UNIVERSITÀ
DEGLI STUDI
DI PADOVA

Sede Amministrativa: Università degli Studi di Padova
Dipartimento di Scienze Medico-Diagnostiche e Terapie Speciali

SCUOLA DI DOTTORATO DI RICERCA IN SCIENZE MEDICHE, CLINICHE E SPERIMENTALI
INDIRIZZO "SCIENZE CARDIOVASCOLARI"
XXIV CICLO

Identification of a novel gene involved in Arrhythmogenic Right Ventricular Cardiomyopathy/Dysplasia

Direttore della Scuola : Ch.mo Prof. Gaetano Thiene
Coordinatore d'indirizzo: Ch.mo Prof. Gaetano Thiene
Supervisore: Ch.ma Prof.ssa Alessandra Rampazzo

Dottoranda: Dr.ssa Martina Calore

31 gennaio 2012

INDEX

ABSTRACT

Introduction- Arrhythmogenic right ventricular cardiomiopathy/displasia (ARVC/D) is a genetic cardiac disease inherited as an autosomal dominant trait with incomplete penetrance and variable expressivity. Its main feature is the progressive substitution of the myocardium with fatty or fibrofatty tissue, involving predominantly the right ventricle. Clinically, ARVC/D is characterized by ventricular arrhythmias, often associated with syncope and sudden cardiac death, especially in the young and athletes. Up to now, ten disease genes have been identified, including 5 encoding desmosomal proteins: plakoglobin (JUP), desmoplakin (DSP), plakophilin-2 (PKP2), desmoglein-2 (DSG2), and desmocollin-2 (DSC2). Less frequently, pathogenic mutations have been detected in genes encoding cardiac ryanodine receptor-2 (RYR2), transforming growth factor beta-3 (TGFβ3), the inner nuclear membrane protein LUMA (TMEM43), desmin (DES), and titin (TTN). Despite mutations in desmosomal genes account for pathogenic phenotype of about half of ARVC/D probands, there is still a significant proportion of probands negative for mutations in known genes, thus suggesting the presence of further genetic heterogeneity.

Methods- Mutation screening for desmosomal genes has been performed by dHPLC (denaturing high performance/pressure liquid chromatography) and direct sequencing in 80 consecutive unrelated Italian index cases. Clinical diagnosis of ARVC/D was based on major and minor criteria established by the International Task Force in 2010. Genetic analysis was then extended to available family members of porbands who resulted to carry a disease-gene mutation. Mutation screening was performed in CTNNA3 candidate gene in 76 affected subjects, negative for mutations in desmosomal genes. To evaluate pathogenicity of mutations detected in CTNNA3 gene, appropriate constructs have been obtained by site-directed mutagenesis PCR. Cellular localization of wild type and mutated proteins has been analyzed by transfection and immunofluorescence experiments performed in neonatal rat cardiomyocytes and in HL-1 cardiac cell line. Interactions with different molecular partners have been studied by yeast two-hybrid assay. Moreover, to better understand the aberrant behaviour of p.del765L-alphaT-catenin, transfection experiments have been performed also in HEK293T cells, that don't express CTNNA3 gene.

Results- Mutation screening in desmosomal genes led to the identification of mutations in 44% of probands. In particular, 12 (15%) probands resulted to carry a single mutation in PKP2 gene, 6 (7,5%) in DSP gene, 5 (6%) in DSG2 gene, and 2 (2,5%) in JUP gene, whereas no mutations have been detected in DSC2 gene. Moreover, compound or double heterozygosity has been identified in 10 (12,5%) probands. On the contrary, any mutation wasn't detected in 56% of the probands. On the basis of alphaT-catenin cellular localization and function, mutation screening was performed in CTNNA3 candidate gene in 76 index cases, negative for mutations in desmosomal genes. Four novel exonic mutations (p.V94D, p.Q260R, p.V583A, p.del765L), absent in 250 healthy controls and located in important functional domains of alphaT-catenin, have been detected. Cellular localization of wild-type

and mutated proteins has been analyzed by transfection and immunofluorescence experiments performed in neonatal rat cardiomyocytes and in HL-1 cells. These experiments showed that the p.V94D mutant protein localized mainly into the cytoplasm, whereas in all the other cases, the proteins were correctly localized in the plasma membrane. Interactions with different alphaT-catenin molecolar partners have been studied by yeast two-hybrid assay. p.V94D mutant protein lost its ability to bind beta-catenin and plakoglobin. This result represents also a new data, because so far the interaction between alphaT-catenin and plakoglobin was never demonstrated. Yeast two-hybrid assay revealed also that the p.del765L mutant protein was able to dimerize more strongly, interacting both with mutated and wild type proteins. Transfection experiments performed in HEK293T cells that do not express alphaT-catenin showed that the mutated proteins formed aggregates into the cytoplasm surrounded by a vimentin cage, called aggresomes.

Discussion- An accurate genotyping and the identification of disease-causing mutations facilitate timely diagnosis and consequently allow the prevention of complications and the reduction of morbidity and mortality. However, a crucial aspect of mutation screening is the assessment of pathogenicity of ARVC/D mutations, to discriminate pathogenic mutations from rare polymorphisms. This is particular relevant since in the last revision of the diagnostic criteria, the identification of a pathogenic mutation has been considered as a major diagnostic criteria.

Since half of the probands resulted negative for mutation screening, additional genes have to be identified. CTNNA3 gene encodes for alphaT-catenin, a protein highly expressed in cardiac intercalated discs in adherens junctions and in *area composita*, a recently discovered mixed junction, exclusively present in cardiomyocytes, composed both by proteins of desmosomes and of adherens junctions. In this study, for the first time mutations in αT-catenin have been identified and associated to ARVC. However, how *CTNNA3* mutations perturb the assembly and function of the areae compositae in ARVC hearts is still unclear. We can speculate that expression of mutant αT-catenins may lead to weakened cell-cell contacts between adjacent cardiomyocytes, and to disruption of tissue integrity particularly in response to excessive mechanical stress.

Most mutations causing ARVC have been identified in *JUP*, *DSP*, *PKP2*, *DSG2* and *DSC2* genes, all of which encode proteins present in both desmosomes and areae compositae. As αT-catenin is present only in the area composita and not in the desmosomes, ARVC may be considered a disease of the area composita, rather than a classical desmosomal disease.

RIASSUNTO IN ITALIANO

Introduzione- La cardiomiopatia aritmogena del ventricolo destro (ARVC/D) è una malattia genetica cardiaca, ereditata come carattere autosomico dominante a penetranza incompleta ed espressività variabile. La sua caratteristica principale è la progressiva sostituzione del miocardio del ventricolo destro con tessuto adiposo e/o fibroadiposo, con formazione di circuiti anatomici di rientro e conseguenti aritmie e morte improvvisa, specie nei giovani. Attualmente sono noti dieci geni malattia, di cui cinque sono codificanti per le proteine desmosomali placofilina-2, desmoplachina, desmogleina-2, desmocollina-2 e placoglobina. Meno frequentemente, sono state trovate mutazioni in soggetti affetti nei geni che codificano per il recettore rianodinico cardiaco, il fattore di crescita beta-3 (TGFβ3), la proteina della membrana nucleare interna LUMA, e più recentemente nei geni che codificano per la desmina e la titina. Nonostante le mutazioni nei geni desmosomali siano responsabili della determinazione genetica della malattia in circa la metà dei soggetti analizzati, rimane una cospicua parte degli individui affetti in cui non è stata trovata nessuna mutazione nei geni malattia noti, suggerendo la presenza di ulteriore eterogeneità genetica.

Metodi- 80 casi indice italiani non imparentati tra loro e diagnosticati affetti da ARVC/D in base ai criteri diagnostici della Task Force del 2010, sono stati sottoposti a *screening* per la ricerca di mutazioni nei cinque geni desmosomali tramite dHPLC (*denaturing high performance/pressure liquid chromatography*) e sequenziamento diretto. L'analisi genetica è stata successivamente estesa ai familiari disponibili. Lo *screening* per la ricerca di mutazioni nel gene CTNNA3 è stato eseguito con le stesse metodiche in 76 soggetti affetti, negativi per mutazioni nei geni desmosomali. Allo scopo di valutare la patogenicità di mutazioni identificate nel gene CTNNA3, sono stati preparati dei costrutti tramite PCR di mutagenesi sito specifica. La localizzazione cellulare delle proteine mutate è stata analizzata eseguendo esperimenti di trasfezione e immunofluorescenza nelle cellule cardiache HL-1 e nei cardiomiociti primari di ratto. L'interazione delle alphaT-catenine mutate con vari *partners* molecolari è stata invece studiata tramite saggi del doppio ibrido in lievito. Sono stati inoltre eseguiti esperimenti di trasfezione nelle cellule HEK293T, in cui l'alphaT-catenina non viene sintetizzata, per studiare il comportamento anomalo della proteina che porta la delezione p.del765L.

Risultati- La ricerca di mutazioni nei geni desmosomali ha portato all'identificazione di mutazioni nel 44% dei casi. In particolare, 12 (15%) probandi sono risultati portatori di una singola mutazione nel gene PKP2, 6 (7,5%) nel gene DSP, 5 (6%) nel gene DSG2 e 2 (2,5%) nel gene JUP; al contrario, nel gene DSC2 non è stata rilevata nessuna mutazione. Inoltre, 10 (12,5%) casi indice sono risultati essere portatori di mutazioni multiple, mentre nel 56% dei probandi analizzati non è stata osservata nessuna variazione patogena. In virtù della funzione e della localizzazione cellulare dell'alphaT-catenina, è stato svolto lo *screening* di mutazioni nel gene candidato CTNNA3 in 76 casi indice negativi per mutazioni nei geni desmosomali. Sono state identificate quattro nuove variazioni esoniche (p.V94D, p.Q260R, p.V583A e p.del765L), assenti in 250 soggetti sani di controllo e presenti in domini di interazione importanti dell'alphaT-catenina. Esperimenti di trasfezione e

immunofluorescenza eseguiti nelle cellule HL-1 e in cardiomiociti neonatali di ratto hanno evidenziato che la proteina che porta la variazione p.V94D si localizza in modo anomalo a livello del citoplasma, a differenza delle altre forme mutate e della proteina wild type, che sono correttamente presenti nella membrana plasmatica. Mediante saggi di doppio ibrido in lievito, è stato dimostrato che proteina mutata p.V94D non è in grado di interagire con la beta-catenina e la placoglobina. Tale risultato rappresenta anche un aspetto nuovo, in quanto finora non era mai stata riportata l'interazione tra alphaT-catenina e placoglobina. Il saggio del doppio ibrido in lievito ha inoltre evidenziato che la proteina che porta la delezione p.del765L è in grado di formare dei dimeri più forti, coinvolgendo sia un'altra proteina mutata, che una wild type. Per approfondire questo aspetto, sono stati svolti esperimenti di trasfezione anche nelle cellule HEK293T. Da ciò è emerso che tale proteina forma degli aggregati circondati da vimentina nel citoplasma, chiamati aggresomi.

Discussione- L'identificazione di mutazioni patogene si pone alla base della diagnosi precoce dell'ARVC/D, oltre che della prevenzione e della riduzione dei casi di morte improvvisa. Un aspetto importante nella ricerca di mutazioni è stabilire la patogenicità delle mutazioni e discriminare tra mutazioni patogene e polimorfismi rari. Questo aspetto è particolarmente rilevante in quanto nell'ultima revisione dei criteri diagnostici la presenza di una mutazione patogena è considerata un criterio maggiore di diagnosi.

Poiché circa la metà dei probandi è risultata negativa allo screening per la ricerca di mutazioni, altri geni devono essere implicati nella patologia.

Il gene CTNNA3 codifica per l'alphaT-catenina, una proteina abbondantemente espressa nei dischi intercalari cardiaci a livello delle giunzioni aderenti e dell'*area composita*, una giunzione mista, presente esclusivamente nei cardiomiociti, costituita da proteine dei desmosomi e delle giunzioni aderenti, scoperta recentemente. Proprio a livello dell'*area composita*, è stata identificata la specifica interazione tra l'alphaT-catenina e la placofilina-2. Alla luce di questi aspetti, nel nostro laboratorio, il gene CTNNA3 è stato considerato un buon candidato per l'ARVC/D. In questo studio sono state identificate per la prima volta mutazioni nel gene CTNNA3 e sono state associate all'ARVC. Tuttavia non è ancora noto come queste mutazioni alterino l'assemblaggio e la funzione dell'area composita nei cuori affetti. Si può ipotizzare che mutazioni nel gene CTNNA3 potrebbero portare all'indebolimento delle giunzioni intercellulari e alla conseguente perdita dell'integrità del miocardio in risposta allo stress meccanico.

La maggior parte delle mutazioni che causano ARVC sono state identificate in geni che codificano per proteine presenti sia nei desmosomi che nell'area composita. Poiché l'alfa-T catenina è presente solo nell'area composita e non nei desmosomi, l'ARVC potrebbe essere considerata una malattia dell'area composita piuttosto che desmosomale.

1. INTRODUCTION

Cardiomyopathies are an inherited, clinically heterogenous group of heart diseases, characterized by an abnormal cardiac structure and/or function, without ischaemia, that can lead to sudden cardiac death (SCD). Clinical evaluation of affected individuals and genotype profiling, if possible, are the current tools for the classification of cardiomyopathies. Beyond channelopathies, up to now, cardiomyopathies are divided into major phenotypic categories in hypertrophic, dilated, restrictive, and arrhythmogenic right ventricular cardiomyopathy/dysplasia (ARVC/D) (Elliott, et al., 2008; Maron et al., 2006).

Among them, ARVC/D is a heritable progressive cardiac disease associated with arrhythmia, heart failure and sudden death (Thiene et al., 1988; Nava et al., 1988). ARVC/D is mostly inherited as an autosomal dominant trait with reduced penetrance and variable expression, although autosomal recessive forms have been reported (Nava et al., 2000; McKoy et al., 2000).

The main characteristic of the disorder is the replacement of myocytes by adipose and/or fibrous tissue (Thiene et al., 1988). This substitution interests mostly the right ventricle (RV) and the name of the disease reflects this aspect; however, recognition of subtypes with left involvement supports the adoption of the wider term “arrhythmogenic cardiomyopathy” (ACM) (Sen-Chowdhry et al., 2007; Corrado et al., 1997; Basso et al., 1996). Thus, while familiar, the term ARVC/D does not reflect accurately the width of the phenotypes known of this disease. For this reason, the term ACM has been suggested by HRS/EHRA Expert Consensus Statement of the State of Genetic Testing for Channelopathies and Cardiomyopathies (Ackerman et al., 2011)

Clinically, ARVC/D manifests with structural and functional changes of ventricles, electrocardiogram abnormalities, and fibro-fatty replacement. In some cases, sudden death can be the first symptom of the disease. ARVC/D accounts for SCD mainly among young people between the second and the fourth decade of life, engaged in physical exercise, as a consequence of ventricular tachycardia (VT) and ventricular fibrillation (VF) (Tabib et al., 1999; Furlanello et al., 1998; Corrado et al., 1990; Thiene et al., 1988; Fontaine et al., 1988).

1.1 EPIDEMIOLOGY OF ARVC/D

In the general population, the prevalence of ARVC/D spans from 1:2000 to 1:5000 (Norman et al., 1999; Nava et al., 1988) and it’s considered the second most common cause of SCD among young and athletes, after hypetrophic cardiomyopathy (Corrado et al., 1998). ARVC/D results to be familiar in 30-50% of cases; anyway, in the isolated cases, familiarity cannot be excluded due to the incomplete penetrance or limited expression. For the same reason, it must be considered that the prevalence of the disease in the population could be underestimated (Hamid et al., 2002). Moreover, ARVC/D affects men more frequently than women, with a ratio ranging from 1.3 to 2.4 (Bauce et al., 2008; Saffitz et al., 2009). The classical form of ARVC/D is manifested in teenagers or in young adults in about 80% of

cases (Marcus et al., 1982; Marcus and Fontaine, 1995; Fontaine et al., 1988), but it can be discovered at any age and in both sexes.

1.2 ARVC/D: HISTORICAL NOTES

The first historical description of ARVC/D was published in 1736 in the "*De Motu Cordis et Aneurysmatibus"* by Giovanni Maria Lancisi who reported the recurrence of the disease in four-generations of a family whose members showed palpitations, heart failure, dilatation and aneurysms of the RV, and sudden death (Lancisi, 1736). In the next two centuries, other pathological descriptions of the disease were reported, like the one made by Sir William Osler in 1905 about a 40-year-old man who died suddenly while climbing a hill, whose heart showed biventricular atrophy, thinning and translucency of ventricular free walls (Osler, 1905). In 1961, Sergio Dalla Volta and colleagues described cases with "auricularization" (strong right atrial contraction) of the RV pressure to emphasize the behavior of the RV without an effective systolic contraction, pushing the blood into the pulmonary artery mostly thanks to the right atrial systole (Dalla Volta et al., 1965). Thirty years later, an original patient reported by Dalla Volta underwent cardiac transplantation. Post operation analysis showed a normal LV, while RV was hugely dilated with thinning of the free wall and complete disappearence of the myocardium (Thiene et al., 2007). Only in the eighties a detailed clinical description was documented; in 1982, Marcus and coworkers reported 24 adult cases showing VT with right bundle-branch morphology (Marcus et al., 1982), and in 1984, Fontaine and colleagues reported for the first time the electrocardiographic aspects of the disorder, such as epsilon waves (Fontaine et al., 1984). In 1988, Nava and colleagues described polymorphous clinical features of the disease, like different kinds of arrhythmias in affected subjects, and the autosomal dominant mode of transmission with incomplete penetrance of the disease (Nava et al., 1988). In the same year, Thiene and co-workers described several cases of sudden death in young people (≤35 years), occurred almost during effort. These subjects showed typical electrical ARVC/D features, like inverted T waves in the right precordial leads and ventricular arrhythmias with left bundle branch block (LBBB), together with fibrofatty replacement in the right ventricular free wall (Thiene et al., 1988). For the first time ARVC/D had been considered among the main causes of sudden death, above all among young and sporty people. From this time, the disease identification in athletes was considered a key point of prevention during pre-partecipation screening for sport activity (Corrado et al., 2006). Thus, due to the importance and the complexity of the diagnosis, in 1994 an International Task Force published the diagnostic criteria to define the guidelines for clinical diagnosis of ARVC/D (McKenna et al., 1994). More recently, due to the great advances made in the diagnostic features, new Task Force criteria have been adopted from the scientific community in ARVC/D diagnosis (Marcus et al., 2010). In the nineties, Basso and colleagues deepened the ultrastructural aspect of the disease and the progressive myocardial loss due to genetically-determined cardiomyocytes death (Basso et al., 1996), whereas Valente and co-workers linked apoptosis to cardiomyocytes death in ARVC/D (Valente et al., 1997).

In parallel to the clinical advances on ARVC/D, linkage analyses were performed in order to map and to identify the disease gene/s: in 1994, Rampazzo and colleagues gave rise to a long series of molecular studies leading to the identification of the first disease *locus*, ARVD1, mapped on in the chromosome 14 (Rampazzo et al., 1994); subsequently the same group identified four disease genes: RYR2, DSP, TGFβ3, and, later, DSG2 (Tiso et al., 2001; Rampazzo et al., 2002; Beffagna et al., 2005; Pilichou et al:, 2006). In few years, several chromosomal *loci* and disease genes, mostly encoding desmosomal proteins, had been identified, leading in 2004-2005 to the definition of ARVC/D as a "desmosomal disease" (Basso et al., 2006). Up to now, genetic analysis worldwide led to the identification of 12 *loci* independently involved in the determination of the disease and 10 disease genes.

Another interesting aspect regards the correlation genotype-phenotype, representing a complex aspect of ARVC/D, due to the clinical heterogeneity of the disease. Bauce and colleagues showed that DSP mutation carriers often showed a biventricular form of the disease (Bauce et al., 2005).

1.3 CLINICAL PRESENTATION OF ARVC/D

ARVC/D usually manifests between the second and the fourth decades of life. Its course can be divided in four main phases, described on the basis of the long-term follow-up of clinical data:

1) Subclinical phase with concealed structural abnormalities: in this first phase, functional and structural abnormalities are subtle or absent, with or without ventricular arrhythmias. Patients are thus usually asymptomatic and SCD can be the first manifestation of the disease, mainly in athletes or in subjects under effort (Thiene et al., 1988).
2) Overt arrhythmic phase: in this phase symptomatic right ventricular arrhythmias may occur, possibly inducing sudden cardiac arrest associated with overt right ventricular functional and structural abnormalities (Corrado et al., 1990).
3) Global RV dysfunctional phase: it's the phase of the extension of the disease to the whole RV, while generally LV is preserved and conserves its functionality (Corrado et al., 1998).
4) End-stage phase: it is characterized by pronounced involvement of both ventricles, making it difficult to differentiate clinically ARVC/D from biventricular dilated cardiomyopathy. In this phase, congestive heart failure and related complications can occur, also requiring cardiac transplantation. These data and those produced by other authors confirm that the disorder develops progressively (Blomstrom-Lunqvist et al., 1987).

The main electropathological mechanism that causes arrhythmias is the re-entry in the areas affected by the fibrofatty replacement (Basso et al., 1996; Thiene et al., 1988). Scars originated from the substitution alter, blocking or delaying, the conduction in the RV and could provide the substrate for re-entrant circuits and the development of ventricular

arrhythmias. Also, abnormalities in gap junctions could alter the correct propagation of the electric impulse, thus generating arrhythmias (Kaplan et al., 2004; Kostetskii et al., 2005).
Clinically, the disease is characterized by palpitations, presyncope or syncope in subjects generally considered normal on physical examination. Weakness and dizzy spells are sometimes referred. Typical clinical features of the disease can be evidenced by a 12-lead electrocardiogram (ECG) during the events or by a 24-h Holter monitoring. Arrhythmias can vary from isolated premature ventricular beats to sustained VT with LBBB morphology (Figure 1), or VF. The origin of arrhythmias in a VT with LBBB morphology is reflected by QRS morphology and axis, that can be inferior for arrhythmias originated from the RV outflow tract (RVOT), or superior for arrhythmias originated from the RV inferior wall. Obviously, when also the LV is affected, ventricular arrhythmias may appear polymorphic, originating from different cardiac regions.
Also, ventricular extrasystoles of LBBB configuration have been recorded in the majority of patients. However, it is necessary to consider that a VT with LBBB cannot be strictly connected to ARVC/D.

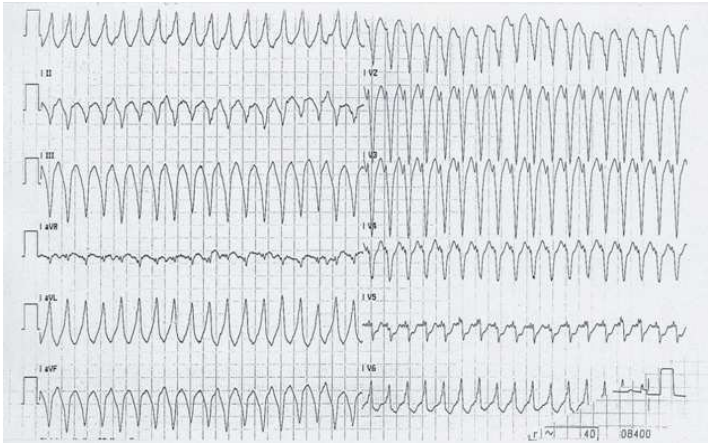

Fig.1: 12-lead ECG recording VT with left
bundle branch block (LBBB) morphology (Thiene at al., 2007).

T-waves inversion beyond precordial lead V1-V5 after 14 years of age, incomplete right bundle branch block (RBBB) or prolongation of QRS duration greater than 110 ms on V1-V2 are typical aspects of ARVC/D as well (Figure 2). Moreover, epsilon waves (Figure 2) are strongly indicative of intraventricular impulse conduction delay. Epsilon waves are probably caused by the delayed depolarization in the surviving myocytes interspersed with fatty and fibrous tissue. Also, fibro-fatty infiltration in the atrial myocardium may explain palpitations that in about 24% of cases are not exclusively associated with ventricular arrhythmias but also with atrial extrasystoles, atrial flutter or fibrillation. Only secondary this can be due to hemodynamic impairment of the right ventricle (Fontaine et al., 1988).
Sometimes chest pain associated with transient alterations of repolarization, such as ST segment elevation or negative T waves on inferior or precordial leads can be evidenced.

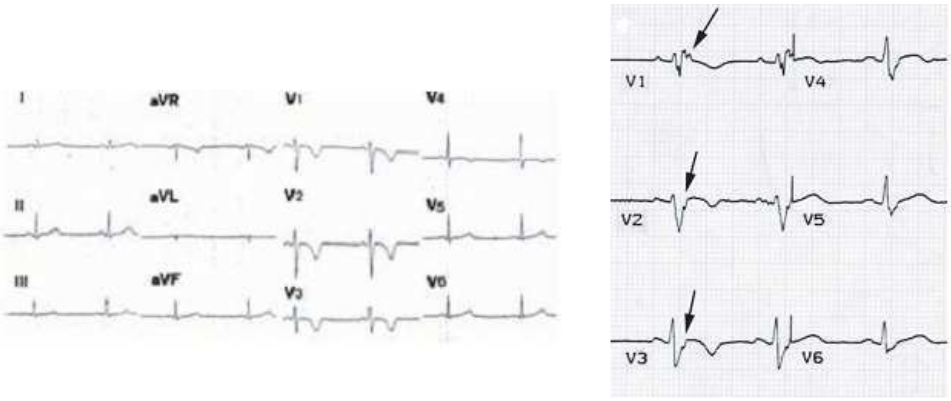

Fig. 2: (Left) 12-lead ECG of a 17 year old asymptomatic male athlete who died suddenly during a soccer game. Inverted T waves up to V4 are present (Basso et al., 1996). (Right) post-excitation epsilon wave (arrows) in right precordial leads (Thiene et al., 2007).

Signal average ECG (SAECG) reveals low amplitude late potentials at the end of the QRS complex, which corresponds to epsilon waves on surface ECG.

Morphologic changes accounting for global and/or regional dysfunction are detectable by noninvasive techniques as echocardiography, angiography, radionuclide scintigraphy, or cardiac magnetic resonance imaging (MRI). Echocardiography is a non-invasive widely used technique representing the first-line imaging approach for evaluation of patients with suspected ARVC/D or for screening of family members. This technique is also used to assess the disease onset and progression during the follow-up. RV angiography is usually reported as the gold standard for the diagnosis of ARVC/D. Angiographic evidence of akinetic/diskinetic bulgings localized in infundibular, apical and subtricuspid region has a high diagnostic specificity (>90%) (Daliento et al., 1990). Radionuclide angiography is also an accurate non-invasive imaging technique for detection of global RV dysfunction and regional wall motion abnormalities. Its diagnostic concordance with RV angiography is nearly 90% (Le Guludec et al., 1995). MRI is a non-invasive imaging used to characterize tissue by distinguishing fat from muscle (Figure 3). However, an interobserved variability in evaluating fatty deposition has been shown, comparably with what is detected also in normal hearts (Tandri et al., 2005). Cine-MRI may be of value in estimating RV volume and wall motion abnormalities with akinesia, dyskinesia and aneurysms.

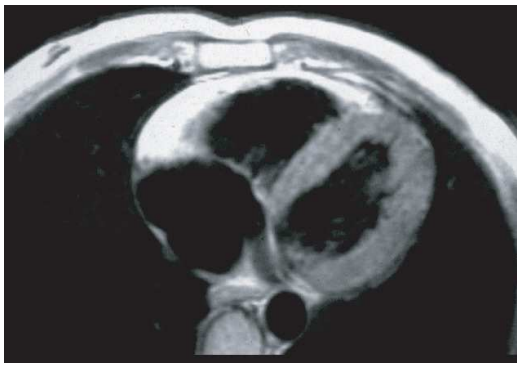

Fig.3: MRI: long axis view of the RV of a patient affected by ARVC/D. Transmural diffuse bright signal in the RV free wall due to massive myocardial atrophy with fatty replacement is evidenced (Thiene et al., 2007).

Endomyocardial biopsy can identify fibro-fatty replacement (Figure 4), thus distinguishing ARVC/D from myocarditis and sarcoidosis (Chimenti et al., 2004; Ott et al., 2003; Thiene and Basso 2001; Angelini et al., 1996). Since the ventricular septum in usually spared, samples should be taken from the right ventricular free wall preferably using electrocardiography or MRI, and to diagnose the disease the residual amount of myocardium should be less of 60% (Avella et al., 2008; Basso et al., 2008).

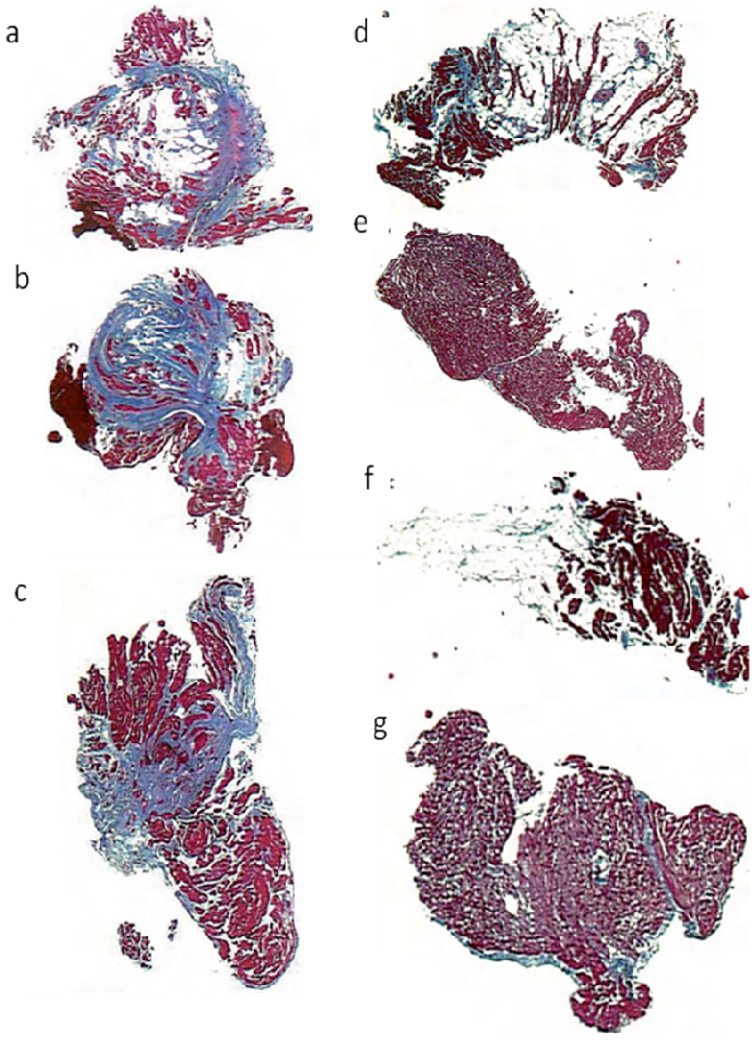

Fig.4: (Left) Endomyocardial biopsy findings in a proband affected by a diffuse form of ARVC/D: the extensive fibro-fatty replacement is ecident in all three bioptic samplec (a,b,c). (Right) Endomyocardial biopsy findings in a proband affected by a localized form of ARVC/D: only cuts d and f have either extensive or focal fibro-fatty tissue replacement, whereas the other two (e,g) are normal (Basso and Thiene, 2007).

In the last years new diagnostic tools have been introduced in the clinical management of ARVC/D patients. MRI with gadolinium late enhancement is a non-invasive technique used to detect fibrosis in the RV and LV myocardium (Tandri et al., 2005). Among invasive procedures, three dimensional electroanatomic mapping is a tool showing low voltage areas corresponding to fibro-fatty myocardial replacement, thus differentiating ARVC/D from inflammatory cardiomyopathy mimicking ARVC/D (Corrado et al., 2005).

1.4 TASK FORCE CRITERIA

Due to the difficulties in diagnosis and to the heterogeneous pattern of phenotypic expression evidenced in ARVC/D patients in several years, in 1994 International Task Force criteria were published to define guidelines for the clinical diagnosis of ARVC/D (Table 1) (McKenna et al., 1994). This Task Force experienced clinicians in the field of cardiomyopathy and it was convened under the auspices of the European Society of Cardiology (Working Group on Myocardialand Pericardial Diseases) and the International Society and Federation of Cardiology (Scientific Council). The defined criteria were based on six different groupings (structural, histological, electrocardiographical (repolarization and depolarization/conduction abnormalities), arrhythmic, and familial aspects of the disease) and were divided into major and minor features, according to the specificity of their association with ARVC/D. The diagnosis of ARVC/D is fulfilled by the presence of two major criteria, one major and two minor criteria, or four minor criteria of different groups (Table 1). During the last decades, experience with ARVC/D lead to the development of additional diagnostic tools, such as echocardiography and imaging techniques, and the improvement of genetic mutation analysis. Thus, in 2010, Marcus and colleagues proposed modified criteria considering the updated knowledge and diagnostic sensitivity, and at the same time maintaining the diagnostic specificity (Table 1) (Marcus et al., 2010). With the new criteria, ARVC/D diagnosis is now considered fulfilled by the presence of 2 major, or 1 major and 2 minor criteria, or 4 minor criteria from different categories. Moreover, a borderline condition is contemplated in the presence of 1 major and 1 minor, or 3 minor criteria from different groups, while a possible condition is held in the presence with 1 major or 2 minor criteria from different categories.

Original Task Force Criteria	**Revised Task Force Criteria**
I. Global or regional dysfunction and structural alterations*	
Major -Severe dilatation and reduction of RV ejection fraction with no (or only mild) LV impairment -Localized RV aneurysms (akinetic or dyskinetic areas with diastolic bulging) -Severe segmental dilatation of the RV	**Major** **By 2D echo:** -Regional RV akinesia, dyskinesia, or aneurysm -and 1 of the following (end diastole): -PLAX RVOT ≥ 32 mm (corrected for body size [PLAX/BSA] ≥ 19 mm/m^2) - PSAX RVOT ≥ 36 mm (corrected for body size [PSAX/BSA] ≥ 21 mm/m^2) -Or fractional area change ≤ 33% **By MRI:** -Regional RV akinesia or dyskinesia or dyssynchronous RV contraction -and 1 of the following: -Ratio of RV end-diastolic volume to BSA ≥ 110 mL/m^2 (male) or ≥ 100 mL/m^2 (female) -Or RV ejection fraction ≤ 40% **By RV angiography:** -Regional RV akinesia, dyskinesia, or aneurysm
Minor -Mild global RV dilatation and/or ejection fraction reduction with normal LV -Mild segmental dilatation of the RV -Regional RV hypokinesia	**Minor** **By 2D echo:** -Regional RV akinesia or dyskinesia -and 1 of the following (end-diastole): -PLAX RVOT ≥29 to <32 mm (corrected for body size [PLAX/BSA] ≥16 to <19 mm/m^2) -PSAX/RVOT 32 to <36 mm (corrected for body size [PSAX/BSA] ≥ 18 to <21 mm/m^2) -Or fractional area change >33% to ≤ 40% **By MRI:** -Regional RV akinesia or dyskinesia or dyssynchronous RV conctraction

	-and 1 of the following: -Ratio of RV end-diastolic volume to BSA ≥100 to <110 mL/m^2 (male) or ≥90 to <100mL/m^2 (female) -or RV ejection fraction >40% to ≤ 45%
II. Tissue characterization of wall	
Major -Fibrofatty replacement of myocardium on endomyocardial biopsy **Minor**	**Major** -Residual myocytes <60% by morphometric analysis (or <50% if estimated), with fibrous replacement of the RV free wall myocardium in ≥1 sample, with or without fatty replacement of tissue on endomyocardial biopsy **Minor** -Residual myocytes 60% to 75% by morphometric analysis (or 50% to 65% if estimated), with fibrous replacement of the RV free wall myocardium in ≥1 sample, with or without fatty replacement of tissue on endomyocardial biopsy
III. Repolarization abnormalities	
Major **Minor** -Inverted T waves in precordial leads (V_2 and V_3) (people age >12 years, in absence of right bundle-branch block)	**Major** -Inverted T waves in right precordial leads (V_1, V_2, and V_3) or beyond in individuals >14 years of age (in the absence of complete right bundle-branch block QRS ≥120 ms) **Minor** -Inverted T waves in leads V_1 and V_2 in individuals >14 years of age (in the absence of complete right bundle-branch block) or in V4, V5, or V6 - Inverted T waves in leads V1, V2, V3, and V4 in individuals >14 years of age in the presence of complete right bundle-branch block
IV. Depolarization/conduction abnormalities	
Major -Epsilon waves or localized prolongation (>110 ms) of the QRS complex in right precordial leads (V1 to V3) **Minor** Late potentials (SAECG)	**Major** - Epsilon wave (reproducible low-amplitude signals between end of QRS complex to onset of the T wave) in the right precordial leads (V1 to V3) **Minor** -Late potentials by SAECG in ≥_1 of 3 parameters in the absence of a QRS duration of ≥110 ms on the standard ECG -Filtered QRS duration (fQRS) ≥114 ms - Duration of terminal QRS <40 μV (low-amplitude signal duration) ≥38 ms - Root-mean-square voltage of terminal 40 ms <20 μV - Terminal activation duration of QRS ≥55 ms measured from the nadir of the S wave to the end of the QRS, including R', in V1, V2, or V3, in the absence of complete right bundle-branch block
V. Arrhythmias	
Major **Minor** -Left bundle-branch block-type ventricular tachycardia (sustained and nonsustained) (ECG, Holter, exercise) - Frequent ventricular extrasystoles (>1000 per 24 hours) (Holter)	**Major** -Nonsustained or sustained ventricular tachycardia of left bundle-branch morphology with superior axis (negative or indeterminate QRS in leads II, III, and aVF and positive in lead aVL) **Minor** -Nonsustained or sustained ventricular tachycardia of RV outflow configuration, left bundle-branch block morphology with inferior axis (positive QRS in leads II, III, and aVF and negative in lead aVL) or of unknown axis - >500 ventricular extrasystoles per 24 hours (Holter)
VI. Family history	
Major **-** Familial disease confirmed at necropsy or surgery **Minor** -Family history of premature sudden death (<35 years of age) due to suspected ARVC - Familial history (clinical diagnosis based on present criteria)	**Major** -ARVC confirmed in a first-degree relative who meets current Task Force criteria -ARVC confirmed pathologically at autopsy or surgery in a first-degree relative -Identification of a pathogenic mutation** categorized as associated or probably associated with ARVC in the patient under evaluation **Minor** -History of ARVC in a first-degree relative in whom it is not possible or practical to determine whether the family member meets current Task Force criteria - Premature sudden death (<35 years of age) due to suspected ARVC in a first-degree relative - ARVC confirmed pathologically or by current Task Force Criteria in second-degree relative
PLAX indicates parasternal long-axis view; RVOT, RV outflow tract; BSA, body surface area; PSAX, parasternal short-axis view; aVF, augmented voltage unipolar left foot lead; and aVL, augmented voltage unipolar left arm lead. *Hypokinesis is not included in this or subsequent definitions of RV regional wall motion abnormalities for the proposed modified criteria. **A pathogenic mutation is a DNA alteration associated with ARVC/D that alters or is expected to alter the encoded protein, is unobserved or rare in a large non-ARVC control population, and either alters or is predicted to alter the structure or function of the protein or has demonstrated linkage to the disease phenotype in a conclusive pedigree.	

Tab.1: International Task Force ARVC/D diagnostic criteria. Original criteria are listed in the left column, the revised criteria in the right column.

ARVC/D diagnosis in probands' relatives has been considered complex as well, due to the heterogeneity of disease expression, even within relatives carrying the same gene mutation. Phenotypic expression in proband's family members could be so heterogenous to include clinical features of the disease which were not as marked as in the proband. This could be explained considering both incomplete and age-related penetrance (Nava et al., 1988). Identification of specific gene mutations responsible for ARVC/D provided evidence of mutation(s) carriers with some features of ARVC/D but insufficient to fulfill the Task Force criteria. Diagnostic criteria were then also proposed for relatives' diagnosis for familial ARVC/D by Hamid et al. (Hamid et al., 2002). In first-degree relatives of an ARVC/D patient, diagnosis is made considering electrical, functional and structural aspects, listed in Table 2.

ARVC in first-degree relatives plus one of the following:	
I. ECG	T-wave inversion in right precordial leads (V_2 and V_3)
II. SAEGC	Late potentials seen on signal-averaged ECG
III. Arrhythmia	-LBBB type VT on ECG, Holter monitoring or during exercise testing -Extrasystoles >200 in 24 hours
IV. Structural or functional abnormality of the RV	-Mild global RV dilatation and/or ejection fraction reduction with normal LV -Mild segmental dilatation of the RV -Regional RV hypokinesia

Tab.2: Proposed modification of Task Force Criteria for the diagnosis of familial ARVC/D.

1.5 ARVC/D PATHOLOGY

The main aspect of the disease is the progressive replacement of the right ventricular myocardium by fatty or fibrofatty tissue, starting from the epicardium or myocardium and extending to the endocardium as to become transmural. Myocardial atrophy accounts for a parchment-like, translucent look of the wall, even though the distance between the epicardium and the endocardium may be preserved (Figure 5) (Thiene et al., 1988).

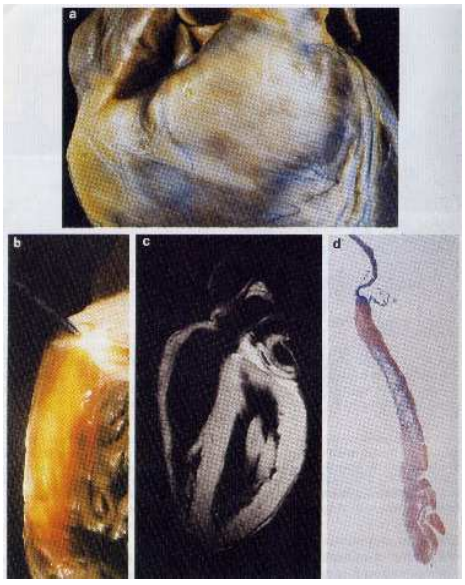

Fig. 5: ARVC/D in a 26-year-old male cyclist died suddenly at rest. Gross view of the heart specimen showing a yellow, dilated pulmonary infundibulum. (b) The pulmunary infundibulum appears translucent. (c) Bright streaks visible in the infundibular region by an *in vitro* nuclear magnetic resonance. (d) Macrohistologic slide of the RV from the apex to the pulmunary valve showing a localized fibro-fatty replacement in the infundibular region (Basso et al., 1997).

Due to the weak thickness of the right ventricle free wall, the disease evolvement leads to aneurysms located in the so-called “triangle of dysplasia”, that is the areas of the wall less resistant: apex, inflow, outflow (Figure 6). Only in the more severe forms of ARVC/D all the three areas are involved, while usually only one or two regions are affected in the minor cases (Thiene et al., 2007). During pathological analysis, some peculiar alterations of the RV should be taken into account. At external examination, the right side of the heart appears yellowish or whitish, compared with the brownish left side, due to a different tissue composition of the underlying myocardium. The suspicion of fibrofatty substitution may be easily confirmed by cutting the free wall along the inflow-outflow tracts, which appears fatty, and by checking the wall transparency with a light source (Figure 6).

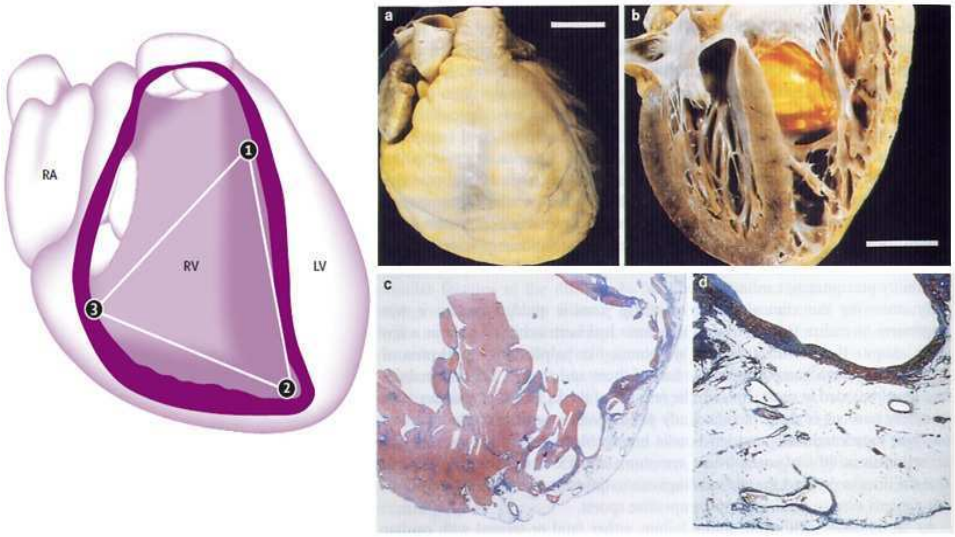

Fig.6: (Left) Triangle of dysplasia, which shows the characteristic areas of the right ventricle affected by abnormalities. RA= right atrium. RV= right ventricle. LV= left ventricle (Basso C., et al., 2009). (Right). Case of ARVC/D in a 25-year-old man who died suddenly at rest. (a) External anterior view showing the yellow appearance of the RV. (b) Four chamber cut of the heart seen from behind. Note the isolated fatty replacement of the right ventricular free wall and translucent infundibulum (c) Macrohistologic slide showing the involvement of the right ventricular free wall, the LV and the ventricular septum. (d) Close up of (c) showing the transmural fatty replacement. Scale bar= 30 mm. (Basso et al., 1997).

Aneurysms of the right ventricular free wall are a typical feature of ARVC/D and are considered to be pathognomonic of the disease. They may appear as a true external bulging or as an “*ex vacuo*” hollow, the latter being explained by the empty cavity in the specimen (Figure 7).

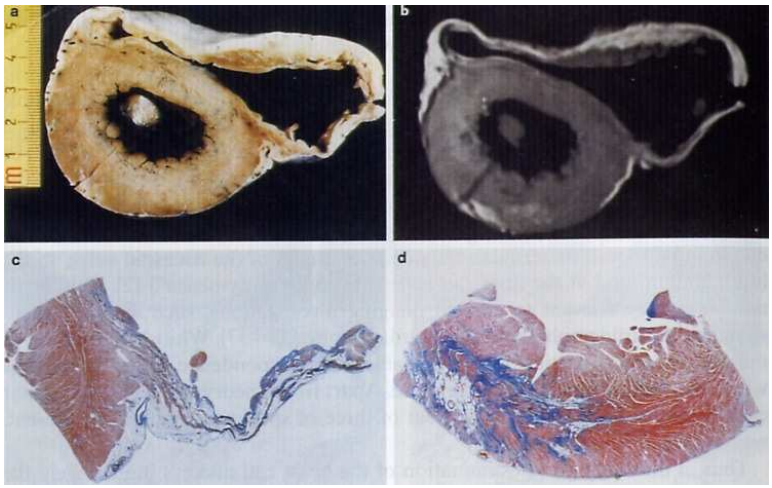

Fig.7: Aneurysms in the right ventricle of a 17-years-old boy affected by ARVC/D who died suddenly during a soccer game. (a) Cross section of the heart specimen with infundibular and inferior subtricuspidal aneurysms (b) Corresponding view of (a) of the *in vitro* MRI cross-sectional view showing a uniformly whitish right ventricular free wall with anterior and inferior aneurysms; note a spotty involvement of the posterolateral wall of the LV. (c) Panoramic histological view of the inferior aneurysm showing wall thinning with fibro-fatty replacement (Azan stain) (d) Macrohistologic slide of postero-lateral free wall of the LV with a large spot of fibro-fatty replacement (Basso et al., 1996).

1.6 PATHOLOGIC SUBSTRATES

Histologically, two different patterns, fatty and fibro-fatty, can be identified. The fatty pattern is mainly characterized by transmural adipose infiltration in the RV free wall, generally localized in the anterior wall and in the infundibulum. The residual myocytes appear interspersed within the fatty tissue. This pattern is regularly associated with a normal or even thickened wall, without scarring or aneurysms (Thiene et al., 1997). In the fibro-fatty pattern, right ventricular aneurysms and focal myocarditis, consisting of patchy inflammatory infiltrates of lymphocytes associated with myocardial necrosis, are frequently evidenced (Thiene et al., 1991; Basso et al., 1996). Moreover, an exclusive feature of the fibro-fatty substitution is the LV and the ventricular septum involvement (Thiene et al., 1997). The fibro-fatty replacement of the myocardium interferes with the intraventricular conduction of the electric impulse accounting for delay (late potentials, epsilon wave, parietal right bundle branch block) and onset of re-entrant phenomena which are the mechanism of ventricular arrhythmias. Fibro-fatty substitution doesn't occur since the birth, as seen in Uhl's disease, but it most likely starts in the adolescence (Uhl, 1952; Daliento et al., 1995). Fatty infiltration of the RV should not be considered "*per se*" a sufficient morphologic hallmark of ARVC/D. Indeed, ARVC/D must be distinguished from "*adipositas cordis*", the physiological presence of intramyocardial fat in healthy hearts, located in the antero-lateral and apical wall of the RV. In about more than 50% of old subjects a significant fatty infiltration has been identified (Basso and Thiene, 2005). Moreover, several forms of ARVC/D without fatty substitution, like Carvajal syndrome, have been reported (Sen-Chowdhry et al., 2005; Kaplan et al., 2004). These evidences indicate that fibrofatty replacement in the RV alone isn't pathognomonic of ARVC/D, thus, presence of replacement-type fibrosis and myocyte degenerative changes are essential to provide a clear-cut diagnosis, besides remarkable fat replacement (Basso and Thiene, 2005; Thiene et al., 2007).

1.7 ETIOPATHOGENETIC THEORIES

Several etiopathogenetic theories have been developed to justify the fibrofatty replacement in the affected myocardium. Originally, ARVC/D was thought to be a congenital dysplasia or hypoplasia of the free wall of the RV (Marcus et al., 1982). This dystrophic theory was postulated before the discovery of the disease-causing genes, evidencing similarities between ARVC/D and skeletal muscle dystrophies at ultrastructural level, such as a progressive muscular atrophy with fibro-fatty replacement. Another theory asserted the idea that the progressive loss of myocardium could be due to genetic metabolic or ultrastructural defects (Valente et al., 1997). Inflammatory theory is supported by several histological analysis, such as inflammatory infiltrates detected around the areas interested by fibro-fatty replacement in 73% of cardiac autopsies. It has been suggested a possible involvement of inflammatory infiltrates in triggering life-threatening arrhythmias (Thiene and Basso; 2001). However, whether inflammatory cells are a consequence of cell death, of immune or infective mechanisms, or of exposition to environmental or toxic factors remains unknown (Thiene et al., 2001; Corrado et al., 1997). Beside inflammatory theory, it has been ipothesized that cardiomyocytes could accumulate lipidic droplets and transform into adipocytes (d'Amati et al., 2000). This theory, however, is still controversial, due to the limited capabilities in de-differentiation of adult cardiac cells. On the other hand, an apoptotic process has been proposed to justify the loss of myocardium and the replacement by fibro-fatty tissue in ARVC/D, as arises from studies performed by Mallat and coworkers (Mallat et al., 1996). Evidence of apoptotic cells was also found in 35% of endomyocardial biopsies analyzed by Valente and colleagues by TUNEL and transmission electron microscope (TEM) (Valente et al., 1997).

1.8 ARVC/D RISK STRATIFICATION AND TREATMENTS

Besides very young subjects, among ARVC/D patients, those most likely to undergo arrhythmic death are the ones that have been resuscitated from SCD, that underwent syncope, and that showed marked right ventricular involvement (Muthappan and Calkins; 2008). Turrini and colleagues in 2001 reported that QRS dispersion (≥40 ms) was the strongest independent predictor of sudden death in ARVC/D and that risk stratification in these patients was refined by syncope, negative T-wave beyond V1 and QT dispersion >65 ms (Turrini et al., 2001). Hulot and colleagues reported that subjects who manifested signs of heart failure and/or left ventricular dysfunction and VT could be at high risk of cardiac events. On the contrary, the lowest risk regards patients presenting without VT (Hulot et al., 2004). Thus, subjects at risk of cardiac events should manage a particular lifestyle, such as avoiding competitive training and limiting sport to low intensity activity. Furthermore, in some cases ARVC/D patients undergo a pharmacological therapy. Anti-arrhythmic therapy, consisting of beta-blockers, sotalol, mexiletine, and amiodarone can be useful for controlling arrhythmia and for reducing appropriate and inappropriate ICD interventions in patients with an implantable cardioverter defibrillator (ICD), Moreover, in ARVC/D patients the implantation of ICD is mandatory in subjects who underwent cardiac arrest or VF, despite

antiarrhythmic drug therapy. In the 5%-8% and in the 14%-22% of patients who received an ICD, the device discharged appropriately in the presence of VF and overall, respectively, thus demonstrating that ICD is potentially life-saving and compelling for the secondary prevention (Corrado et al., 2003; Wichter et al., 2004). Also, catheter ablation could be considered in ARVC/D patients that show drug-refractory, or monomorphic and well-tolerated VT with localized forms of the disease, or frequent ICD discharges. Anyway, in patients with intractable VT, it is still used as a palliative treatment, due the progression of ARVC/D in these subjects (Zou et al., 2004). Finally, heart transplantation should be considered in the case of patients with progressive heart failure and refractory recurrent ventricular arrhythmias (Lacroix et al., 2005).

1.9 GENETIC BASIS OF ARVC/D

ARVC/D is a genetic disease generally inherited as an autosomal dominant trait with incomplete penetrance and variable expressivity (Nava et al., 1988). In about 50% of cases, the disease is familiar; however, this percentage could be underestimated due to asymptomatic subjects, low penetrance, complexity in diagnosis, and poor family history (Hamid et al., 2002). The discovery of disease-genes offered the potential to increase the diagnosis of ARVC/D by genotyping confirmation in a proband with a clinical suspicion of ARVC/D. Moreover, the molecular diagnosis allows to discriminate among family members the healthy ones from those that, carrying a pathogenic mutation, are at risk to develop the disease and thus that could undergo targeted clinical controls (Sen-Chowdhry et al., 2005; Corrado et al., 2006; Sen-Chowdhry et al., 2007). ARVC/D is a genetically heterogeneous disease: so far ten disease genes have been identified (Table 3).

Gene	Encoded protein	Chromosomal locus	Mode of inheritance	Reference
Desmosomal				
JUP	Plakoglobin	17q21	AD/AR	McKoy et al., 2000/Asimaki et al., 2007
DSP	Desmoplakin	6p24	AD/AR	Rampazzo et al., 2002
PKP2	Plakophilin-2	12p11	AD/AR	Gerull et al., 2004
DSG2	Desmoglein-2	18q12	AD	Pilichou et al., 2006
DSC2	Desmocollin-2	18q12	AD/AR	Syrris et al., 2006
Non-desmosomal				
TGFβ3	Transforming growth factor β3	14q23-q24	AD	Beffagna et al., 2005
RYR2	Cardiac ryanodine receptor	1q42-q43	AD	Tiso et al., 2001
TMEM43	Transmembrane protein 43	3p25	AD	Merner et al., 2008
DES	Desmin	2q35	AD	Klauke et al., 2010
TTN	Titin	2q32	AD	Taylor et al., 2011

Tab. 3: Genes involved in ARVC/D identified so far. AD= autosomal dominant. AR= autosomal recessive.

Among the known disease-genes, 5 encode proteins of desmosome, a cell-cell junction complex that provides mechanical integrity of heart tissue affording an intercellular connection between adjacent cells. Desmosomes are abundant in those tissues, like heart and skin, that are frequently subjected to mechanical stress; however, different isoforms of desmosomal proteins are expressed in the different tissues. This junction has five major component proteins, the desmosomal cadherins (desmoglein and desmocollin), the armadillo proteins (plakoglobin and plakophilin), and the cytolinker desmoplakin (Garrod et al., 2002; Green and Simpson, 2007). The disease-genes identified so far and their involvement in ARVC/D are described below.

1.9.1 Desmosomal genes

JUP

In 2000 McKoy and colleagues identified JUP, encoding plakoglobin, as the gene causing Naxos disease, a triad of ARVC/D, wooly hair and palmoplantar keratoderma. This syndrome takes its name from the Greek island of Naxos, where its prevalence exceeds 1 in 1000, despite autosomal recessive inheritance. While the cutaneous phenotype is expressed from infancy, cardiac symptoms are present from adolescence to the fourth decade of life (McKoy et al., 2000).

Later, in the same gene, a heterozygous three base pairs (bp) insertion (c.118_119insGCA) was identified by Asimaki et al. in a subject affected by a typical form of ARVC/D, without skin or hair abnormalities (Asimaki et al., 2007). This different phenotype is probably due to the dominant inheritance of the mutation.

Plakoglobin, an armadillo family member, is a key constituent of both desmosomes and adherens junctions (AJ), another intercellular junction in intercalated discs that provides strong cell-cell adhesion mediated by linkage of the cadherin-catenin complex to the actin cytoskeleton (Gumbiner, 2000). In desmosomes, plakoglobin bridges the cytoplasmic tail of desmosomal cadherins to intermediate filaments through desmoplakin binding, supporting the intercellular adhesion.

It has also been reported that plakoglobin, beyond its structural role in cellular junctions, is engaged in intracellular signal transduction (Garrod & Chidgey, 2008). Plakoglobin is known to interact and compete with beta-catenin at multiple cellular levels with a net negative effect on the canonical Wnt/beta-catenin signaling pathway through T cell/lymphoid-enhancing binding (Tcf/Lef) transcription factors (Zhurinsky, et al., 2000; Klymkowsky et al., 1999; Ben Ze'ev and Geiger, 1998). Inhibition or suppression of Wnt/beta-catenin signaling, characterized by low levels of beta-catenin, switches on adipogenesis and leads to proliferation of adipocytes (Ross et al., 2000). In contrast, upon Wnt/beta-catenin pathway activation, beta-catenin accumulates in the cytoplasm and enters the nucleus, where it acts as a transcription factor. As a consequence, myogenesis is enhanced, adipogenic transcription factors C/EBP-a and PPAR-gamma are inhibited, and preadipocytes are maintained in an undifferentiated state (Ross et al., 2000; Polesskaya et al., 2003; Chen et

al., 2005; Liu and Farmer, 2004). It has been demonstrated that mutations in desmosomal genes leading a compromised assembly of desmosome cause the transfer of plakoglobin into the nucleus, where it competes with beta-catenin, suppressing the Wnt/beta catenin pathway and stimulating the adipogenesis in the myocardium in ARVC/D patients (Garcia-Gras et al., 2006).

DSP

DSP, encoding desmoplakin, was the first gene associated to a classical form of ARVC/D. In 2002, Rampazzo and coworkers identified the heterozygous p.S299R missense mutation in a patient belonging to a large family (Rampazzo et al., 2002). This mutation is thought to disrupt a protein kinase C (PKC) phosphorylation site which is involved in plakoglobin binding and in clustering of desmosomal cadherin-plakoglobin complexes. Although the vast majority of DSP mutations are associated to classical-autosomal dominant forms of ARVC/D, few cases of recessive cardiomyopathy linked to skin and hair abnormalities have been reported. Autosomal recessive mutations are responsible of a cardiocutaneous syndrome, the Carvajal syndrome, described in families from India and Ecuador, consisting of plamoplantar keratoderma, wooly hair and dilated biventricular cardiomyopathy (Norgett et al., 2000). Some other dominant mutations in DSP gene have been linked to plamoplantar keratoderma, without cardiac involvement (Whittock et al., 1999, Armstrong et al., 1999).
In cardiac desmosomes, desmoplakin acts like a cellular linker between plakoglobin and plakophilin-2, and desmin cytoskeletal intermediate filaments, interacting through its N-terminal and C-terminal domains, respectively (Stappenbeck et al., 1993; Troyanovsky at al., 1994; Bornslaeger et al., 1996; Choi et al., 2002).

PKP2

The most frequently mutated gene identified so far in ARVC/D is PKP2, encoding plakophilin-2. In a study involving 120 unrelated probands, Gerull and co-workers detected 25 different heterozygous mutations, including insertions, deletions, nonsense, missense and splice site (Gerull et al., 2004). Also, a recessive mutation in PKP2 gene has been reported to cause ARVC/D, without skin and hair abnormalities (Awad et al., 2006).
As plakoglobin and beta-catenin, plakophilin-2 belongs to armadillo family. It is located in the outer dense plaque of desmosomes, where it links desmosomal cadherins to desmoplakin and the intermediate filament system. Plakophilin-2 has been also identified in the nucleus, where it may play a role in transcriptional regulation (Mertens et al, 2001). Gerull et al. speculated that lack of plakophilin-2 or incorporation of mutant plakophilin-2 in the cardiac desmosomes might impair cell-cell contacts and, as a consequence, might disrupt association between adjacent cardiomyocytes (Gerull et al., 2004).

DSG2

DSG2 encodes desmoglein2, one of the two desmosomal cadherins expressed in cardiac myocytes. Thanks to its five extracellular domains (EC1-5), it anchors desmosomal

cadherins of adjacent cells to plakoglobin and plakophilin-2, thus generating a cellular array, which binds to intermediate filaments.
In 2006, Pilichou and coworkers detected in DSG2 gene nine heterozygous mutations in 8 out of 50 (12%) unrelated ARVC/D probands. Among these, 5 were missense mutations, 2 were insertion-deletions, 1 was a nonsense and 1 was a splice site mutation; one patient had two different DSG2 mutations (compound heterozygote). Endomyocardial biopsy, obtained from 5 patients, showed extensive loss of myocytes with fibro-fatty tissue replacement. In 3 patients, electron microscopy showed intercalated disc paleness, decreased desmosome number, and intercellular gap widening (Pilichou et al., 2006).
Together with DSP and PKP2 genes, DSG2 is one of the genes the most frequently mutated in ARVC (Awad et al., 2008).

DSC2

Like DSG2, DSC2 encoding desmocollin-2, the other constituent of desmosomal cadherins, was considered an important candidate gene. Pathogenic mutations have been found in 2006 by Syrris and colleagues; later on, only other few mutations have been found in DSC2 gene (Syrris et al., 2006; Heuser et al., 2006; Beffagna et al., 2007). Beffagna et al. reported that two heterozygous mutations in the N-terminal domain of desmocollin-2 affect the correct cellular localization of the protein, as it is located into the cytoplasm instead of in the plasma membrane (Beffagna et al., 2007).
So far, mutations affecting desmosomal cadherins haven't been associated to skin and hair abnormalities. This can probably due to the absence of the cardiac isoforms (DSG2 and DSC2) in skin and hair, where other isoforms are expressed.

1.9.2 Non desmosomal genes

Less frequently, ARVC/D may be determined by mutations in non desmosomal genes, described hereinafter.

TGFβ3

TGFβ3 encodes a cytokine essential in cellular homeostasis and development. It is involved in the stimulation of expression of genes of cellular matrix and in the inhibition of other genes involved in the degradation of the extracellular matrix, thus stimulating fibrosis in several tissues (Leask et al., 2004; Varga et al., 1986; Overall et al., 1989). Moreover, TGFβ3 belongs to TGFβ family, whose members seem to be involved in the regulation of expression of desmosomal genes in different cells.
In 2005, two mutations in 5' and 3' UTR of TGFβ3 gene have been found in a large family with recurrence of ARVC/D and in a subject with family history of SCD (Beffagna et al., 2005). The authors reported that these mutations induce in vitro an overexpression of TGFβ3 and thus an overproduction of fibrous tissue in the heart that could induce arrhythmias. Moreover, it is known that proteins of TGFβ3 family could influence the

expression of JUP gene (Ota et al., 2002); hence, mutations in TGFβ3 gene could affect also the stability of intercellular junctions and provoke ARVC/D.

RYR2

Mutations affecting RYR2 gene are responsible of a form of ARVC/D characterized by ventricular polymorphic arrhythmias, induced by effort (Tiso et al., 2001). RYR2 mutations have been identified as well in patients affected with Catecholaminergic Polymorphic Ventricular Tachycardia (CPVT) (Priori et al., 2001).

RYR2 encodes the ryanodynic cardiac receptor, a calcium channel localized in the membrane of the sarcoplasmic reticulum of myocardium. RYR2 is essential for calcium intracellular homeostasis and thus for the excitation-contraction coupling in the cardiac muscle (Stokes and Wagenknecht, 2000; Missiaen et al., 2000). Mutations in RYR2 gene are most frequently localized in three specific regions and involve highly conserved amino acids. Functional studies in vitro demonstrated that these mutations induce an increased channel activity and, as a consequence, a raising of intracellular calcium concentration (George et al., 2003).

TMEM43

In 2008, Merner and colleagues identified the missense substitution p.S358L in TMEM43 gene, correlated to a lethal form of ARVC/D inherited with complete penetrance and sex related (Merner et al., 2008). Later, Christensen and co-workers identified a mutation in the same gene, associated with a classical ARVC/D phenotype (Christensen et al., 2011). Immunohistochemistry experiments revealed that patients carrying mutations in TMEM43 gene showed a reduction of immunoreactive signal levels both for TMEM43 and plakoglobin, while signal levels for plakophilin-2 and connexin-43 (a gap junction protein) were comparable to wild-type (Christensen et al., 2011).

Up to now, the role of the genic product of TMEM43, transmembrane protein 43, hasn't been clarified yet. It is hypotesized that it could be a transription factor involved in the adipogenic pathway, as it possesses a sequence recognized by the transcription factor PPAR-gamma. It has been speculated that a deregulation of this pathway can induce the fibro-fatty substitution in the myocardium in ARVC/D patients (Merner et al., 2008). More recently, it has been proposed that TMEM43 encodes for LUMA, a nuclear membrane protein that binds emerin and lamin, involved in the organization of nuclear membrane (Bengtsson and Otto, 2008).

DES

In 2010, Klauke et al identified p.N116S missense mutation in DES gene in a patient with ARVC/D and terminal heart failure (Klauke et al., 2010). DES encodes desmin, a cytoskeletal filament protein located in the myocardial z- and intercalated disc and connected to the desomosomal plaque proteins via desmoplakin, thus supporting the resistance to mechanical stress of cardiomyocytes (Lapouge et al., 2006). Mutations in DES gene are

often involved in skeletal abnormalities. The proband carrying p.N116S mutation thus was also examined for skeletal muscle disease and he showed complaining of exercise-induced muscle pain, fatigability and weakness when walking uphill or climbing stairs. Moreover, neurological examination at the age of 20 revealed only a slight proximal weakness of the lower extremities and that her standing up from a squatting position was slowed (Klauke et al., 2010). In a previous study, Van Tintelen and colleagues identified p.S13F variant in DES gene in patients with an ARVC/D-like phenotype (Van Tintelen et al., 2009).

TTN

Titin, after myosin and actin, is the third most abundant protein of striated muscle and connects the Z-line to the M-line in the sarcomere (Granzier and Labeit). In the sarcomeric I-band region, titin is extendible and acts as a molecular spring that develops the force that determines the passive stiffness in cariomyocytes (Granzier and Irving., 1995; Labeit et al., 1997; Wu et al., 2000).

Very recently, Taylor and coworkers identified in TTN gene the p.T2896I missense variant segregating in an ARVC/D family in a candidate-gene approach study (Taylor at al., 2011). Functional experiments performed in this mutated protein revealed that p.T2896I-titin shows a reduced electrophoretic mobility and that it is likely to adopt an unfolded state. Moreover, incubation with protease trypsin resulted to cause more a prominent proteolysis of the mutated protein, if compared to the wild type. The authors speculated that titin mutations found in subjects affected by ARVC/D may induce titin degradation, consequently initiating the pathological process that eventually leads to the disease (Taylor et al., 2011).

1.10 MUTATION FREQUENCY IN DESMOSOMAL GENES

Genetic screening of desmosomal genes in a wide population of ARVC/D patients, performed in different laboratories worldwide, allowed to define the mutational spectrum of the disease-genes (Table 4).

The percentage of mutation carriers is related to the geographic area of investigated probands, but the mutational trend is almost conserved among different populations. In every case, the most frequently mutated genes in ARVC/D are the so-called “the three big genes”: PKP2, DSP, and DSG2, with frequencies spanning from 7% to 45%, 1% to 16%, and 0% to 12%, respectively (Gerull et al., 2004; Van Tintelen et al., 2006; Pilichou et al., 2006; Dalal et al., 2006; Syrris et al., 2007; Awad et al., 2006; Heuser et al., 2006; Yang et al., 2006; Lahtinen et al., 2008; Christensen et al., 2010; Bhuiyan et al., 2009; Den Haan et al., 2009; Bauce et al., 2010; Fressart et al., 2010). Only few mutations have been reported so far in DSC2 and JUP genes (Syrris et al., 2006; Heuser et al., 2006; Asimaki et al., 2007; Ly et al., 2008; Den Haan et al., 2009; Bhuiyan et al., 2009; Bauce et al., 2010; Fressart et al., 2010; Xu et al., 2010, De Bortoli et al., 2010).

Population	PKP2	DSP	DSG2	DSC2	JUP	% probands carrying mutations in desmosomal genes	References
Germany	27%			1%			Gerull et al., 2004; Heuser et al., 2006
Holland	43%; 40%		7%	1%			Van Tintelen et al., 2006; Bhuiyan et al., 2009
Denmark	15%						Christensen et al., 2010
Finland	10%						Lahtinen et al., 2008
Italy	14%; 7%	16%; 5%	10%, 9.5%	1.5%, 5%	0%	43%	Pilichou et al., 2006; Bauce et al., 2010
UK			10.45%		5%		Syrris et al., 2007; Syrris et al., 2006
France	31%	4.5%	10%	1.5%		46%	Fressart et al., 2010
USA		6%	12%				Yang et al., 2006; Awad et al., 2006
North USA	45%; 43%	1%	9%	0%	1%	52%	Den Haan et al., 2009; Dalal et al., 2006

Tab. 4: Trend of desmosomal genes mutation carriers in different populations.

In probands from the Northern America and from Holland there's the highest percentage of mutations in PKP2 gene (40%-45%) (Bhuiyan et al., 2009; Den Haan et al., 2009; Van Tintelen et al., 2006; Dalal et al., 2006). Despite the inheritance of a common haplotype found in Dutch patients carrying the same PKP2 mutations, that suggests a founder effect, analysis performed in larger and more heterogeneous populations in North America and Western Europe confirmed the inheritance of identical mutations in patients carrying a different haplotype (Van Tintelen et al., 2006; Dalal et al., 2006; Gerull et al., 2004). In these cases, the recurrent mutations may be explained by mutational hot spots in PKP2 gene, or simply by selection bias.

Data published independently from different research groups indicate that comprehensive exonic sequence analysis of the known desmosomal genes involved in ARVD/C currently identifies a responsible mutation in approximately 50% of ARVD/C probands (Den Haan et al., 2009, Fressart et al., 2010; Bauce et al., 2010) (Table 4). This redundancy suggests that ARVC/D could be characterized by further genetic heterogeneity. Two main different approaches can be held to identify novel disease genes: the genome wide scan and the candidate gene approach, in which on the basis of function, tissue, molecular partners, and cellular expression, a gene is supposed to be involved in the disease.

1.11 DESMOSOMAL ABNORMALITIES AND PATHOPHYSIOLOGICAL MECHANISMS

Since mutations causing ARVC/D have been identified so far in five genes encoding desmosomal proteins, this cardiomyopathy has been considered as “a disease of the desmosome”.

Desmosomes are adhesive, multiprotein, symmetric disk-shaped intercellular junctions. They are composed of three protein families: transmembraneous proteins (cadherins): desmogleins and desmocollins; linker-proteins (armadillo): plakoglobin and plakophilin; and plakins: desmoplakin and plectin (Garrod and Chidgey, 2008) (Figure 8).

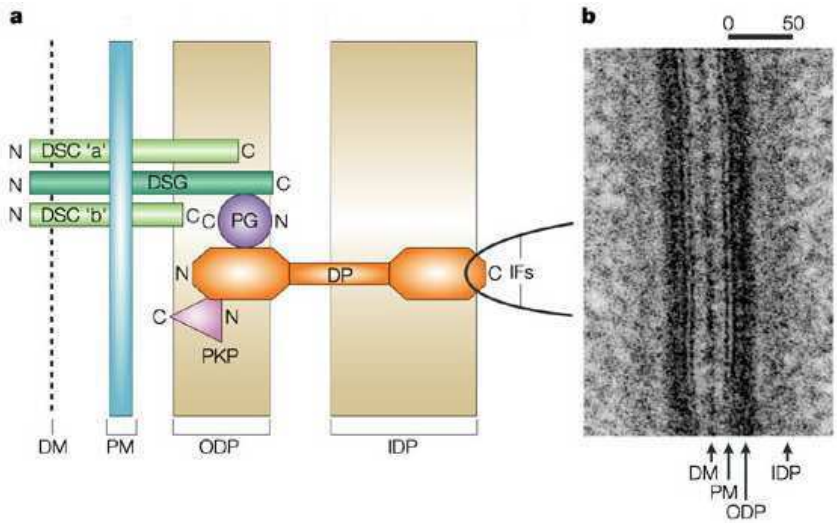

Fig.8: Schematic representation of a desmosome showing the locations of the five major proteins. (*A*) Schematic representation of desmosomal proteins and relative distance from the plasma membrane. IF=intermediate filaments; IDP=inner dense plaque; ODP=outer dense plaque; DM= dense midline; PM=plasma membrane; DP=desmoplakin ; PG=plakoglobin ; PKP=plakophilin; DSC= desmocollin; DSG= desmoglein. (*B*) Electron micrograph of a desmosome. (adapted from Getsios et al., 2004).

Following the proposed model, in the cardiac desmosomes, within the “outer dense plaque” (ODP), extracellular domains of desmoglein-2 and desmocollin-2 interact with extracellular domains of other desmosomal cadherins of adjacent cells, while in the “inner dense plaque” (IDP), desmoplakin interacts with plakophilin-2 and plakoglobin, through its N-terminal domain, and with desmin intermediate filaments through its C-terminal domain (Garrod et al., 2002; Green and Simpson, 2007) (Figure 8). It has been speculated that ARVC/D could be caused by structural abnormalities of desmosomes. Mutations affecting a desmosomal protein could cause the joining in the structure of the aberrant element, or the insufficient incorporation of a wild-type protein in a dimer, in the case of haploinsufficiency. As a consequence, these events could eliminate essential protein-protein interactions, or alter the correct assembly of other elements in the cellular junction, leading to a disturbed formation or reduced numbers of functional desmosomes (Kostetskii et al., 2005). Microscopic investigations on endomyocardial biopsies in mutation carriers with ARVC/D revealed intercalated disc remodeling and desmosomal abnormalities. This is exemplified by studies of Basso and colleagues, which showed decreased desmosome numbers, increased desmosome lengths, and widened gap junctions in myocardial tissue of mutation carriers

(Basso et al., 2006) (Figure 9). Mechanical stress can induce the flanking of the aberrant desmosomes, resulting in detachment of cardiomyocytes and in fibro-fatty replacement (Kostetskii et al., 2005).

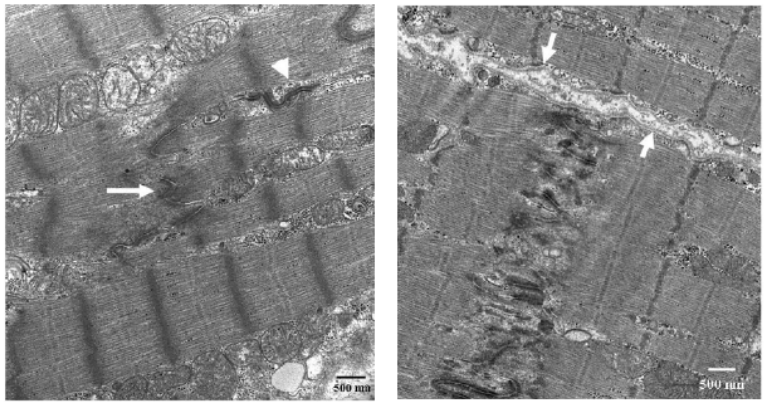

Fig.9: Panoramic view of intercalated discs in cardiomyocytes. (Left) ARVC/D patient with DSP gene splice site mutation. The abnormal position of long desmosomes (arrowhead) and the widened gap of fascia aherens (arrow) are evidenced. (Right) Control sample. Regular membrane (arrows) and intercalated disc between adjacent cardiomyocytes. Original magnification: x15 000 (Basso et al., 2006).

Moreover, it has also been postulated that the development of the disease could depend not only on primary abnormalities of the desmosome, but also on the strong association between desmosomes, gap junctions, and adherens junctions (Delmar and McKenna, 2010). Indeed, it has been described a thick crosstalk among these three cellular junctions resulting in integrity of the ICD and in both mechanical and electrical cellular stability, dependent on correct functioning of all three subunits (Delmar 2004).

More recently, in the last years the concept of a final common pathway of genetically determined cardiomyopathies has been proposed. Immunohistochemical investigations performed on intercellular junctions by Asimaki and colleagues showed that in nearly every case of ARVC/D, the signal of plakoglobin diminished at ICD and seemed to be specific for the disease (Asimaki et al., 2011) (Figure 10).

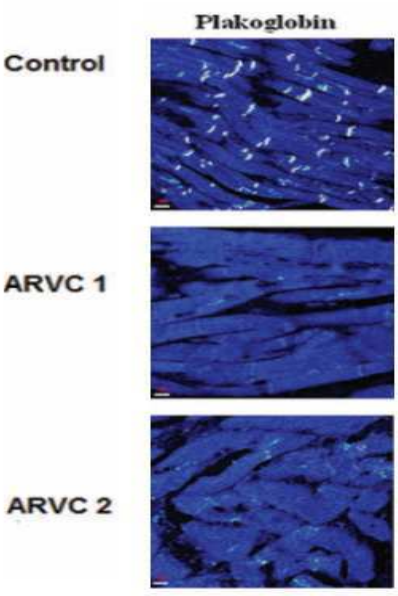

Fig.10: Plakoglobin immunofluorescence signal in myocardium of two examples of autosomal dominant ARVC/D and in a control. Signal for plakoglobin at ICD is reduced in both cases of ARVC, compared to control (adapted from Asimaki and Saffitz., 2011).

Considering these results, the investigators suggested that the analysis of the localization of desmosomal proteins by immunohistochemical assays on endomiocardial biopsy samples represent a promising test for ARVC/D diagnosis. However, more recently, Munkholm and co-workers performed this immunohistochemical analysis in myocardial biopsies with fibrofatty replacement from 50 patients. Following evaluation revealed that this diagnostic test has a sensivity of 85% and a specificity of 57%, suggesting that this approach should be considered with caution in ARVC/D clinical evaluation (Munkholm et al., 2011).

Beyond structural abnormalities, it has been speculated that the pathogenesis of the disease could be linked to interference on signaling pathways. Desmosome components are involved in intercellular signaling networks via the Wnt/β-catenin pathway (Getsios et al., 2004). Wnt signaling is concerned in cell proliferation and differentiation, and in the development of tissues and organs. As demonstrated by several studies, aberrations in desmosomes result in detachment and nuclear translocation of plakoglobin. Due to its high similarity to beta-catenin, plakoglobin competes with this protein for the regulation of the Wnt/bcatenin signaling, causing its inhibition and finally the shift of cardiomyocytes to adipocytes (Klymkowsky et al., 1999; Garcia-Gras et al., 2006).

On the other hand, effects of desmosomal mutations on biochemical behavior may depend on how a specific mutation affects the binding and the localization of other junctional proteins. It has been demonstrated through studies in HEK cells engineered to express mutant forms of plakoglobin that phenotype in terms on strength of cell-cell adhesion depended on the expressed mutation (Huang et al., 2008). Thus the model of aberrations in desmosomes induced by stress and causing abnormal cellular signaling resulting in fibro-fatty substitution is an appealing but largely speculative hypothesis.

1.12 ANIMAL MODELS FOR ARVC/D

1.12.1 Spontaneous models

ARVC/D is a disease that affects also animals. Several cases have been reported in the literature, regarding affected dogs and cats that show a phenotype mimicking human ARVC/D. In 1983, the first reported canine model of the disease concerned Boxer dogs showing fatty or fibro-fatty replacement of the right ventricular myocardium (Harpster et al., 1983). Despite the different breeds, affected dogs showed common aspects of human ARVC/D, including fatty or fibro-fatty replacement of the myocardium in the RV, right ventricular chamber enlargement and aneurysm, left ventricular involvement, and conduction aberrations such as monomorphic VT with LBBB morphology, syncope, and SCD. In some cases, also myocarditis and apoptosis were also reported (Santilli et al., 2009; Elliott et al., 2008; Basso et al., 2004; Fernández del Palacio et al., 2001; Möhr et al., 2000; Simpson et al., 1994).

Moreover, in a study conducted by Basso and colleagues in 23 canine cases, several among the affected Boxer dogs investigated were related, suggesting that also canine ARVC/D is an inherited disease (Basso et al., 2004).

Also affected cats recapitulate the human phenotype. Indeed, typical feline ARVC/D features are arrhythmias, including VT and atrial fibrillation; right atrial and ventricular dilation, and thin, hypokinetic right ventricular wall segments with aneurysm, especially those localized in the apical and subtricuspid regions (Fox et al., 2000; Harvey 2005; Ciaramella et al., 2009). Moreover, also fibro-fatty replacement of right ventricular myocardium, left ventricular involvement, and inflammatory infiltrates have been reported (Fox et al., 2000).
Spontaneous models of ARVC/D are remarkably similar to that condition in human patients with respect to both clinical and pathological features. Consequently, these animals would provide an useful tool to investigate this disease and contribute valuable insights into its complex clinical and pathogenic mechanisms.

1.12.2 Genetically-engineered models

In the last two decades, animal models have been generated to recapitulate important aspects of ARVC/D phenotype and to study the molecular pathogenesis of the disease. Genes the most frequently studied are those encoding desmosomal proteins, above all through mouse models generation; however, in addition, using morpholino, in some cases embryonic studies on zebrafish have been performed to evaluate the effects of gene inhibition on morphogenesis.

a.DSP mouse models

Mice DSP-/- carrying a cardiac-restricted exon 2 deletion in DSP generated by Garcia-Gras and co-workers are characterized by high rate of lethality at embryonic stage E10-E12 (Garcia-Gras et al., 2006). This result recapitulated the phenotype of knockout DSP mouse model (DSP-/-) generated by Gallicano and co-workers (Gallicano et al., 2001; 1998). Histopathologic evaluation evidenced formed hearts with no chamber specification and unorganized cardiac myocytes. Furthermore, an excess number of cells resembling adipocytes, dispersed between myocytes and localized to adjacent areas, were also detected. On the contrary, heterozygous mice DSP+/- developed normally during embryonic life, but recapitulated human ARVC/D phenotype, as it manifested excess adipocytes and fibrosis in the myocardium, increased myocyte apoptosis, cardiac dysfunction, ventricular arrhythmias, and 20% incidence of premature death (Garcia-Gras et al., 2006). Moreover, the authors demonstrated that in DSP-deficient mice plakoglobin released from desmosomes and accumulated into the nucleus. Accordingly, the authors showed that expression of genes targeted by Wnt/Beta-catenin pathway was reduced, while the expression of adipogenic genes (normally at low levels) was increased. Similarly, apoptosis was increased. On the basis of these results, the authors proposed that the suppression of DSP caused the detachment of plakoglobin from the desmosomes and its accumulation in the nucleus. As a consequence, the negative regulation of Wnt/Beta-catenin pathway lead to adipogenesis, fibrogenesis and myocyte apoptosis, typical ARVC/D features. Most recently, by analyzing mouse and human hearts, the same group speculated that adipogenesis in ARVC/D, derived by the suppression of Wnt/Beta-catenin pathway, interested the second

heart field progenitor cells. These data could explain the predominant involvement of the RV in the disease (Lombardi et al., 2009).

In another study of 2006, Yang and colleagues showed that cardiac-specific overexpression of p.V30M or p.Q90R mutant desmoplakin in transgenic mice caused embryonic lethality (Yang et al., 2006). On the contrary, overexpression in mice of the cardiac-restricted C-terminal DSP p.R2834H mutation resulted in viable mice, but lead to reduced biventricular function, lipid accumulation, increased apoptosis and fibrosis, and aberrant desmin filaments localization at ICD. A consequence of the impairment of the interaction between desmoplakin and desmin may be the desmosomal instability together with the aberrant localization of other junctional proteins, included gap junctions' molecules, and compromised resistance to mechanical stress (Yang et al., 2006).

Taken together, these results underline the role of desmoplakin in mantaining desmosomal stability and thus heart tissue integrity.

b.PKP2 mouse models

In 2004, Grossman and colleagues generated a PKP2 knock-out mouse. The nonviable embryos showed disarrayed cytoskeleton, reduced trabeculations within the ventricles, atrial wall thinning, cardiac wall rupture, blood leakage into the pericardium and death at midgestation (E10.5 to E11). Moreover, the loss of plakophilin-2 lead the aberrant desmoplakin localization into the cytoplasm, and the reduction of desmoglein-2 levels. On the contrary, embryonic epithelia showed normal junctions. These data indicate that plakophilin-2 is essential for the correct association of the junctional proteins and for the cardiac architecture (Grossman et al., 2004).

c.JUP mouse models

The first knock-out JUP mouse models were created independently in 1996 by Ruiz's and Bierkamp's groups and showed contradictory findings. Ruiz's mouse, obtained by homologous recombination in embryonic stem cells, showed absence of desmosomes, replaced by extended adherens junctions containing desmosomal proteins such as desmoplakin, but have impaired architectural stability and function. Due to defects in cardiac stability, structure, and function, the JUP null mouse experienced embryonic lethality between 12 and 16 days of development, while heterozygous mutants (JUP+/-) and WT animals were born and showed normal development (Ruiz et al., 1996). Also Bierkamp's mouse showed embrionic lethality (E10.5) due to severe heart defects. Anyway, in some cases, development proceeded longer, but not over the birth because of cardiac alterations, skin blistering and subcorneal acantholyisis. Moreover, in this mouse, both in skin and heart, desmosomes were structurally altered and reduced in number (Bierkamp et al., 1999; Bierkamp et al., 1996). Despite the few differences between these two models, data obtained demonstrated the importance of plakoglobin in desmosome assembly and function. Later, other JUP mouse models were studied. On the contrary to what reported by null JUP mice studies, heterozygous JUP-deficient mouse (JUP+/-) at birth was comparable to wild

type, but showed dysfunction and RV dilatation and ventricular arrhythmia at 6 months of age. Moreover, in this model no fibrofatty substitution, nor structural desmosomal changes have been detected (Kirchhof et al., 2006).

Very recently, Li and colleagues generated a cardiac restricted JUP knock out mouse (Li et al., 2011). Phenotype in this mouse recapitulated the clinical manifestation of human ARVC/D: fibrofatty replacement, ventricular dilation and aneurysm, cardiac dysfunction and ventricular arrhythmias. Structurally, adherens and gap junctions were preserved, but desmosomes were absent. Moreover, even if β-catenin at adherens junctions was augmented, the Wnt/β-catenin mediated signaling was not altered. On the contrary, TGFβ mediated signaling was increased in the cardiomyocytes of this mouse at the early stage of cardiomyopathy. The authors speculated that the latter pathway could be involved in pathogenesis of JUP-related ARVC/D.

Radice and colleagues produced an inducible cardiorestricted JUP knockout mouse showing progressive loss of myocytes, inflammatory infiltration, fibrous replacement, and cardiac dysfunctions comparable to those observed in ARVC/D patients. Moreover, ultrastructure of desmosomes in the heart was altered, due to a decrease in desmosomal proteins in ICD; alteration in gap junction was observed as well. The authors investigated the antagonistic role of JUP in beta-catenin/Wnt signaling resulting in increased β-catenin/Tcf transcriptional activity, which may contribute to ARVC pathogenesis (Li et al., 2011).

d.Morpholino-induced knockdown of JUP expression on zebrafish

In 2009, Martin and colleagues generated a zebrafish model with reduced Jup expression showing small hearts, edema and valvular dysfunction leading to intrachamber reflux. Moreover, morphants exhibited reduced number of desmosomes and AJs in ICD (Martin et al., 2009).

e.DSG-2 mouse models

The first mouse model for DSG2 was studied in 2002 by Eshkind and colleagues (Eshkind et al., 2002). As seen in the models described above, DSG2-/- mouse showed embryonic lethality (E3.5 to E5.5). Even if blastocysts DSG2-/- apparently grew normally, immunofluorescence showed that, in these cells, expression levels of desmosomal proteins, such as desmoplakin and plakophilin-2, were highly decreased, suggesting that alterations in a gene encoding a given desmosomal protein could negatively affect the expression of other proteins.

More recently, Pilichou et al., developed a transgenic mouse overexpressing the mouse homologue of the human mutation p.N266S (Pilichou et al., 2009). The mouse model didn't manifest embryonic lethality; 30% of mice died by 3.6 weeks and only 20% survived by 20 weeks. Also, this mouse manifested a phenotype close to human ARVC/D: biventricular cardiomyopathy, aneurysms, ventricular arrhythmias, and sudden death. Histologically, the hearts of 2 weeks of age mice showed pronounced myocardial damage, thinning, aneurysms and chamber dilatation in both ventricles at later stages.

Finally, the homozygous DSG2 mutant mouse lacking two extracellular domains (DSG2 $^{mt/mt}$) generated by Krusche and coworkers, showed myocardial fibrosis and calcification (Krusche et al., 2011). These data demonstrate that desmoglein-2 is important in embryonic viability and that mutations affecting DSG2 gene may be causative of ARVC/D.

f.Morpholino-induced knockdown of DSC2 expression on zebrafish

Hearts of dsc2 morphants generated by Heuser and coworkers showed edema, bradycardia, and reduced desmosomal areas and contractility. Co-injection of wild-type human *DSC2* mRNA rescued the morphant phenotype, thus indicating desmocollin-2 as a protein essential for the desmosomal function (Heuser at al., 2006).

g.DES mouse model

DES mutations are associated to desmin-related myopathies (DRM) (Olivé et al., 2004; Dalakas et al., 2000). This group of disorders is characterized by abnormal intrasarcoplasmic misfolded desmin accumulation and by the production of soluble pre-amyloid oligomers, which lead to weakened cardiac, or cardiac and skeletal, muscle (Abraham et al.,1998). Cardiac manifestation usually include conduction blocks, often requiring pacemaker insertion, and cardiomyocyte death (Goldfarb and Dalakas, 2009). DES animal models obtained up to now recapitulate phenotypes evidenced in clinical cases of DRM, but they are pretty far from ARVC/D features. A transgenic mouse carrying a 7-amino acid deletion (R173 through E179) desmin showed aberrant desmin intrasarcoplasmic aggregates, characteristic of human DRM. Also, intermediate filament network was significantly disrupted and myofibril alignment was abnormal. Clinically, even if systolic function was preserved, the heart showed reduced ability to respond to beta-agonistic stimulation (Wang et al., 2001).

Moreover, desmin null mice showed dilated cardiomyopathy occurring with extensive cardiomyocyte death, fibrosis, and heart failure. Analysis of mitochondrial proteome in desmin wild-type and null mice showed differences in apoptosis, calcium homeostasis, fibrosis, and in different signaling pathways. Some of these changes are comparable with desminopathies phenotype (Fountoulakis et al., 2005), but none recapitulated ARVC/D.

Also the transgenic mouse expressing low levels of p.L345P-desmin showed mitochondrial abberrancies, such as swelling and vacuolization. In these mice, mitochondrial calcium levels was significantly increased both in skeletal and in cardiomyocytes respect to wild-type, during and after contractions. At cardiac level, mice showed left ventricular wall hypertrophy and a reduction in left ventricular chamber dimension (Kostareva et al., 2008). Taken together, these data suggest that mutations in DES gene resulting in the absence or in aberrations of desmin in cardiomyocytes lead to abnormal mitochondrial behaviour and fuction, thus probably inducing heart failure.

h.TTN mouse model

In 2003, Gotthardt and co-workers used a conditional knock-out approach to selectively delete the exons encoding a kinase-like region in TTN gene in skeletal and in heart. Exons

were deleted in different stages in embryonic development: mice died *in utero,* if excision occurred in early embryonic stages, or at 5 weeks of age, due to progressive myopathy, in the case of a late embryonic deletion. Ultrastructural analysis showed a quick disassembly of sarcomere, when mutant titins were incorporated. (Gotthardt et al., 2003). These results indicate an important role of titin in cardiac development and in mantaining sarcomere structural integrity.

Using homologous recombination, a knock-out mouse lacking in TTN gene only the N2B exon 49, and a knock-out mouse lacking exons 219-225 encoding PEVK domain specific of cardiac titin, were generated (Radke et al., 2007; Granzier et al., 2009). In both cases, animals survived to adulthood and were fertile but they showed diastolic dysfunction, reduced sarcomere length and increased passive tension. However, probably due to differential binding to specific molecular partners, N2B knock-out mice showed atrophy, whereas PEVK knock-out mice showed hypertophy (Granzier et al., 2009). Anyway, again, these models underline the key role of titin in cardiac growth and in sarcomere integrity.

Moreover, TTN is a gene involved also in dilated cardiomyopathy (DCM). Knock-in mice mimicking the c.43628insAT insertion found in DCM showed embryonic lethality at E9.5 due to defects in sarcomere formation, while heterozygous mouse was viable and showed normal heart structure and function. Even if at resting conditions heterozygous mouse showed high levels of wild-type protein (suggesting that a compensation mechanism occurred), when chronically exposed to angiotensin II or isoproterenol, this mouse developed marked left ventricular dilatation and diffuse myocardial fibrosis, thus mimicking human DCM features (Gramlich et al., 2009).

i.RYR2 mouse model

p.R176Q mutation in RYR2 gene was considered in a study performed by Kannankeril et al. in 2006. This variation recurred in a family with effort-induced polymorphic VT and mild ARVC/D. Knock-in $RYR2^{R176Q}/+$ and wt mice showed no fibrofatty infiltration, nor evidence of structural abnormalities. This model appeared more consistent with a CPVT phenotype than that of a classic form of ARVC/D (Kannankeril et al., 2006).

Taken together, these animal models support the concept of ARVC/D as a desmosomal disease (Vatta et al., 2007). It would be interesting to concentrate efforts on animal models to understand the pathogenic mechanisms that lead to the development of the different features of the disease, such as fibro-fatty replacement and arrhythmias.

2. AIM OF THE STUDY

Arrhythmogenic right ventricular cardiomyopathy/dysplasia is a clinical and genetic heterogenous disease inherited as an autosomal dominant trait with incomplete penetrance and variable expressivity. Histopathologically, it is characterized by the progressive fatty or fibro-fatty replacement in the myocardium, primarily occurring in the right ventricle. Clinically, the main features are arrhythmias and sudden death, often manifesting as the first sign of the disease. Early clinical diagnosis together with the detection of susceptible genotypes by DNA analysis is a crucial tool to prevent sudden cardiac death in patients and then in their relatives. Up to now, ten genes are known to be involved in this disease and, since the majority of pathogenic mutations in affected subjects have been detected in genes encoding desmosomal proteins, ARVC/D has been defined a “desmosomal disease”.

The aim of the present study was to perform a comprehensive mutation screening in desmosomal genes in a cohort of affected subjects. Genetic screening is considered a valid tool in confirmation of the diagnosis in borderline subjects or in probands with a clinical suspicion of the disease. Moreover, it allows the identification of asymptomatic genetically-affected relatives that could undergo pointed clinical management and modify their lifestyle.

However, up to now, several data underlined that in a significant number of ARVC/D patients (about 50%) no pathogenic mutation has been detected, suggesting that additional genes could be involved in this cardiomyopathy. Two main approaches could be employed to identify novel disease-genes: genome-wide linkage analysis and candidate gene approach, that have specific advantages and disadvantages. Linkage studies should be performed in large families showing recurrence of the disease in several generations, whereas candidate gene approach is limited by its reliance on existing knowledge about the known pathophysiology of the phenotype under investigation.

CTNNA3 was considered in our lab a good candidate gene for ARVC/D because its product, alphaT-catenin, specifically interacts with the desmosomal protein plakophilin-2 in the *area composita*, a recently identified mixed junction composed by both desmosomal and adherens junction’s elements, existing exclusively in cardiac intercalated discs. Therefore, in this study, mutation screening in CTNNA3 gene was performed in ARVC/D probands, negative for mutations in desmosomal genes. Moreover, functional studies were accomplished to test the pathogenic potential of detected exonic mutations: proteins’ cellular localization was checked by cardiomyocytes transfection and immunofluorescence experiments, while proteins’ interaction with several molecular partners was studied by the yeast two-hybrid assay.

Discovering additional disease-genes should enable mutation identification in an increasing number of affected subjects, thus preventing more extensively sudden death.

3. MATERIALS AND METHODS

3.1 CLINICAL EVALUATION

The study involved a cohort of 80 unrelated patients of Italian descent, for desmosomal genes screening, and a cohort of 76 unrelated patients of Italian descent, for CTNNA3 gene screening, in which a clinical diagnosis of ARVC/D was made on the basis of major and minor criteria established by the European Society of Cardiology/International Society and Federation of Cardiology Task Force (Marcus et al., 2010). After written informed consent, blood for DNA extraction was obtained from all participating individuals, according to the pertinent Italian legislation and in compliance with Helsinki declaration. Clinical evaluation consisted of a detailed personal/family history, physical examination, 12-lead electrocardiogram (ECG), signal-averaged ECG (SAECG), 24-hour Holter ECG, and 2-dimensional echocardiography (2D-echo).

3.2 GENETIC STUDY PROTOCOLS

3.2.1 Mutation screening

DNA for genetic analysis was isolated from peripheral blood samples according to the salting out procedure. Mutation screening was performed by denaturing high performance/pressure liquid chromatography (dHPLC) and direct sequencing in 80 probands (54 males mean age 44±16) for PKP2, DSP, DSG2, DSC2, and JUP genes and in 76 Italian probands (52 males, mean age 42±12), negative for mutations in desmosomal genes, for CTNNA3 gene. Polymerase chain reaction (PCR) primers were designed by PRIMER3 software to give amplicons including all coding sequences and 50-150 base pairs (bp) of flanking intronic sequences. The longest exons were split into different and overlapping fragments, while in some cases, short adjacent exons were unified in a single amplicon. A control group of 250 healthy and unrelated subjects (500 alleles) from the Italian population was used to exclude (through dHPLC analysis, or direct sequencing) that detected mutations could be common DNA polymorphisms. All the controls were matched to the probands by ancestry.

Mutation screening was performed in all available family members of index cases in which a pathogenic mutation was detected.

All considered cDNA and translation sequences for screened genes are available in NCBI website; the ID numbers are reported below (Table 5).

Human gene	cDNA sequence ID	translation sequence ID
PKP2	NM_001005242	NP_001005242
DSP	NM_004415	NP_004406
DSG2	BC099657	NP_001934
DSC2	NM_004949	NP_004940
JUP	NM_002230	NP_002221
CTNNA3	NM_013266	NP_037398

Tab. 5. ID numbers of considered cDNA and translation sequences for investigated genes.

3.2.2 Sample retrieval and DNA extraction from blood

DNA was extracted from blood samples stored at -20°C in EDTA vacutainer tubes with the salting out procedure, designed by Miller et al., 1998, and modified by Dr. M. Rosa, Human Genetic Laboratory of University of Padua.

To facilitate haemolysis of Red Blood Cells, fresh samples were stored for a few hours in a freezer. N-N solution (NaCl 0,9%, Nonidet 0,1%) was added to the blood, already thawed and transferred into a Falcon tube, to a final volume of 40 mL. After two sample centrifugations for 35 minutes at 6000 rpm at 4°C, pellets were resuspended in 4 mL of TEN solution (TrisHCl 10mM; EDTA 2mM, pH 8; NaCl 400 mM) and well vortexed. Then, 300 μL of SDS 20% detergent were added and the mixture was incubated at 80°C for three hours under vigorous mixing, to denature cellular proteins.

1 mL of saturate NaCl was added to the mixture to induce protein precipitation and, after tubes spinning for 10 minutes at 6000 rpm at room temperature, supernatant was poured off into a fresh tube. An isovolume of chloroform was added and the samples were inverted for 10-15 times to be centrifuged for 10 minutes at 6000 rpm at room temperature, thus obtaining three different phases: the upper containing nucleic acids, the second composed of proteins and cellular debris, and the third, consisting of chloroform. The upper phase was transferred into a fresh tube and an equal volume of isopropanol was added: DNA was precipitated by gentle swirling of the tube and observed visually as a white thread. Samples were then centrifuged for 10 minutes at 6000 rpm at room temperature; the pellet was washed twice with 2 mL of 70% ethanol, centrifuged for 10 minutes at 6000 rpm at room temperature and dried from excess of ethanol. Finally, after resuspension of the pellet in 300-500 μL TE buffer, DNA concentration was checked on spectrophotometer.

3.2.3 DNA quantification

a. Spectrophotometric quantification of DNA

The measurement of DNA concentration was made using NanoDrop ND-1000 Spectrophotometer (CELBIO). It is a full-spectrum (220-750 nm) spectrophotometer that can measure 1 μL samples with high accuracy and reproducibility. This spectrophotometer uses a patented sample retention technology employing surface tension alone to hold the sample in place. This eliminates the use of clumsy cuvettes or other devices for sample containment and allows for clean up within seconds. Moreover, this instrument can measure highly concentrated samples without dilution. Thanks to the use of a specific pc software, samples concentrations are obtained directly in ng/μL. Samples readings at 260 nm and at 280 nm provide directly DNA and proteins concentration in the sample, respectively. Absorbances ratio calculated at 260 nm and at 280 nm gives the purity index: pure DNA preparations have ratio values between 1.8 and 2.0. A ratio inferior than 1.8 indicates that there may be proteins and/or ultraviolet (UV) absorbers in the sample, thus it is commendable to reprecipitate the DNA. A ratio higher than 2.0 indicates that samples may be contaminated with chloroform or phenol and should be reprecipitated with ethanol.

After concentration measurement by NanoDrop, DNA was finally diluted in sterile bidistilled water to a final concentration of 50 ng/µL, to perform polymerase chain reaction (PCR).

b. DNA quantification through agarose gel electrophoresis

The electrophoresis is a technique that allows to separate different molecules on the basis of their molecular weight and charge, given an electric field. Nucleic acid molecules, negatively charged, move from the anode to the cathode through an agarose matrix. Shorter molecules move faster and migrate farther than longer ones because shorter molecules migrate more easily through the pores of the gel. Adding ethidium bromide to the agarose, it is possible to visualize the molecules sieving. Ethidium bromide fluoresces under UV light when intercalated into DNA (or RNA). Thus, by running DNA through an ethidium bromide-treated gel and visualizing it with UV light, the DNA becomes distinctly visible. Because the amount of fluorescence is proportional to the total mass of DNA, the quantity of DNA is estimated by comparing the fluorescent yield of the sample with that of a series of appropriate standards. As little as 1-5 ng of DNA can be detected by this method.

Using gels of different concentrations, it is possible to resolve a wide size range of DNA molecules (i.e., 0.9% w/v agarose gel separates efficient linear DNA molecules of 0.5-7 kb, 2.0% w/v agarose gel separates efficient linear DNA molecules of 0.1-2 kb).

The agarose was melted into TAE running buffer (0.04 M Tris-acetate; 0.001 M EDTA), then ethidium bromide was added at a final concentration of 10 mg/mL and the mixture was polymerized. 1 µL DNA samples to be analyzed was loaded onto the gel in the presence of Orange G gel-loading 5X buffer (10 mM EDTA; 30% glycerol; 0.25% orange G) and separated by applying a voltage of 1-5 V/cm. DNA fragments sieved were visualized by exposing the gel by UV light (250-320 nm). By comparing sample bands with those from the known molecular-weight markers, DNA can be detected and quantified.

3.2.4 DNA amplification by PCR

PCR is a technique that allows to obtain big amount of a specific DNA sequence, amplified from a few initial DNA molecules. Two oligonucleotides complementary to the ends of the target sequence are used as primers for a series of synthetic reactions catalysed by a DNA polymerase. PCR consists of a series of cycles of three successive reactions:

- *DNA denaturation*, typically set at about 93-95°C for human genomic DNA. At this temperature, double strand DNA melts and opens in two single strands;
- *primer annealing,* that is the primers pairing up (annealing) with the single-stranded DNA ("template"). This phase depends on the melting temperature (Tm, usually from about 50°C to 70°C) of the expected duplex.
- *extension*, typically fixed at about 70-75°C, consists of the synthesis of the new DNA molecule, using DNA precursors.

The DNA polymerases most frequently used are heat-stable (they need to elongate efficiently at 70–75°C and should not be adversely affected by the denaturation steps).

In the presence of a suitable heat-stable DNA polymerase and DNA precursors (the four deoxynucleoside triphosphates (dNTPs): dATP, dCTP, dGTP and dTTP), primers annealing gives rise to the synthesis of new DNA filaments, which are complementary to the individual DNA strands of the target sequence. At the end of each cycle, the sequence of interest is copied in both filaments. This technique allows to synthesize the sequence target in exponential progression and, after n PCR cycles, it is possible to obtain 2^n molecules of the same target sequence (Figure 11).

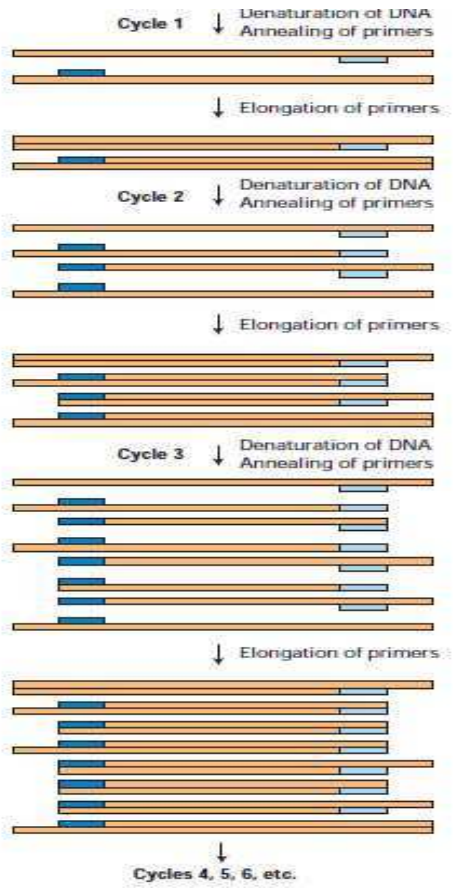

Fig. 11: Exponential amplification in PCR. The PCR is an *in vitro* method widely used to amplify DNA regions of known sequences using specific primers. During each PCR cycle, the reaction mixture is first heated to separate the strands and then cooled to allow the primers to bind to complementary sequences flanking the region to be amplified. Taq polymerase then extends each primer from its 3' end, generating newly synthesized strands that extend in the 3' direction to the 5' end of the template strand. After 35 cycles there is a massive increase (amplification) of the starting DNA (from Lodish 5th ed Molecular Cell Biology, 2003).

DNA fragments to be analyzed for mutation detection were PCR amplicons of ARVC/D desmosomal genes and of CTNNA3 candidate gene, whose nucleotide sequences are available in NCBI website. Primers flanking target regions for the presence of mutations were designed by PRIMER3 software (http://www.genome.wi.mit.edu/cgi-in/primer/primer3.cgi) to obtain the whole exonic sequences flanked by small intronic portions and fragments dimensions from 100 bp to 700 bp, to be properly analyzed by dHPLC. To check the occurred DNA amplification by PCR, an electrophoresis on 2% agarose gel was performed, in order to separate fragments of 200-500 bp.

a. Standard PCR

Each fragment was amplified from patient genomic DNA (for amplicons size, primers sequences and amplification conditions see Appendix). About 50 ng of DNA solution was placed into a sterile micro centrifuge tube and a mix was added to a final volume of 25 μL.

The mix contained 10 pmol/μL of each primer, dNTPs 1 mM, specific buffer depending on the DNA polymerase used, and 5 U/μL of DNA polymerase. After activation of the enzyme at 95°C, the cycling conditions (denaturation at 95°C for 30 sec, annealing at the working temperature for 30 sec, extension at 72°C for 30-45 sec) were repeated 35 times in a thermal cycler. The presence of the PCR product was then checked loading the sample onto an agarose gel.

b. GC-Rich PCR

Sequences of primers flanking exon 1 of PKP2 gene were kindly provided by Syrris P. The amplicon nucleotide sequence showed high GC content, thus the amplification was performed by using the GC-RICH PCR System (Roche diagnostic GmbH).

Approximately 50 ng of DNA solution were placed into a sterile micro centrifuge tube. Storing the reagents on ice, the "Master Mix 1" was prepared mixing 10 pmol/μL of each primer, dNTPs 1 mM, 1.5 mM $MgCl_2$, 1 M Resolution Solution and water to a final volume of 9 μL. Similarly, the "Master Mix 2" was then prepared mixing 1X Reaction Buffer and 0.5 U of GC-RICH Enzyme in a final volume of 2.5 μL. 9 μL of "Master Mix 1" and 2.5 μL of "Master Mix 2" were combined in the sterile micro centrifuge tube containing the DNA and the mixture was gently vortexed. After activation of the enzyme (95°C for 3 minutes), cycling conditions (denaturation at 95°C for 30 sec, annealing at 60°C for 30 sec, extension at 72°C for 45 sec) were repeated 35 times. The presence of the PCR product was then checked loading the sample onto an agarose gel.

c. Touch-Down (TD) PCR

A frequently encountered problem in PCR amplification of target gene sequence is the appearance of spurious smaller bands in the product spectrum. This is usually interpreted to be due to mispriming by one or both of the oligonucleotide amplimers internal or external to the target template. A way of increasing the specificity of a PCR reaction is to perform a TD PCR. The thermal cycler was programmed to perform runs in which the annealing temperature is lowered incrementally during the PCR cycling from an initial value above the expected Tm to a value below the Tm. By keeping the stringency of hybridization initially very high, the formation of spurious products is discouraged, allowing the expected sequence to predominate (Don et al., 1991).

3.2.5 Mutation screening by dHPLC

dHPLC is a high-capacity technique employed to detect mutations (SNPs, short insertions/ deletions and tandem repeats) on a DNA sequence. It is an ion-pair reversed-phase chromatography. The cartridge contains a nonporous alkylated polystyrene-divinylbenzene separation matrix. DNA sample, injected onto a chromatography column, binds to the column hydrophobic matrix through interactions mediated by triethylammonium acetate (TEAA); acetonytrile disrupts this interaction and causes DNA elution out of the column. Elution of the sample appears as a peak of absorbance at 260 nm versus time.

This technique exploits the differential melting properties of DNA homoduplex (made by the association of two wild-type molecules) and heteroduplex (made by the association of a wild-type molecule and a mutated one) that are obtained by denaturation (5 minutes at 95°C) and next renaturation at room temperature.

At a non-denaturing temperature analysis, the concentration of acetonytrile required to remove any given fragment depends on size and sequence. Therefore, any DNA fragment elutes at a characteristic point in a linear gradient of acetonytrile, which corresponds to a characteristic retention time on a plot of absorbance versus time. When the temperature of the column increases, elution takes place at progressively lower acetonytrile concentrations as the DNA fragment starts to denaturate. Heteroduplex (mismatched) DNA fragment has different melting characteristics compared to homoduplex and under condition of partial denaturation (at temperatures opportunely chosen in the range of 50–70°C, depending on the GC-content of the DNA under investigation) has a reduced retention on the chromatographic separation matrix. As a consequence, one or more additional peaks usually appear in the chromatogram, with different mutations yielding. Typically, a single peak from a wild type sample changes to multiple peaks from sample containing sequence variations (Figure 12).

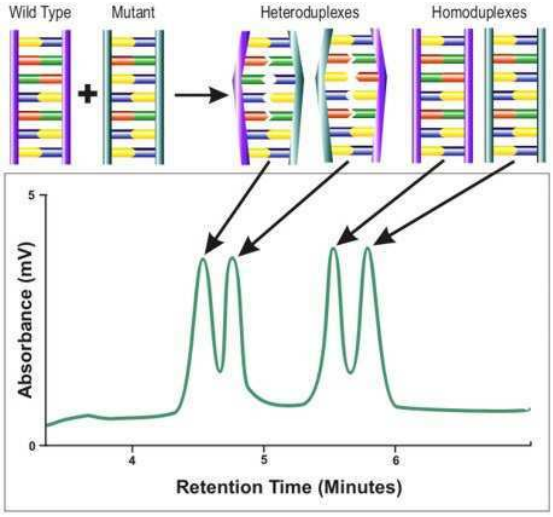

Fig. 12: Principle of dHPLC. (Up) Prior to chromatography, a DNA fragment is amplified by PCR from at least two chromosomes. In the presence of a mutation in one of the chromosomes, two original homoduplex and two different heteroduplex species are formed after denaturation. (Bottom) Example of chromatographic separation of the homoduplex and heteroduplex (http://www.transgenomic.com/pd/Systems.asp?tab=2).

Several studies have estimated dHPLC to be a highly sensitive and specific technique. While it is clear that analysis at multiple temperatures can increase the detection rate, there are still mutations which remain undetected after analysis at all temperatures. The true sensitivity of dHPLC must therefore be under 100%. (Jones et al., 1999; Arnold et al., 1999; Ellis et al., 2000; Bagattin et al., 2004).

a. Sample preparation for dHPLC (quantity and quality)

Samples suitable for mutation detection by dHPLC are PCR products in the range 100-700 bp (Xiao and Oefner, 2001). Fragments larger than 700 bp can be run but the sensitivity may

be reduced, while fragments shorter than 100-200 bp don't give satisfactory results, as the fragments melt over at a too narrow temperature range.

Moreover, it must be considered that poor quality PCR products will produce poor quality results. Thus, PCR products should be sufficiently concentrated (at least 20 ng/μL), considering that usually 3-10 μL (approximately 50-200 ng) of sample would be injected onto the column. Also, PCR products do not require purification: unincorporated nucleotides and primers will elute significantly ahead of the sample peak. On the contrary, primer dimers, smears and contaminating products of a similar size to the sample could interfere with analysis and thus they should be eliminated by optimization of the PCR.

b. Identification of mutations

Mutations are detected only in a heteroduplex molecule, and are easily formed by heating the sample, in the presence of a wild type DNA spike if necessary, to 95°C for 5 minutes, followed by slow cooling to room temperature.

Heteroduplex has different retention properties on the column respect to homoduplex. The presence of heteroduplex, and hence of a mutation in the sample, is detected as a change in the number of peaks. Depending on several factors, including, among others, size of the fragments, influence of nearest neighbour on the stability of both matched and mismatched base pairs, and column temperature, either all four species (two homoduplexes and two heteroduplexes) may be resolved completely or only in part. In the presence of a mutation, the wild-type peak pattern is changed to a two, three or four peaks pattern. Two peaks pattern accounts for the majority of mutations. In principle, homozygous mutations can be detected on the basis of a shift in retention time of more than 0.1 minutes (Gross et al., 1999). In practice, this is not reliable as the retention time shifts are often within the range of normal variation (Ellis et al., 2000). To detect homozygous mutations, heteroduplex must be generated by mixing equal quantities of mutant and wild type samples.

Sample showing a change in dHPLC may contain a pathogenic mutation, so it is necessary to re-amplify it for direct sequencing.

To proceed with the identification of mutations, after the formation of the homo/heteroduplexes, each DNA sample was injected onto the chromatography column of the Wave DNA Fragment Analysis System. Eluent conditions are sequence-dependent and are predicted by Wave NavigatorTM software, which uses a modified Fixman-Freire algorithm (Fixman and Freire, 1977). Eluent flow rates for all analyses were 0.9 mL/min in the Standard Analysis Mode, or 1.5 mL/min in the Rapid Analysis Mode. Mutation detection under partially denaturing conditions is automatically performed at temperature(s) specific for each fragment (the analyzing temperatures are chosen on the basis of the software predicted temperatures). Whenever fragments showed distinct melting domains, additional analyzing temperatures were performed. For amplicons size and analysis conditions see Appendix. Chromatograms were recorded at a wavelength of 260 nm. Samples showing a change in dHPLC pattern were identified as containing potential mutations and re-amplified for direct sequencing.

3.2.6 Automated DNA sequencing

PCR products showing aberrant patterns by dHPLC were reamplified and sequenced. Moreover, in some cases it wasn't possible to perform a dHPLC analysis, due to the presence in the sequence of long mononucleotidic repetitions or domains with very different melting temperatures; thus amplicons were amplified and sequenced directly.

To be sequenced, amplicons had to be purified to eliminate possible dNTPs and primers not used in the amplification that could interfere with the sequencing reaction. Amplicons purification was carried out with two enzymes: SAP, an alkaline phosphatase, that removes exceeding nucleotides, and EXOI, an exonuclease that removes single strand filaments and primers. In each micro centrifuge tube, 0,5 μL of each enzyme were added to about 5 μL of PCR product (3 ng of DNA every 100 bp of length). The mixture was then incubated at 37°C for 15 minutes and then at 80°C for other 15 minutes to inactivate the enzymes. The result was a cleaner PCR product, ready to be sequenced with standard sequencing reagents. DNA sequencing was performed at the B.M.R. Genomics by the automated ABI PRISM 3730XL DNA Sequencer (Applied Biosystem).

The automated DNA sequencing was accomplished by using labeled nucleotides for incorporation into a copy of a DNA sequence. Firstly, the sequencing primer bound specifically to a region 3' of the DNA sequence and primes synthesis of a complementary DNA strand in the 5'-3' direction. Four parallel base-specific reactions were automatically carried out, each with all four dNTPs and with one ddNTP. Dideoxy DNA sequencing relied on random incorporation of base-specific chain terminators during in vitro DNA synthesis. During electrophoresis a monitor detected and recorded the fluorescence signal of the incorporated ddNTPs in order of appearance and the correct sequence data were provided.

The electropherograms were visualized by two programs: Chromas, to see the chromatogram of a single sequence, and Seqman II, to align and compare perfectly the sequence obtained with the consensus sequence and individuate polimorphisms, mutations, insertions and deletions both carried in heterozygosity and homozygosity. Amplicons showing putative mutations were resequenced, with the product of an independent PCR reaction used as template.

3.3 FUNCTIONAL STUDIES

3.3.1 Constructs used

Constructs containing wild type cDNA of CTNNA3 gene to be used in functional experiments were kindly provided by Prof. Frans Van Roy, director of Department for Molecular Biomedical Research (DMBR), University of Ghent, Belgium.

pEGFPC2-haTctn construct (Figure 13) was used for transfections of mammalian cells. In this plasmid, wild type cDNA of human alphaT-catenin was in frame N-terminally fused to the enhanced red-shifted variant of the *Aequorea victoria* green fluorescent protein gene (EGFP), optimized for brighter fluorescence and higher expression in mammalian cells (excitation maximum= 490 nm; emission maximum= 509 nm). The fusion gene was

expressed under control of the human cytomegalovirus immediate early promoter (hCMV). Moreover, sequences flanking EGFP have been converted to a Kozak consensus translation initiation site to further increase the translation efficiency in eukaryotic cells. SV40 polyadenylation signal downstream of the EGFP gene directed proper processing of the 3' end of the EGFP mRNA. The vector carried also Amp^r for selection in *E. Coli*.

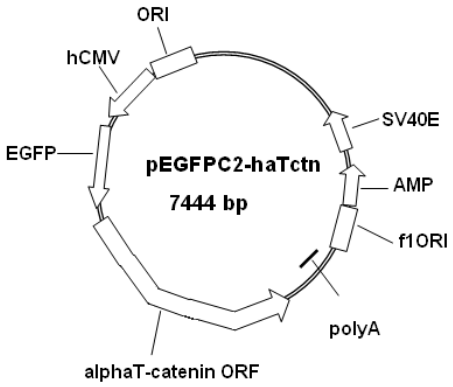

Fig. 13: Construct used for transfections of mammalian cells.

pEGADT7-haTctn and pEGBKT7-haTctn prey and bait constructs (Figure 14) were used in Y2H experiments. pEGADT7-haTctn was designed to express a fusion protein consisting of GAL4 activation domain (AD) and alphaT-catenin full length. The fusion protein was expressed at high levels from the full-length ADH1 promoter. Moreover, the vector carried Amp^r for selection in *E. coli* and the LEU2 nutritional marker for selection in yeast. Similarly, pEGBKT7-haTctn was designed to express a fusion protein consisting of GAL4 DNA-binding domain (DNA-BD) and alphaT-catenin full length. The fusion protein was expressed at high levels from the medium ADH1 promoter. The vector carried the Kan^r for selection in *E. coli* and the TRP1 nutritional marker for selection in yeast. Both vectors, to facilitate *in vitro* transcription/translation, included the T7 promoter.

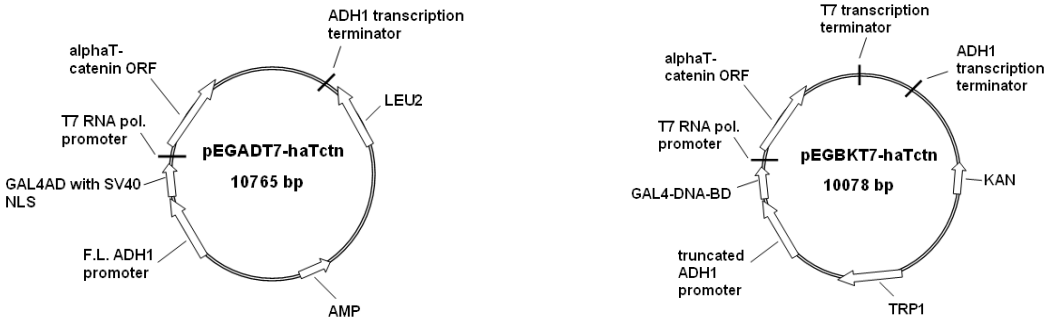

Fig. 14: Prey (left) and bait (right) constructs used for yeast two-hybrid experiments.

Site-directed mutagenesis was performed on the three described plasmids to obtain the constructs carrying the mutated CTNNA3 cDNA.

3.3.2 Site-directed mutagenesis

The cloning strategy used to obtain the different mutated constructs used in this study is based on site-directed mutagenesis. The cDNA to be mutagenized has been amplified using pEGFPC2-haTctn, pEGADT7-haTctn, and pEGBKT7-haTctn constructs as template and specific primers containing the point variations of interest in the middle of the sequences, in order to reproduce the four mutations naturally occurring in CTNNA3. The following primers, designed by PRIMER3, were used:

CTA3-V94D-F: GGCTTCACTTGAGGAAGATCGCAAAGAAAGTGAAGC;
CTA3-Q260R-R: GCTTCACAAGGGATCCGGAATATGACAACCCCACC;
CTA3-V583A-F:GGCAACATTCACTTGTGTTGCAAATTCAGGAATTACAG;
CTA3-DEL765L-F: CTGTTCCAGGTAGGCCAAGTCCTGTTTACAAGATG.

PCR reactions were performed with 300 ng DNA, 5 μM primer (Eurofins MWG Operons), 5 mM deoxynucleotide triphosphates (dNTPs) (Invitrogen), 10X PfuUltra II Buffer (Stratagene) 2.5 U/μL PfuUltra II polymerase (Stratagene), and water to a final volume of 25 μL. Cycling conditions (denaturation at 95°C for 30 seconds, annealing at 60°C for 1,30 minutes, extension at 68°C for 18 minutes) were repeated for 22 times.

3.3.3 Enzymatic restriction of mutagenesis PCR product

Restriction endonucleases are enzymes obtained from bacteria that cut DNA double strand at specific recognition sites. In particular, DpnI targets only methylated DNA sequences and can thereby cleave the DNA template isolated from most *E. coli* strains, but not the PCR product, as it isn't methylated. In this way, DNA mutagenized remains intact and can be used for subsequent bacteria transformation.
PCR products obtained from site-directed mutagenesis PCR were thus restricted with 1 μL DpnI (Euroclone) for 1 hour at 37°C.

3.3.4 Bacterial cultures

a. Culture media

To produce constructs carrying wild type and mutated CTNNA3 cDNA, bacterial cultures were prepared. Culture media used were prepared in lab as follows:

Luria-Bertani (LB) medium	
peptone (Fluka)	10 gr
yeast extract (Gibco)	5 gr
NaCl (Carlo Erba)	10 gr
Agar (Invitrogen)	15 gr (only for solid LB medium)
H_2O	to 1L

Specific selection antibodies were added to the medium, on the basis of the used construct. To select bacteria transformed with pEGFPC2-haTctn and pEGADT7-haTctn, 1 mL/L

Ampicillin (50 mg/mL Sigma-Aldrich) was used, while for selection of bacteria transformed with pEGBKT7-haTctn construct, 0,8 mL/L Kanamycin 50 mg/mL (Sigma-Aldrich) were used. For solid LB medium, about 20-25 mL of medium were aliquoted in every Petri dish; after polymerization of agar, dishes were stored at 4°C.

b. Bacterial transformation

Bacterial transformation is the process to introduce an exogenous plasmid into bacteria; in this way, bacteria are used to amplify the foreign DNA in order to obtain large quantities of it. Plasmids containing wild type or mutagenized CTNNA3 cDNA were used to transform One Shot® TOP10 *E.Coli* chemically competent cells (Invitrogen). These cells are provided at a transformation efficiency of 1 x $10e^9$ cfu/µg supercoiled DNA and are ideal for high-efficiency cloning and plasmid propagation. Since DNA is a very hydrophilic molecule, it does not normally pass through bacterial cell's membrane. In order to make bacteria take in the plasmid, they must first be made "competent". The plasmid can then be forced into cells by incubating the bacteria and the DNA together on ice, placing them briefly at 42^{o}C (heat shock), and then putting them back on ice. This causes the bacteria to take in the DNA. Transformation of Top10 *E.coli* cells occurred following the manifacturer's protocol, using about 100 ng of DNA of interest. 100 ng of DNA were added to a thawed vial of Top10 cells. After incubation on ice for 30 minutes, cells were heat shocked for 30 seconds at 42°C and rapidly placed in ice for two minutes. Then, 250 µL pre-warmed Super Optimal broth with Catabolite repression (S.O.C) medium, supplied with the kit, were added to the vial and the cells were stirred horizontally at 37°C for 1 hour at 225 rpm. About 50-200 µL from the transformation were spread on a pre-warmed selective LB-agar plate which was then inverted and incubated overnight at 37°C. It could be useful plate two different volumes of transformed bacteria, to ensure that at least one plate will have well-spaced colonies. The morning after, in the plate only colonies from transformed bacteria were grown. In fact, only bacteria that received the construct, and thus the antibiotic resistance, could grow in the selective medium.

c. Preparation of a bacterial glycerol stock

To make a long term stock of bacteria containing the construct of interest, a colony from an LB-agar plate containing the appropriate antibody was picked off and grown overnight in 1 mL of selectable liquid LB medium. Bacteria grown were then transferred into a sterile micro centrifuge tube containing 20% sterile glycerol. After mixing, the glycerol stock was stored at -80°C.

d. Preparation of a bacterial culture from a glycerol stock

To prepare a bacterial culture from a glycerol stock, it was sufficient to scratch the top of the glycerol stock (it doesn't have to thaw) with a sterile tip and transferred it into a culture of selective liquid LB medium. Bacteria grew under horizontal stirring at 37°C overnight.

e. Mini-prep plasmid DNA extraction

To select colonies carrying the construct with the correct insert, a little volume of bacterial culture obtained by picking off a colony from a selective agar plate was prepared in order to extract a low amount of plasmid and check its quality through digestion pattern on agarose gel.

Bacterial cultures were prepared using 3 mL of selectable liquid LB medium and grown overnight at 37°C under horizontal stirring. Plasmid DNA was extracted with the PureYield™ Plasmid Miniprep System (Promega), following the manifacturer's protocol. This system is designed to rapidly isolate highly pure plasmid DNA using a silica-membrane column, providing a rapid method for purification of up to 15 µg of plasmid DNA from 600 µL to 3 mL of bacterial culture. Moreover, it incorporates a unique Endotoxin Removal Wash designed to remove substantial amounts of protein, RNA and endotoxin contaminants from purified plasmid DNA. Purification is achieved without isopropanol precipitation or extensive centrifugation, providing rapid purification of highly concentrated plasmid DNA.

f. Maxi-prep plasmid DNA extraction

To obtain a significant amount of pure plasmid DNA to transfect the eukaryotic cells, Maxi prep plasmid DNA extraction was performed using PureYield™ Plasmid Maxiprep System kit (Promega). The system provides a rapid method for purification using a silica-membrane column. Plasmid DNA can be purified in approximately 60 minutes, greatly reducing the time spent on purification compared to silica-resin or other membrane column methods.

The system also incorporates a unique Endotoxin Removal Wash designed to remove substantial amounts of protein, RNA and endotoxin contaminants from purified plasmid DNA, and improve the robustness of sensitive applications such as eukaryotic transfection and in vitro transcription. Purification is achieved without isopropanol precipitation of purified plasmid DNA, providing rapid purification as well as a high concentration of pure plasmid DNA. The PureYield™ Plasmid Maxiprep System purifies up to 1 mg of plasmid DNA with an A_{260}/A_{280} >1.7 from 250 ml of overnight bacterial culture, transformed with a high-copy-number plasmid.

The day before plasmid DNA extraction, a 300 mL culture from glycerol stock of *E.coli* cells containing the construct of interest was prepared in selective LB medium and grown overnight at 37°C under stirring. Plasmid DNA extraction was performed following the protocol provided by the manufacturer. DNA concentration was then measured by NanoDrop and DNA quality was verified loading 1 µL of DNA onto 1% agarose gel. Extracted plasmid DNA was then digested with specific restriction enzymes and sequenced.

g. Enzymatic digestion

To check that the plasmid contained the insert of interest and that any recombination, like insertion, deletion or duplication didn't happened, extracted plasmid DNA was digested with appropriate restriction enzymes (See appendix for conditions). Finally, plasmid DNA of colonies positive to restriction was sequenced to be sure that point variations didn't occur.

3.3.5 Cellular cultures

To evaluate the pathogenicity of mutations identified in CTNNA3 gene, localization of wild type and mutated proteins was checked through transfection and immunofluorescence experiments in HL-1 cells and in neonatal rat cardiomyocytes.

3.3.5.1 HL-1 cells

The HL-1 immortal cell line was isolated by Claycomb and colleagues in 1998 from a culture of AT-1 cells. HL-1 are cells forming desmosomes that can be serially propagated in culture with an apparently unlimited life span retaining a differentiated phenotype during continuous passages in culture. Moreover, HL-1 cell line manifests a phenotype similar to adult cardiomyocytes. These cardiac characteristics of HL-1 cells include an ultrastructure similar to primary cultures of adult atrial cardiac myocytes and AT-1 cells; cytoplasmic reorganization and myofibrillogenesis similar to that observed in mitotic cardiomyocytes of the developing heart; presence of highly ordered myofibrils and cardiac-specific junctions in the form of intercalated discs; the ability to undergo spontaneous contractions while remaining in a mitotic state typical of normal *in vivo* immature mitotic cardiomyocytes (under selective culture conditions, they retain the ability to contract through at least passage 240); expression of ANF, a-MHC, cardiac actin, desmin, and connexin-43, and presence of several voltage-dependent currents that are characteristic of cardiac myocyte phenotype, particularly the Ikr current, which has not been identified in noncardiac tissues.

a. Culturing HL-1 cells

HL-1 cells were plated in in gelatin/fibronectin-coated polypropylene T75 flasks (Falcon). To coat the flasks, 15 μL of bovin fibronectin (Sigma-Aldrich) in 3 mL of 0.02% gelatin in water were added to each T75 flask, which was then incubated at 37°C overnight. Cells were maintained in 15 mL Claycomb medium (Sigma-Aldrich) supplemented with L-glutammine 2 mM (Invitrogen), penicillin and streptomycin 100 U/mL (Sigma-Aldrich), 10% fetal bovin serum (FBS, JRH), and norepinephrine 0,1 mM (Sigma-Aldrich). The cells were cultivated at 37°C in a humidified air atmosphere containing 5% CO_2.

b. HL-1 splitting protocol

Once HL-1 cells reached confluency, cell culture was split 1 to 3, and this was designated as a passage.

Cells were rinsed briefly with 0,05% trypsin-EDTA (Invitrogen) warmed at 37°C and then incubated twice with 0,05% trypsin-EDTA at 37°C for 3 minutes. After addition of 3 mL soybean trypsin inhibitor (Gibco) to neutralize trypsin activity, flask was rinsed with Claycomb medium to collect as many cells as possible. Cells were then centrifuged for 5 minutes at 1300 rpm. Once the supernatant was discarded, the pellet was resuspended in 3 mL Claycomb medium and finally 1 mL of resuspended cells was transferred into each of the three T75 flasks, gelatin-fibronectin coated, containing 14 mL of fresh supplemented Claycomb medium.

c. HL-1 freezing protocol

HL-1 cells grown at confluency in a T75 flask were freezed into one cryovial. Once detached from the flask and centrifuged as described in the splitting protocol, cells were resuspended in 1,5 mL of freezing medium (95% FBS/5% Dimethyl sulfoxide (DMSO) (Carlo Erba)) and transferred into a cryovial. After a few hours at -80°C, the vial was transferred to a liquid nitrogen dewar, where cells can be stored forever.

d. HL-1 thawning protocol

When cells were needed, a cryovial containing freezed cells was thawned into one T75 flask. Cells were quickly thawned in a 37°C water bath (about 2 minutes) and transferred into a 15 mL centrifuge tube containing 5 mL of Claycomb medium, previously warmed at 37°C, and centrifuged for 5 minutes at 1300 rpm. After supernatant discard, cells were resuspended in supplemented Claycomb medium and transferred into a T75 flask containing warm fresh medium. To be sure that cells could grow in DMSO-free conditions, medium was replaced with fresh supplemented Claycomb medium after 4 hours (after cells attached).

3.3.5.2 Culturing neonatal rat cardiomyocytes

Neonatal rat cardiomyocytes were isolated from ventricular tissue of Crl:(WI)BR-Wistar rats from Charles River Laboratories (Wilmington, MA) at the age of 1–3 days in collaboration with Dr. Mongillo's group. All animal procedures were in accordance with the institutional guidelines for animal research. The ventricles were excised and transferred firstly into a Petri dish containing cold 1X ADS buffer to be minced, and then to a Falcon tube to be precipitated. Once supernatant was discarded, the tissue was enzymatically digested by incubation with 7-9 mL Collagenase A/Pancreatin (Roche/Sigma Aldrich) for 5 minutes at 37°C, gently stirring. The supernatant was discarded and cells were incubated again with the enzyme solution for 20 minutes at 37°C under stirring. 1 mL of normal chicken serum (NCS) was then added to the supernatant and the mix was centrifuged at 1250 rpm for 5 minutes. Cells were then resuspended in 2 mL NCS. Step with enzymatic incubation were repeated three to four more times until the fragments completely disappeared. After processing the supernatant from each digestion step, all the dissociated cells from each step were pooled, centrifuged, and resuspended in complete DMEM medium (Invitrogen) supplemented with 10% horse serum (Gibco), 5% newborn calf serum (Gibco), L-glutammine 2 mM (Invitrogen), penicillin and streptomycin 100 U/mL (Sigma-Aldrich). To segregate myocytes from nonmyocytes, the cell suspension was plated into a Petri dish and incubated for 1 hour into the incubator. Then the supernatant was centrifuged at 1250 rpm for 5 minutes and cell pellet was resuspended in 10 mL complete DMEM medium to be finally plated onto laminin-coated 24-mm glass coverslips (Roche). The cells were cultivated at 37°C in a humidified air atmosphere containing 5% CO_2.

3.3.5.3 Culturing HEK293T cells

HEK293T is a cell line derived from human embryonic kidney cells transformed with adenovirus and expressing SV40 large T antigen. Cells were grown in T75-flasks (Falcon) in DMEM medium supplemented with penicillin and streptomycin 100 U/mL (Sigma-Aldrich) and 10% fetal bovin serum (FBS, Gibco) at 37°C in a humidified air atmosphere containing 5% CO_2. HEK293T cells were splitted using 0,25% trypsin-EDTA (Invitrogen) using the same protocol described for HL-1 cells. Also, freezing and thawning protocols followed were the same used for HL-1 cells, with the use of 0,25% trypsin-EDTA and DMEM medium.

3.3.5.4 Transient cellular transfection

Transfection is the process of introduction of esogenous DNA into an eukaryotic cell, through chemical or physical methods. In the transient transfection, the DNA introduced can be mantained into the cell just for a certain period that usually spans between 24 and 72 hours: since the DNA introduced through transient transfection process is not integrated into the nuclear genome, the foreign DNA will be diluted through mitosis or degraded.

Among the different transient transfection methods, lipoplexes (lipid-DNA complexes) are widely used to deliver DNA into mammalian cells, owing to their potential advantages over viral vectors, such as their safety, versatility and low immunogenicity. For successful transfection, a nucleic acid, which carries a net negative charge under normal physiological conditions, must come into contact with a cell membrane that also carries a net negative charge. Lipoplexes allow the entrance of the DNA into the cell, wrapping the nucleic acid during its passage through the cell membrane.

In this study, HL-1 and HEK293T cells were transfected using Lipofectamine 2000 kit (Invitrogen), while neonatal rat cardiomyocytes were transfected using TransFectin lipid reagent (Bio-Rad). Both Lipofectamine 2000 and TransFectin are cationic liposome formulations that function by complexing with nucleic acid molecules, allowing them to overcome the electrostatic repulsion of the cell membrane and to be taken up by the cell.

After two days in culture, HL-1 and HEK293T cells were detached from a T75 flask as described above, resuspended in supplemented fresh medium (Claycomb for HL-1 and DMEM for HEK293T) -FBS and antibiotic-free and plated into a 6 wells-plate containing glass coverslips gelatin/fibronectin-coated to be transfected. For each well, a mix containing 3 μg of plasmid DNA and 50 μL of Opti-MEM I Medium (Invitrogen) and a mix containing 1 μL of Lipofectamine 2000 and 50 μL of Opti-MEM I Medium were prepared. After incubation of the two mixes at room temperature for 5 minutes, the mix containing the DNA was added to the mix containing the Lipofectamine 2000 and incubated for 20 minutes at room temperature. About 100 μL of Lipofectamine 2000-DNA complex was then added to each well containing cells and the plates were incubated at 37°C.

Similarly to the Lipofectamine 2000 protocol, also in the case of transfection with Trans-Fectin two mixes were prepared. The first contained 2 μL of Trans-Fectin and 50 μL of Optimem medium, while the second contained 3 μg of DNA and 50 μL of Optimem medium.

After mixing of the two solutions and incubation at room temperature for 20 minutes, the transfection complex was added to confluent cells and the plates were incubated at 37°C.
At 48 hours post-transfection, cells were fixed with methanol/acetone (1:1), or with 4% paraphormaldeyde (PFA).

3.3.5.5 Cells fixation

To ensure free access of the antibody to its antigen, cells must be fixed on the coverslip. In general, fixation strengths and times are considerably shorter for cells than on the thicker, structurally complex tissue section. For immunocytochemistry, sample preparation essentially entails fixing the target cells to the slide. Perfect fixation would immobilize the antigens, while retaining authentic cellular and subcellular architecture and permitting unhindered access of antibodies to all cells and subcellular compartments. Wide ranges of fixatives are commonly used, and the correct choice of method depends on the nature of the antigen being examined and on the properties of the antibody used. Fixation methods fall generally into two classes: organic solvents and cross-linking reagents. Organic solvents (such as alcohols and acetone) remove lipids and dehydrate the cells, while precipitating the proteins on the cellular architecture. Cross-linking reagents (such as PFA) form intermolecular bridges, normally through free amino groups, thus creating a network of linked antigens. Cross-linkers preserve cell structure better than organic solvents, but may reduce the antigenicity of some cell components and require the addition of a permeabilization step to allow access of the antibody to the specimen. The appropriate fixation method should be chosen according to the relevant application.
On the basis of the antibody used, transfected cells were fixed using two different protocols.

a. Cells 4% PFA fixation

Cardiomyocytes to be incubated with phalloidin in direct immunofluorescence assay to detect cellular localization of F-actin and HEK293T cells were fixed in PFA 4%. After aspiration of the medium, cells were firstly rinsed twice with 1X Phosphate Buffered Saline (PBS) (Gibco) and then incubated with 4% PFA (w/v) in 1X PBS at room temperature for 10 minutes. Then, cells were stored at 4°C in 1X PBS for 4-5 days.

b. Cells methanol/acetone (1:1) fixation

Cells to be incubated with anti beta-catenin and anti-plakoglobin in indirect immunofluorescence experiments were fixed with methanol/acetone (1:1). After aspiration of the medium, cells were firstly rinsed twice with 1X PBS and then incubated with cold methanol/acetone 1:1 at -20°C for 20 minutes. The solution was then removed, cells were washed again with 1X PBS and stored at 4°C for 4-5 days.

3.3.6 Immunofluorescence experiments

Immunofluorescence is a technique allowing the visualization of a specific protein or antigen in cells or tissue sections by binding a specific antibody chemically conjugated with a

fluorescent dye. There are two major types of immunofluorescence staining methods: direct immunofluorescence staining, in which the primary antibody is labeled with a fluorescence dye, and indirect immunofluorescence staining, in which a secondary antibody labeled with a fluorochrome is used to recognize a primary antibody.

In this study, HL-1 cells, neonatal rat cardiomyocytes and HEK293T cells were transfected with a construct containing CTNNA3 cDNA fused with EGFP, thus exogenous wild-type or mutated alphaT-catenin synthesized could be visualized thanks to the green fluorescence. To check colocalization of the protein with its binding partners in the cell and if other molecules could be affected by the presence of the mutated protein, it was necessary to stain specific endogenous proteins of certain cellular regions, like beta catenin and plakoglobin, as plasma membrane proteins, cytoskeletric F-actin, and intermediate filaments' vimentin. To distinguish the two proteins in the transfected cells, it was necessary to use different fluorochromes. Considering that EGFP conjugated to alphaT-catenin gave a green signal, the other protein must be stained with a secondary antibody labeled with a fluorochrome emitting in the red scale.

a. Indirect immunofluorescence

To check the localization of wild-type and mutated alphaT-catenin, experiments of indirect immunofluorescence were performed in HL-1 cells and in neonatal rat cardiomyocytes. Beta catenin and plakoglobin were chosen as markers of plasma membrane. Beta-catenin and plakoglobin are essential components of AJs, and are also present in *area composita.* Moreover, plakoglobin is also a component of desmosome. Moreover, in HEK293T cells transfected with the construct carrying the sequence of p.del765L-alphaT-catenin, immunofluorescence experiments were performed to detect the organization of vimentin, a protein of intermediate filaments.

As primary antibodies, a monoclonal mouse anti-beta-catenin (clone 6F9, Sigma), diluted 1:150, a monoclonal mouse anti-plakoglobin (clone PG-11E4, Zymed, Invitrogen), diluted 1:100, and a monoclonal mouse anti-vimentin (clone V9;Dako) diluted 1:500 were chosen. As secondary antibody, a polyclonal rabbit anti-mouse/TRITC (Dako-Cytomations), diluted 1:40, was used.

Transfected cells were washed with 1X PBS for 10 minutes and then saturated for 1 hour in 1X PBS-1%BSA, to avoid aspecific interactions of the antibody. After three rinses in 1X PBS, cells were incubated with the primary antibody for 1 hour at room temperature. Followed other three washes in 1X PBS and incubation with secondary antibody for 1 hour at room temperature. Cells were finally washed 3-4 times in 1X PBS for 5 minutes each and then mounted onto a clear glass slide (sample-side down) using the mounting medium. After incubation overnight at room temperature to harden the mounting medium, samples were stored in the dark at 4°C. Slides were inspected and photographed using a Radiance 2000 confocal microscope (BioRad) with a 60x oil objective or a the SP5 confocal laser scanning microscope from Leica with a 63x oil objective.

b. Phalloidin cells staining (direct immunofluorescence)

Among the different endogenous proteins interacting with alphaT-catenin stained in the immunofluorescence experiments, F-actin is a cytoskeletal protein. Cellular localization of F-actin is usually visualized by phalloidin. It belongs to a family of toxins isolated from the deadly *Amanita phalloides* mushroom and it is commonly used in imaging applications to selectively label F-actin in cells. Phalloidin is conjugated with a fluorochrome, so that cytoskeletric F-actin filaments can be visualized performing a direct immunofluorescence experiment.

For phalloidin staining, after fixation in 2% PFA, cells were incubated for 20 minutes with NH_4Cl 50 mM in order to prevent unspecific binding of phalloidin, blocking free aldehyde groups from the fixation media. To allow the access of phalloidin, cells, after a rinse in 1X PBS, must be permeabilized with 0,1% Triton (BDH) for 10 minutes at room temperature. To avoid aspecific interactions, cells were then saturated in 1X PBS-1% bovine serum albumin (BSA) (Sigma-Aldrich). Finally, cells were incubated for 45 minutes at room temperature with phalloidin (Sigma-Aldrich) diluited 1:700 in 1X PBS and washed twice with 1X PBS. To mount the sample, a drop of mounting medium (20-30 μL) was placed onto the center of a clear glass slide and the coverslip was lowered (sample-side down) onto the mounting medium. After incubation overnight at room temperature to harden the mounting medium, samples were stored in the dark at 4°C. Phalloidin-stained specimens should be imaged within a few days of staining as it will dissociate into the mounting medium over time and produce a background autofluorescence that may obscure fine detail. Slides were inspected and photographed using a Radiance 2000 confocal microscope (BioRad) with a 60x oil objective.

3.3.7 Y2H assay

The Y2H is an assay widely used to test interactions between two proteins. It is based on the fact that eukaryotic transcriptional activators consist of two individual domains: the DNA Binding Domain (BD) and the Activation Domain (AD). Normal transcription requires the interaction of these two domains to form a functional and active transcription complex. This complex then binds to specific sequences within the promoter region and activates the transcription of downstream genes. In the Y2H assay, the protein of interest (X) is expressed as a fusion protein with the DNA-BD in a bait construct and the AD is fused to the protein target (Y) in prey construct. Yeasts are co-transfected with the two constructs containing the sequences encoding X-DNA-BD and Y-AD fusion-proteins: only if X and Y physically interact with one another, DNA-BD and AD are brought together to activate the expression of the downstream reporter genes (Figure 15).

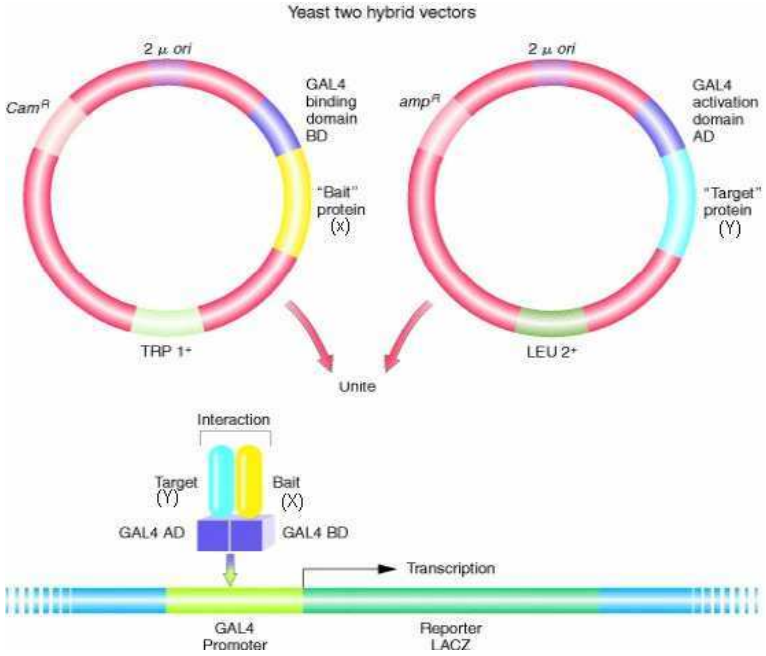

Fig. 15: Principle of Y2H assay. Transcription of reporter gene will occur only if the bait fusion protein and the prey fusion protein interact each other, bringing together the BNA-BD and the AD of the GAL4 transcription complex. Modified from http://www.ncbi.nlm.nih.gov/books/NBK21334/ CBI bookshelf.

To perform Y2H assay, the Matchmaker Gold system (Clontech) was used. This system uses the Y2HGold yeast strain, that harbours four integrated reporter genes, thus avoiding false positives and a high number of background colonies.

One of the reporter genes is MEL1, whose trascriptional product is alpha-galactosidase, an enzyme that catalyzes the hydrolysis of the substrate X-α-gal (5-Bromo-4-Chloro-3-indolyl-a-D-galactopyranoside) added to the medium causing yeast colonies to develop a blue color. X-α-gal itself is colourless, so the presence of blue-colored yeast colonies means that alpha-galactosidase has been activated under the control of GAL4 promoter, that is that the two proteins of interest interact. Another reporter gene carried by Y2H Gold strain is AUR1-C, a dominant mutant version of AUR1 gene. It encodes inositol phosphoryl ceramide synthase and its expression is induced by protein-protein interactions that lead to the activation of GAL4 promoter. Its activation induces the resistance to Aureobasidin A (AbA). Aba is a potent antibiotic, isolated from the filamentous fungus *Aureobasidium pullulans*, toxic to yeast at low concentrations (0.1–0.5 µg/mL). It kills sensitive cells, rather than merely retarding their growth, thus AbA-based selection greatly favors the growth and the identification of genuinely positive clones. Moreover, the employment of AbA can reveal the strength of interaction between bait and prey proteins. The other two reporter genes are ADE2 and HIS3. The Y2H Gold strain is unable to synthesize adenine and histidine and it is therefore unable to grow on media lacking these elements. Only when bait and prey fusion proteins interact each other, GAL-4 responsive ADE2 and HIS3 expressions allow the cell to synthesize these two components and thus to survive in a selective medium lacking adenine or histidine.

Y2H assay was performed in collaboration with Prof. Frans Van Roy's lab.

3.3.7.1 Culture media

a. YPDA medium

For routine culturing of untransformed yeasts, yeast peptone dextrose adenine (YPDA) was used:

YPDA medium	
Bacto yeast extract (Difco)	10 gr
Bacto peptone (Difco)	20 gr
Glucose monohydrate (Sigma-Aldrich)	20 gr
Adenine hemisulfate (Sigma-Aldrich)	40 mg
H_2O	to 800 mL

b. Selective dropout media

Co-transfected yeasts were grown in different selective dropout (SD) media: LT-, LTHA-, LTHA-/+X-α–gal. The variants of SD media differ in the DropOut (DO), that provides various mixtures of amino acids and nucleosides to be added to the minimal SD medium.

-DO solution

To make one litre of 10X –Leu/–Trp/–Ade/–His DO Solution, the following components were combined (autoclave and store at 4°C):

arginine HCl	200 mg
isoleucine	300 mg
lysine HCl	300 mg
methionine	200 mg
phenylalanine	500 mg
threonine	2000 mg
tyrosine	300 mg
uracil	200 mg
valine	1500 mg

A 10X stock of supplement components (when needed) was prepared as follows:

L-Adenine hemisulfate salt	100 mg/ 50ml
L-Histidine HCl monohydrate	100 mg/ 50ml

-LT- **:** In this case, DO lacks leucine and tryptophan for yeast selection. The two constructs used in co-transfection contain the sequences encoding leucine and tryptophan, and so only co-transfected yeasts are able to provide themselves both these elements.

40% Glucose 20X (Sigma-Aldrich)	2,5 mL
DO-LT 10X	5mL
Histidine 100X (Sigma-Aldrich)	0,5 mL
Adenine 100X (Sigma-Aldrich)	0,5 mL
Yeast nitrogen base without amino acids (Sigma-Aldrich)	335 mg
Bacto Agar (Difco)	1000 mg
H_2O	to 50 mL

-LTHA-**:** In this case, DO lacks leucine, tryptophan, histidine, and adenine for yeast selection. The bait and prey constructs contain the sequences encoding tryptophan and leucine, respectively, while synthesis of histidine and adenine is under the control of GAL4 transcription complex. Thus, only co-transfected yeasts are able to provide themselves these four elements.

40% glucose 20X (Sigma-Aldrich)	2,5 mL
DO-LTHA 10X	5 mL
yeast nitrogen base without amino acids (Sigma-Aldrich)	335 mg
Bacto Agar (Difco)	1000 mg
H_2O	to 50 mL

-LTHA-/+X-α–gal: As previously described, DO lacks leucine, tryptophan, histidine and adenine. Moreover, in this medium X-α–Gal is added, so that selection of co-transfected yeasts is made also by a colourimetric assay.

40% glucose 20X (Sigma-Aldrich)	2,5 mL
10X DO-LTHA	5 mL
X-α-GAL (Clontech)	40 µg/ml
yeast nitrogen base without amino acids (Sigma-Aldrich)	335 mg
Bacto Agar (Difco)	1000 mg
Aureobasidin (when needed)	50, 100 or 200 ng/ml
H_2O	to 50 mL

X-α-GAL is light sensitive, so these plates should be stored in the dark.

3.3.7.2 Yeast co-transformation

The day before co-transformation, a 50 mL yeast colture in YPDA medium was prepared and kept in horizonal stirring at 180 rpm at 30°C. When growth stationary phase was reached, the culture was transferred into 300 mL YPDA medium at OD600=0.3. After incubation of about three hours in horizontal stirring at 180 rpm (OD600=0.6), the culture was centrifuged at 2000 g at 20°C for 5 minutes and the pellet was resuspended into 25 mL sterile water.

The pellet was centrifuged again, resuspended into 1,5 mL TE/LiAc (LiAc 100 mM in Tris-HCl 10 mM pH 7,5, EDTA 1 mM), and cells were incubated without agitation at 30°C for 15 min. Aliquots of 50 μL, containing 1 x 10^8 cells, were dispensed into 1.5 mL microcentrifuge tubes.
Then, to each pellet, were added, in order:

PEG (50% w/v)	240 μL
LiAc 1 M	36 μL
DNA carrier (2 mg/ml)	50 μL
previously boiled 5' and then kept on ice	
H_2O with plasmid DNA	34 μL
(1 μg bait and 1 μg prey)	

After being vortexed, the mix was incubated at 30°C for 30 minutes with shaking. Cells were then heat-shocked at 42°C for 15 minutes and then chilled on ice for 2 minutes. Yeasts were centrifuged at 2000 g for 15 minutes and pellets were resuspended in 1 mL water.
Samples were plated on different solid LT- medium plates. Plates were incubated at 30°C for 3-4 days.

3.3.7.3 Replating of co-transfected yeasts in selective SD plates

After 3-4 days, in solid LT- medium plates were grown only co-transfected yeasts, as only those who received both the genes encoding leucine and tryptophan could survive in this selective medium. Each yeast colony was scratched with a sterile tip and transferred into a well of a 96-wells plate containing 200 μL of liquid LT- medium. Then plates were incubated at 30°C overnight. The day after, with the use of a 96-prong replicator, sterilized in ethanol, the yeasts grown into the 96-wells plate were replated on the different selective SD plates. Replates were then incubated at 30°C for 3-4 days to allow yeasts' growth.

3.4 BIOINFORMATIC TOOLS

1000 GENOMES

(http://www.1000genomes.org)

1000 Genomes Project is the first project to sequence the genomes of a large number of people, to provide genetic variants present in the population studied with a frequency of at least 1%. Data obtained are available to the worldwide scientific community through freely accessible public databases. The sequence of a single person's genome is obtained by sequencing short pieces of the DNA, that are then aligned to the reference sequence and joined together.

BCM Search Launcher (Baylor College of Medicine Search Launcher)

(http://searchlauncher.bmc.tmc.edu)

It is a tool that organize molecular biology-related search and analysis services available by function by providing a single point of entry for related searches. Not only nucleic acids and proteins sequences can be provided, but also multiple and pair-wise sequence alignments, protein secondary structure prediction, gene feature analysis, and miscellaneous sequence utilities.

BLAST (Basic Local Alignment Search Tool)

(http://www.ncbi.nlm.nih.gov/BLAST)

It is a database available from the National Center for Biotechnology Information (NCBI) for comparing biological sequence information, such as the amino-acid sequences of different proteins or the nucleotides of DNA sequences. A BLAST search enables to compare a query sequence with a database of sequences, and to identify sequences that resemble the query sequence above a certain threshold. BLAST can be used to infer functional and evolutionary relationships between sequences as well as help identify members of gene families.

Chromas

It's a software for visualize electropherograms obtained from sequencing. It allows to see a single sequence and to detect double peaks.

ClustalW

(http://www2.ebi.ac.uk/clustalw/)

It is a general purpose multiple sequence alignment program for DNA or proteins, provided by European Bioinformatics Institute. It produces biologically meaningful multiple sequence alignments of different sequences. It calculates the best match for the selected sequences, and lines them up so that the identities, similarities and differences can be seen.

dbSNP (Single Nucleotide Polymorphism Database)

(http://www.ncbi.nlm.nih.gov/projects/SNP)

The Single Nucleotide Polymorphism Database (dbSNP) is a free public archive for genetic variations within and across different species developed and hosted by the NCBI. In February 2010, dbSNP contained more than 184 million submissions representing more than 64 million distinct variants for 55 organisms. These quantities of SNPs give a high level of coverage across the genome. Each submitted variation can be identified with an unique identification number, to avoid redundancy, and a reference SNP ID number ("rs#"), that gives the basic information as well as information available from combining the data from multiple submissions (e.g. heterozygosity, genotype frequencies).

Ensembl

(http://www.ensembl.org)

It is a joint project between EMBL - European Bioinformatics Institute (EBI) and the Wellcome Trust Sanger Institute (WTSI) which was launched in 1999 in response to the imminent completion of the Human Genome Project. Ensembl is a database of automated annotation on selected eukaryotic genomes that mimics decision made by a human annotator through the identification of "confirmed" genes that are computationally predicted and also supported by a significant BLAST match to one or more expressed sequence or proteins. The database includes several species, like human, mouse, fruitfly, and zebrafish as well as a wide range of genomic data, like genetic variations and regulatory features. All the data are freely accessible to the world research community.

Entrez

(http://www.ncbi.nlm.nih.gov/entrez)

It is an integrated, text-based search and retrieval system used at NCBI for the major databases, including PubMed, Nucleotide and Protein Sequences, Protein Structures, Complete Genomes, Taxonomy, and others.

GenBank

(http://www.ncbi.nlm.nih.gov/Genbank)

It's a public database produced by NCBI containing sequences of more than 100000 distinct organisms. GenBank continues to grow at an exponential rate, doubling every 10 months. Produced in August 2006, contains over 65 billion nucleotide bases in more than 61 million sequences.

NAVIGATOR SOFTWARE

It's the software used to define the Transgenomic Wave® Nucleic Acid Fragment Analysis System (Wave System), for dHPLC analysis. It contains several options to set up the different parameters. The tool DNA allows to insert the amplicon sequence and to set the analysis temperatures, suggested by using a variant of the Fixman-Freire algorithm. This algorithm is used for the prediction of optimal denaturation conditions for mutation detection based on DNA fragment length, nucleotide sequence and composition, and chromatography

conditions. It calculates the likelihood that for each temperature each nucleotide is in a single strand or in a double strand. The results of this calculation are visualized graphically in four different denaturation curves: the first plot indicates the percentage of double strand at a certain temperature; the second one shows the percentage of double strand beside the position of each base at a given temperature; the third and the fourth plots describe the ratio between melting temperature and base position in the sequence. Among them, the second plot is the most used in the temperature setting. Particularly, the software proposes a temperature that causes a partial denaturation of the sample (75-80% double strand). The tool Injection allows to create a project to load, appoint and number the samples in specific positions in the plate. Through Analysis window, chromatograms obtained are visualized.

NCBI (National Center for Biotechnology Information)
(http://www.ncbi.nlm.gov)
Established in 1988 as a division of the National Library of Medicine (NLM) at the National Institutes of Health (NIH), NCBI represents a national resource for molecular biology information. It creates public databases, conducts research in computational biology, develops software tools for analyzing genome data, and disseminates biomedical information - all for the better understanding of molecular processes affecting human health and disease.

NEB CUTTER V2.0
(http://tools.neb.com/NEBcutter2/index.php)
It's a tool from New England BioLabs to find large, non-overlapping, open reading frames and sites for all restriction enzymes.

OMIM (Online Mendelian Inheritance in Man)
(http://www.ncbi.nlm.nih.gov/OMIM)
This database was initiated in the early 1960s by Dr. Victor A. McKusick as a catalog of mendelian traits and disorders, entitled Mendelian Inheritance in Man (MIM). The online version, OMIM, was created in 1985 by a collaboration between the National Library of Medicine and the William H. Welch Medical Library at Johns Hopkins. In 1995, it was developed for the World Wide Web by NCBI, the National Center for Biotechnology Information. OMIM is a database containing information on all known mendelian disorders and over 12000 genes that focuses on the relationship between phenotype and genotype. It is an excellent resource for providing a brief background biology on genes and diseases, it includes informations on the most common and clinically significant mutations and polymorphisms in genes. Moreover, it is updated daily, and the entries contain copious links to other genetic resources, like the NCBI database family, thus facilitating rapid and direct linking between disease, gene sequence and chromosomal locus.

POLYPHEN2 (**Poly**morphism **Phen**otyping v**2**)

(http://genetics.bwh.harvard.edu/pph2)

It's a software tool which predicts a possible impact of aminoacid substitutions on the structure and function of human proteins using straightforward physical and evolutionary comparative considerations. PolyPhen2 makes functional predictions on the basis of a profile analysis of homologous sequences, the mapping of the relevant substitution to 3D structures, and the sequence-based characterization of the specific substitution site. This analysis classifies mutations as benign and possibly or probably damaging (Ramensky et al. 2002).

Primer3

(http://frodo.wi.mit.edu/primer3/)

It's an online program developed and supported from WI/MIT for designing PCR primers. Primer3 has many different input parameters that can be controlled to choose exactly the characteristics to make good primers, like melting temperature, primer size, target/excluded regions, product size range and others.

Pubmed

(http://www.ncbi.nlm.nih.gov/pubmed/)

PubMed is a free database, first released in 1996, accessing primarily the MEDLINE database of references and abstracts on life sciences and biomedical topics. The search can be made by title, year of publication, author of interest, or keyword. The results are visualized as a list of references and many of them contain links to full text articles, some of which are freely available.

SeqManII (DNASTAR)

SeqManII is a software used to assemble from two to tens of thousands of electropherograms into contigs. Prior to assembly, SeqManII evaluates the quality of the underlying trace data to eliminate contaminating and poor quality data from the projects, thus generating the most accurate consensus sequence possible. SeqmanII can assemble also electropherograms with sequences in FASTA format, thus allowing the comparison of the sequencing results with a reference sequence. This software is then particularly useful to detect nucleotides that differ from the consensus sequence and that could be a pathogenic mutation.

SIFT (sorting **i**ntolerant **f**rom **t**olerant**)**

(http://sift.jcvi.org/)

SIFT is a sequence homology-based tool that sorts intolerant from tolerant amino acid substitutions and predicts whether an amino acid variation in a protein could have a phenotypic effect. This program presumes that important amino acids will be conserved in the protein family, so changes at well-conserved positions tend to be predicted as

deleterious, thus distinguishing between functionally neutral and deleterious amino acid changes.

TrEMBL

(http://www.ebi.ac.uk/trembl/index.html)

It's a protein sequence database of nucleotide translated sequences. UniProtKB/TrEMBL is a computer annotated protein sequence database complementing the UniProt/Swiss-Prot Protein Knowledgebase. UniProt/TrEMBL contains the translations of all coding sequences and also protein sequences extracted from the literature or submitted to UniProt/Swiss-Prot. It was introduced in response to increased dataflow resulting from genome projects.

UCSC Human Genome Browser

(http://genome.ucsc.edu)

It's a browser containing the reference sequence and working draft assemblies for a large collection of genomes. There are several tools useful for genomic analysis. The Browser zooms and scrolls over chromosomes, showing the work of annotators worldwide. Gene Sorter shows expression, homology and other informations on groups of genes that can be related in many ways. Blat maps a sequence to the genome. Moreover, Graphical representation of the fragments making up a region of draft genome can be displayed, showing the relative size and overlaps of each fragment and also whether any gap between fragments are bridged by mRNAs or paired BAC end sequences. This means that one can get an idea of the likely degree of misassembly in a draft region. There is an increasing amount of data becoming available from large-scale gene expression studies.

UniProt-SwissProt

(http://www.ebi.ac.uk/swissprot/)

It's an annotated protein sequence database established in 1986 and maintained collaboratively by the Swiss Institute for Bioinformatics (SIB) and the European Bioinformatics Institute (EBI). It provides a high level of annotation and of integration with other databases, and a minimal level of redundancy.

4. RESULTS

4.1 STUDY POPULATION

Exon by exon analysis of all five desmosomal genes involved in ARVC/D (PKP2, DSP, DSG2, DSC2, and JUP) was performed in 80 Italian unrelated index cases (54 males, mean age 44±16) fulfilling ARVC/D 2010 Task Force diagnostic criteria. For about 50% of them, family history reported the occurence of additional cases of ARVC/D. Moreover, mutation screening of CTNNA3 gene was performed in 76 ARVC/D probands (52 males, 42±12) who fulfilled 2010 Task Force criteria for ARVC/D and negative for mutations in desmosomal genes.

A group of 250 Italian healthy and unrelated subjects (500 chromosomes) were used to exclude that detected variations could be common polymorphisms. DNA variations found in more than 1% of the healthy controls chromosomes have been considered polymorphisms.

The study was conform the Declaration of Helsinki and all the participants gave their written informed consent.

4.2 MUTATION SCREENING

4.2.1 Mutation screening in desmosomal genes involved in ARVC/D

Mutation screening was performed by dHPLC and direct sequencing on amplicons consisting of exons and intronic boundaries of all five desmosomal genes. Primers flanking exons of all investigated genes were designed by PRIMER3 software. For amplicons size, primers sequences, amplification and analysis conditions see Appendix. dHPLC analysis conditions were set up by NAVIGATOR™ software (Transgenomics). Samples showing a change in dHPLC elution pattern were sequenced. Some exons were unsuitable for dHPLC analysis, due to the presence of domains rich in GC, or long mononucleotidic repeats, or different melting temperatures; thus, they were analyzed by direct sequencing. Relative position of mutations detected in desmosomal genes are reported in Figure 16.

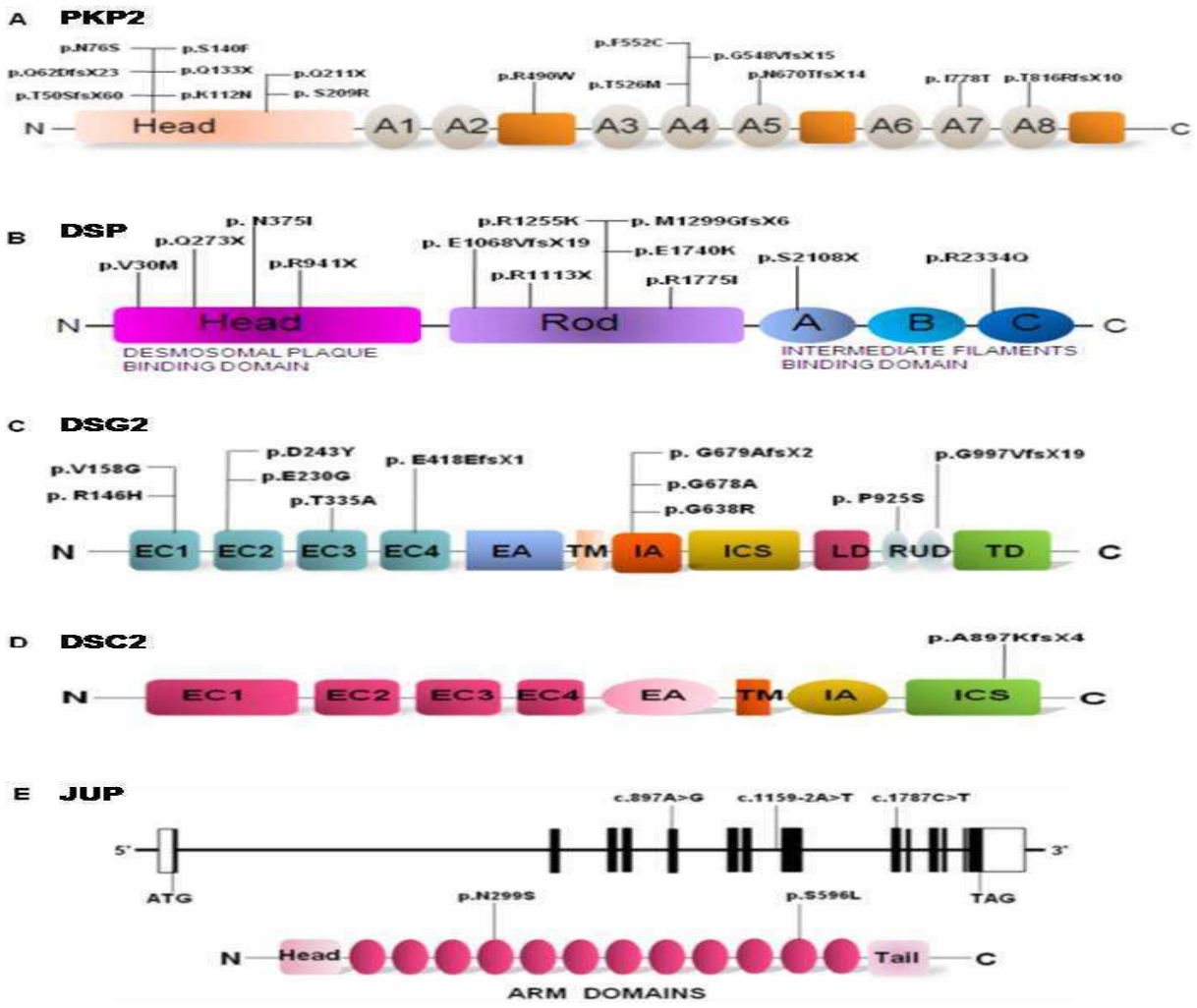

Fig.16: Schematic representation of desmosomal proteins and relative positions of variants identified in this study. **A.** Plakophilin-2 belongs to armadillo protein family. It is composed of an Head domain and 8 Arm domains, composed of imperfect 42aa-repetitions organized in three alpha-helices. The positive charged surface acts as a binding site for different molecular partners, such as cadherins (Huber et al., 1997). The longest isoform plakophilin-2b shows also an additional domain between Arm repeats 5 and 6 that introduces a bend into the overall structure. **B.** Desmoplakin is composed of three main domains. The Head domain is involved in binding of proteins of desmosomal plaque, such as plakophilin-2 and plakoglobin. The C-terminal domain is composed of three repetitions of a 38-amino acids domain forming a platform for desmin intermediate filaments binding. The central Rod domain has an helicoidal structure, involved in homodimerization of the protein. **C-D.** Desmoglein-2 and desmocollin-2 are characterized by the presence of four extracellular domains (EC) followed by an extracellular anchor domain (EA), all essential for homo- and heterodimerization of cadherins Ca^{2+}-dependent. Other cadherin domains are transmembrane domain (TM), intracellular anchor domain (IA), and an intracellular sequence typical of cadherins (ICS). Moreover, in desmoglein-2, an intracellular linker rich in Proline (LD), a variable number of repeated units (RUD) and a terminal domain Glycine-rich (TD) are also present. Up to now, functions of the different desmoglein-2 domains are unknown. **E.** Also plakoglobin belongs to armadillo protein family, due to its 12 Arm repetitions localized between an Head and a Tail domain. Splicing site mutation affecting the acceptor site of exon 8 of JUP gene is also indicated on the top of Figure 15 E.

a. Single mutations found in PKP2 gene

Human PKP2 gene (cDNA and translation sequences are available in NCBI website, NM_001005242 and NP_001005242, respectively) contains 14 coding exons. Alternative splicing of PKP2 gene produces two protein isoforms, differing in length. Mutation screening was performed in PKP2 corresponding to the longest isoform. All the amplified fragments consisted of a single exon flanked by intronic regions, exception made for exons 5, 12, and 14, which were divided in two fragments. Exons 1, 3, 6, 12a, and 12b were analyzed by direct sequencing, because the nucleotide sequences showed denaturation domains unsuitable for dHPLC analysis. Several polymorphisms reported in dbSNP were detected (not reported). In Table 6 pathogenic mutations are listed. Relative position of mutations identified in this study is reported in Figure 15.

EXON	# INDEX CASE	NT SUBSTITUTION	AA SUBSTITUTION	POSITION (PROTEIN DOMAIN)	REFERENCES
1	12, 18, 52	c.145_148delCAGA	p.T50SfsX60	Head	Gerull et al., 2004; Syrris et al., 2006; Dalal et al., 2006; Van Tintelen et al., 2006
	40	c.184_185delCA	p.Q62DfsX23	Head	-
2	46	c.227A>G	p.N76S	Head	-
	33	c.336G>T	p.K112N	Head	-
3	71	c.397C>T	p.Q133X	Head	Van Tintelen et al., 2006, Cox et al., 2011
	58	c.419C>T	p.S140F	Head	Gerull et al., 2004, Dalal et al., 2006; Syrris et al., 2006; den Haan et al., 2009
7	25	c.1642delG	p.G548VfsX15	Arm-4	Gerull et al., 2004; Basso et al., 2006; Dalal et al., 2006
10	7, 77	c.2009delC	p.N670TfsX14	Arm-5	-
12	74	c.2447_2448delCC	p.T816RfsX10	Arm-8	Xu et al., 2010

Tab.6 : Heterozygous PKP2 mutations identified in the present study.

Twelve patients out of 80 investigated (15%) resulted to carry a single mutation in PKP2 gene. Among nine identified mutations, 5 were deletions, one was nonsense, and 3 were missense variations. Five variants not reported in the literature have been classified as mutations due to their absence in the control population, to the involvement of conserved regions and of important interaction domains of plakophilin-2.

In two cases, the same single mutation occurred in more than one proband. The c.145_148delCAGA deletion (Figure 16) was detected in three index cases. This mutation causes a frameshift leading to the insertion of a premature stop codon (p.T50SfsX60) within the Head domain of the protein. Also, the novel single base-pair deletion c.2009delC was found to be carried in heterozygosity by two patients. It causes a frameshift resulting in an earlier termination of translation (p.N670TfsX14) that leads to a protein truncated in the Arm-5 domain of plakophilin-2.

Among the other frameshift mutations detected in this study, the two base-pairs deletion c.184_185delCA resulted in the anticipated introduction of a stop codon (p.Q62DfsX23), truncating the protein within its Head domain. The other two deletions (c.1642delG, causing p.G548VfsX15, and c.2447_2448delCC, causing p.T816RfsX10, Figure 17) resulted in the loss of the last Arm domains.

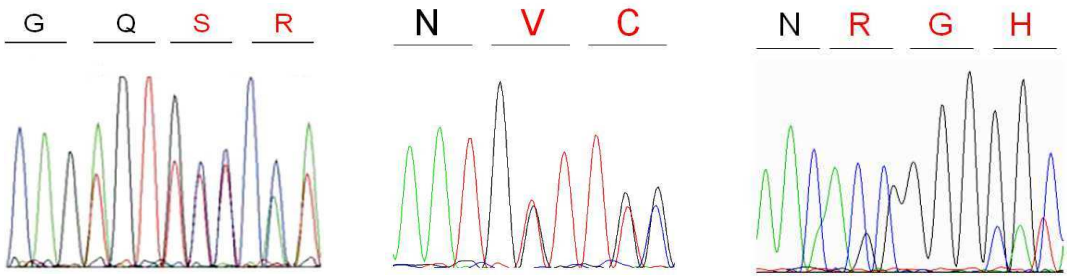

Fig.17: (From left to right) Sequence electropherograms showing the presence of heterozygous deletions found in PKP2 gene (c.145_148delCAGA, c.1642delG, and c.2447_2448delCC), leading to frameshifts mutations p.T50SfsX60, p.G548VfsX15, and p.T816RfsX10.

As far as missense mutations is concerned, only one (c.419C>T; p.S140F) was previously reported (Gerull et al., 2004, Dalal et al., 2006; Syrris et al., 2006; den Haan et al., 2009). Moreover, only p.N76S resulted to be a conservative change. On the contrary, p.K112N replaces a positive-charged amino acid (Lysine) by an hydrophilic one (Asparagine), and p.S140F changed an hydrophilic amino acid (Serine) with an hydrophobic aromatic one (Phenylalanine). All the three missense mutations affect the Head domain of plakophilin-2. Also the only nonsense mutation identified (p.Q133X) resulted to affect the Head domain of the protein. All the amino acids involved in the missense mutations are conserved among different organisms (Figure 18).

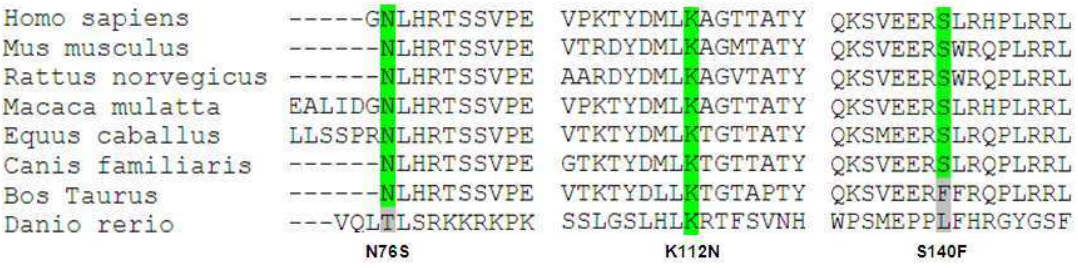

Fig.18: Sequence conservation of the three amino acids involved in the missense mutations detected in plakophilin-2 among different species.

b. Single mutations found in DSP gene

Human DSP gene (cDNA and translation sequences are available in NCBI website, NM_004415 and NP_004406, respectively) contains 24 coding exons. Alternative splicing of DSP gene produces two protein isoforms, but only the isoform I is expressed in cardiac muscle. Mutation screening was performed in DSP corresponding to the isoform I. All the amplified fragments consisted of a single exon flanked by intronic regions, exception made for long exons 23 and 24, which were divided into several shorter overlapping fragments.

Amplicons 8, 18, 22, 24a, 24f and 24i were analyzed by direct sequencing, because the nucleotide sequences showed denaturation domains unsuitable for dHPLC analysis. Several polymorphisms reported in dbSNP were detected (not reported). In Table 7 identified variants are listed. Relative position of substitutions found in this study is reported in Figure 16.

EXON	# INDEX CASE	NT SUBSTITUTION	AA SUBSTITUTION	POSITION (PROTEIN DOMAIN)	REFERENCES
1	42	c.88G>A	p.V30M	Head	Yang et al., 2006
7	30	c.817C>T	p.Q273X	Head	-
20	36	c.3100C>T	p.R941X	Head	Quarta et al., 2011
23	49	c.3337C>T	p.R1113X	Rod	Sen-Chowdhry et al., 2008; Asimaki et al., 2009; Cox et al., 2011
24	4	c.6323C>A	p.S2108X	C-terminal	-
24	61	c.7001G>A	p.R2334Q	C-terminal	-

Tab. 7:. Heterozygous DSP mutations identified in the present study.

Six investigated probands out of 80 (7,5%) resulted to carry a single heterozygous mutation in DSP gene. Among six variations identified in these cases, two were missense and four were nonsense mutations. Only two variations have been previously reported in literature. p.V30M conservative amino acid change occurs in the Head domain of desmoplakin, involved in the binding to plakoglobin and plakophilin-2. *In vitro* studies showed that this missense variation affects the correct localization of desmoplakin, probably disrupting the binding with cytolinker desmosomal proteins (Yang et al., 2006). p.R1113X nonsense mutation causes the introduction of a stop codon within the Rod domain in desmoplakin, that forms homodimeric coiled-coil structures (Sen-Chowdhry et al., 2008; Asimaki et al., 2009, Cox et al., 2011). The predicted truncated molecule lacks most central Rod domain and completely lacks C-terminal domain interacting with desmin intermediate filaments.

The non conservative change p.R2334Q and the other three nonsense variations detected weren't reported in literature and haven't been identified in the control population. In the missense mutation p.R2334Q, a positive Arginine is replaced by an hydrophilic Glutammine in the C-terminal domain of desmoplakin, affecting a conserved amino acid. p.Q273X and p.R941X produce a premature stop codon in the Head domain of desmoplakin, while p.S2108X affects the C-terminal domain. Truncated proteins in the Head and C-terminal domains are predicted to interact abnormally with plakoglobin and plakophilin-2, and with desmin, respectively.

c. Single mutations found in DSG2 gene

Human DSG2 gene (cDNA and translation sequences are available in NCBI website, BC099657 and NP_001934, respectively) contains 15 coding exons. All the amplified fragments consisted of a single exon flanked by intronic regions, exception made for exons 7 and 8, which were amplified as a single fragment, and exons 9, 14, and 15, which, on the contrary, were subdivided into two or more fragments. Amplicons 3, 5, 7+8, 12, and 14d

were analyzed by direct sequencing, because the nucleotide sequences showed denaturation domains unsuitable for dHPLC analysis. Several polymorphisms reported in dbSNP were detected (not shown). In Table 8 identified variants are listed. Relative position of variations found in this study is reported in Figure 16.

EXON	# INDEX CASE	NT SUBSTITUTION	AA SUBSTITUTION	POSITION (PROTEIN DOMAIN)	REFERENCES
5	68	c.473T>G	p.V158G	EC1	Syrris et al., 2007; Posch et al., 2008; Bhuiyan et al., 2009
7	5	c.727G>T	p.D243Y	EC2	-
8	80	c.1003A>G	p.T335A	EC3	den Haan et al., 2009; Bauce et al., 2010; Cox et al., 2011
14	66	c.2033G>C	p.G678A	IA	-
	1	c.2036delG	p.G679AfsX2	IA	Pilichou et al., 2006

Tab. 8: Heterozygous DSG2 mutations identified in the present study.

.

Five probands resulted to carry a single mutation in DSG2 gene (6,25%). Four of the variations found in these patients were missense substitutions, while one was a frameshift mutation caused by a single base pair deletion. As far as missense mutations are concerned, only p.D243Y and p.T335A are non conservative changes, as both involve amino acids with different chemical properties, while all of the four affect conserved residues and interest functional domains important for desmoglein-2 interactions. In fact, extracellular domains (EC), involved in adhesive interactions Ca^{2+}-dependent with other cadherins, are affected by p.V158G (EC1), p.D243Y (EC2), and p.T335A (EC3), and intracellular anchor (IA) domain is affected by p.G678A. A microdeletion of a single base pair (c.2036delG) was also identified. This variation results in a frameshift (p.G679AfsX2) leading the introduction of 2 novel amino acids, in the IA domain of desmoglein-2. The predicted truncated protein would maintain the transmembrane domain, but it would lose all the cytoplasmic portion.

Two novel variations have been identified and weren't detected in the control population (p.D243Y and p.G678A). The p.V158G variant has been reported in two families as potentially pathogenic (Syrris et al., 2007); however, later, it has also been detected by other groups in healthy controls (Posch et al., 2008; Bhuiyan et al., 2009). Similarly, p.T335A was reported as pathogenic by den Haan and coworkers (den Haan et al., 2009), but as unclassified variant by Cox and colleagues (Cox et al., 2011). Thus, at this stage it is difficult to determine whether these variations could be pathogenic mutations, rather than factors that in these patients could modulate the pathogenic effect of variations in other disease-genes, not yet identified.

d. Single mutation found in DSC2 gene

Human DSC2 gene (cDNA and translation sequences are available in NCBI website, NM_004949 and NP_004940, respectively) contains 16 coding exons. Alternative splicing of DSC2 gene produces two protein isoforms, differing in the C-terminal domain. Mutation screening was performed in DSC2 corresponding to the longest isoform. All the amplified

fragments consisted of a single exon flanked by intronic regions, exception made for exon 15, which was subdivided into three fragments. Exons 1 and 2 were analyzed by direct sequencing, because the nucleotide sequences showed denaturation domains unsuitable for dHPLC analysis. Several polymorphisms reported in dbSNP were detected (not shown).

Only one patient out of 80 (1,25%) resulted to carry a two-base pair insertion (c.2687_2688insGA), leading to p.A897KfsX4 frameshift variant, already reported by Syrris and co-workers (Syrris et al., 2006) as pathogenic. The same variation was identified in several probands in our lab together with other substitutions in other desmosomal genes, but only patient #14 resulted to carry this variant alone. Moreover, this insertion has been identified by our group in 6 controls out of 200 (allelic frequency of 1,5%). It affects the last exon of DSC2 gene, encoding the intracellular cadherin-typical segment domain (ICS), which is longer in the isoform DSC2a, while it's absent in the shorter isoform DSC2b, the most expressed in the heart (Figure 19). The five involved aminoacids are quite conserved among species (Figure 19). The same variation was also reported by den Haan as a polymorphism (den Haan et al., 2009).

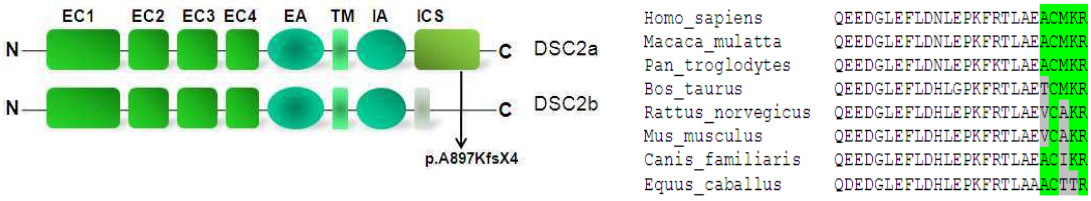

Fig. 19: (Left) p.A897KfsX4 variation identified in desmocollin-2. It affects only the longest DSC2a isoform, and not the DSC2b isoform, the most expressed in human heart. EC= extracellular domain, EA= extracellular anchor domain, TM= transmembrane domain; IA= intracellular anchor domain, ICS= intracellular cadherin-typical segment domain. (Right) Conservation of last five amino acids of desmocollin-2 among different species.

e. Single mutations found in JUP gene

Human JUP gene (cDNA and translation sequences are available in NCBI website, NM_002230 and NP_002221, respectively) contains 14 coding exons. Alternative splicing of JUP gene produces two plakoglobin isoforms, differing in length. Mutation screening was performed in JUP corresponding to the longest isoform. All the amplified fragments consisted of a single exon flanked by intronic regions, exception made for exons 6, 7, 11, and 12, which were amplified in two fragments (6+7 and 11+12), and for exon 14 that, on the contrary, was subdivided into four fragments. Fragments 1, 11+12, 14A and 14C were analyzed by direct sequencing, because the nucleotide sequences showed denaturation domains unsuitable for dHPLC analysis. Several polymorphisms described in dbSNP were detected (not reported). In Table 9 pathogenic mutation are listed. Relative position of mutations detected in this study is reported in Figure 16.

EXON	# INDEX CASE	NT SUBSTITUTION	AA SUBSTITUTION	POSITION (PROTEIN DOMAIN)	REFERENCES
5	21	c.897A>G	p.N299S	Arm-4	-
8	41	c.1159-2A>T	-	-	-

Tab. 9: Heterozygous JUP mutations identified in the present study.

Two probands out of 80 (2,5%) resulted to carry a variation in JUP gene. One of them carried a missense mutation, the other one carried a splice site alteration. Both variants, detected by dHPLC analysis (Figure 20) followed by DNA sequencing, were not reported in literature and weren't found in the healthy controls. The novel missense mutation, affecting Arm-4 domain, consists of a conservative amino acid change, as both Serine and Asparagine are hydrophilic residues. However, Asparagine shows a different sterical crowding, due to the aminic group and to its structural rigidity, given by the double bond of the carbonilic group in its lateral chain, both absent in Serine.

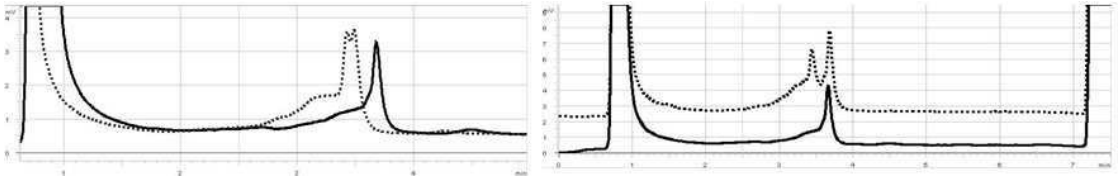

Fig. 20: dHPLC elution patterns of JUP amplicon 5 of proband #21 (left) and amplicon 8 of JUP of proband #41 (right) (dotted) and of healthy control (continuous black line), both at 63.7°C analysis temperature.

The only splice site alteration detected in this study was identified in acceptor site of exon 8 of JUP gene in patient #41 (c.1159-2A>T) and affects a nucleotide conserved among different organisms (Figure 21). This variation could alter the correct splicing of exon 8, with possible consequences on the correct transcription.

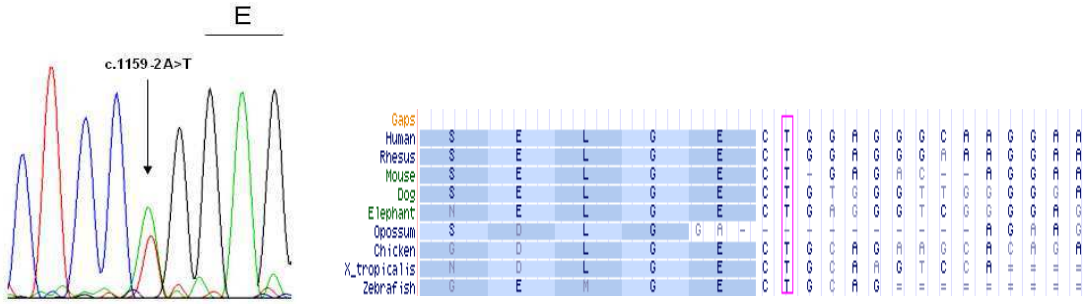

Fig. 21: (Left) Sequence electropherogram showing the presence of the heterozygous mutation c.1159-2A>T detected in amplicon 8 of proband #41. (Right) Reverse complement of sequence of amplicon 8 of JUP gene showing the conservation among different species of Adenine 1159 involved in the change.

Unluckily, proband's cardiac biopsy wasn't available and JUP gene isn't expressed in lymphocytes, thus further studies couldn't be performed to determine the effects of this mutation in mRNA maturation.

f. Multiple mutations found in desmosomal genes

Ten patients out of 80 (12,5%) carried more than one mutation in the same gene (compound heterozygous) or in two different genes (digenic heterozygous). The distribution of the multiple mutations are listed in Table 10.

# INDEX CASE	GENE	EXON	NT SUBSTITUTION	AA SUBSTITUTION	POSITION (PROTEIN DOMAIN)	REFERENCES
2	DSP	9	c.1124A>T	p. N375I	Head	De Bortoli et al., 2010
	DSG2	13	c.1912G>A	p.G638R	IA	De Bortoli et al., 2010
	DSC2	16	c.2687_2688insGA	p.A897KfsX4	ICS	Syrris et al., 2006, De Bortoli et al., 2010, Den haan et al., 2009
8	DSP	9	c.1124A>T	p.N375I	Head	De Bortoli et al., 2010
	PKP2	7	c.1655T>G	p.F552C	Arm-4	De Bortoli et al., 2010
	DSC2	16	c.2687_2688insGA	p.A897KfsX4	ICS	Syrris et al., 2006, De Bortoli et al., 2010, Den haan et al., 2009
16	DSG2	6	c.689A>G	p.E230G	EC2	-
	DSP	23	c.5324G>T	p.R1775I	Rod	Bauce et al., 2005
27	DSG2	9	c. 1254_1257insATGA	p. E418EfsX1	EC4	Pilichou et al., 2006, Basso et al., 2006
		15	c.2983delG	p.G997VfsX19	RUD	-
34	DSP	23	c.3203_3204delAG	p. E1068VfsX19	Rod	-
			c.5218G>A	p.E1740K		-
	DSG2	15	c.2773C>T	p. P925S	RUD	-
55	PKP2	6	c.1468C>T	p.R490W	Portion between Arm-2 and Arm-3	-
		7	c.1577C>T	p.T526M	Arm-4	den Haan et al., 2009
56	DSP	23	c.3764G>A	p.R1255K	Rod	Bauce et al., 2005
	PKP2	3	c.631C>T	p.Q211X	Head	Xu et al.,2010
		12	c.2333T>C	p. I778T	Arm-7	Xu et al., 2010
60	DSP	23	c.3894_3895insGGTC	p. M1299GfsX6	Rod	-
	JUP	11	c.1787C>T	p. S596L	Arm-11	-
63	PKP2	12	c.2447_2448delCC	p.T816RfsX10	Arm-8	Xu et al., 2010
		3	c.627C>G	p. S209R	Head	Xu et al., 2010
	DSG2	5	c.437G>A	p. R146H	EC1	Xu et al., 2010
73	PKP2	1	c.145_148delCAGA	p.T50SfsX60	Head	Gerull et al., 2004; Syrris et al., 2006; Dalal et al., 2006; Van Tintelen et al., 2006
	DSG2	13	c.1912G>A	p.G638R	IA	De Bortoli et al., 2010

Tab. 10: Multiple mutations identified in the present study.

Two cases of compound heterozygosity have been observed. Patient #27 resulted to carry a four base-pairs insertion (c.1254_1257insATGA) and a single base-pair deletion (c.2983delG) in DSG2 gene. Both variations were inherited *in trans* and resulted in the

frameshift mutations p.E418EfsX1 in EC4 domain and p.G997VfsX19 in repeat unit domain (RUD) of desmoglein-2, respectively. The predicted truncated proteins would lack transmembrane and cytoplasmic components, and a small portion of cytoplasmic domain, respectively. Also patient #55, female, showing a classic form of ARVC/D, was a compound heterozygous, as she carried two different mutations in PKP2 gene: c.1468C>T, in exon 6, and c.1577C>T in exon 7. Both substitutions resulted in a non conservative amino acid change (p.R490W and p.T526M). In particular, p.R490W replaces a positive-charged Arginine with an hydrophobic Tryptophan residue, carrying a bigger sterical crowding, given by the aromatic group in the lateral chain. This variation affects a residue belonging to a 44-amino acid sequence, between the second and the third Arm domain of plakophilin-2, while p.T526M affects Arm-4 domain. The latter wasn't detected in Italian control population, but it was reported as a rare polymorphism by den Haan and colleagues (den Haan et al., 2009).

Also several cases of digenic heterozygosity have been detected in the present study.

Proband #16 carried a novel mutation identified in exon 6 of DSG2 gene (c.689A>G), absent in the control population. This transition leads to the missense variation p.E230G, occurring in a residue highly conserved in different species and located in the EC2 domain of desmoglein-2. The negative charged Glutamic acid in position 230 is replaced by an hydrophobic and smaller Glycine. In the same patient, also the known variation c.5324G>T in exon 23 of DSP gene was detected (Bauce et al., 2005). The resulting amino acid substitution, p.R1775I, occurs in the Rod domain of desmoplakin and involves a positive amino acid (Arginine), replaced by an hydrophobic residue (Isoleucine).

Also, two different variants have been identified in DSP and JUP genes in proband #60. The first one is a four base pairs insertion (c.3894_3895insGGTC), resulting in a frameshift variation (p.M1299GfsX6) in Rod domain of desmoplakin, and the other is a non conservative missense mutation in the Arm-11 domain of plakoglobin (p.S596L). The latter replaces an hydrophilic Serine with an hydrophobic Leucine. Both mutations haven't been detected in 250 healthy patients. Genetic analysis was performed in the available family members. It figured out that DSP mutation was inherited from the paternal side (I,1, Figure 22), while JUP mutation from the proband's mother (I,2, Figure 22). Patient's son (III,1, Figure 22) carries only the DSP mutation, while both the two twin doughters aged 13 years old (III,2 and III,3, Figure 22) carry all of the two mutations, but up to now they are asymptomatic.

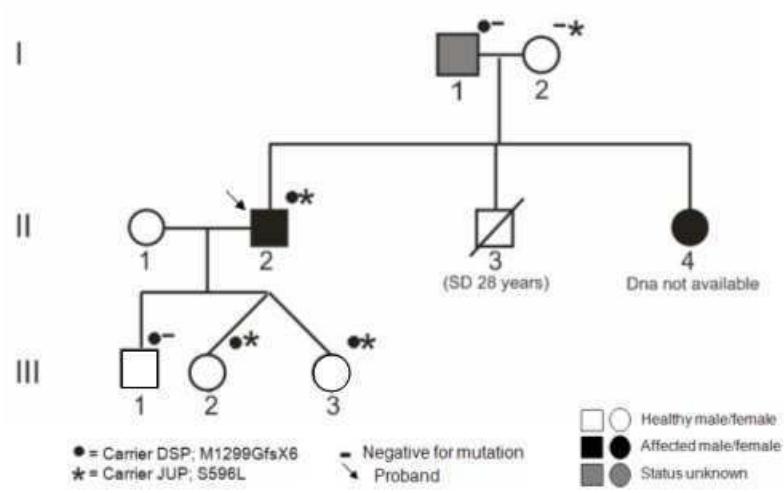

Fig. 22: Pedigree of family of patient #60. Index patient is indicated by an arrow. Black, white and grey symbols represent clinically affected and unaffected individuals, and subjects of unknown disease status, respectively. The trait denotes the absence of mutation.

In proband #73, two different mutations have been identified: the four base-pairs deletion c.145_148delCAGA (p.T50SfsX60) in PKP2 gene and the nucleotide change c.1912G>A (p.G638R) in DSG2 gene. The first affects the Head domain of plakophilin-2 and the latter replaces an hydrophobic Glycine by a positive-charged Arginine in desmoglein-2 intracellular anchor (IA) domain. While c.145_148delCAGA has been previously reported by different groups (Gerull et al., 2004; Syrris et al., 2006; Dalal et al., 2006; Van Tintelen et al., 2006), c.1912G>A was a novel substitution (later published by De Bortoli et al., 2010). Both variations have been detected in other probands investigated in this study: c.145_148delCAGA in index cases #12, #18, and #52, and c.1912G>A in patient #2.

Finally, patients #2 and #8, both showing a severe form of ARVC/D, resulted to carry two mutations and a polymorphism. They shared two variations: the novel mutation c.1124A>T in DSP gene, resulting in the missense change p.R375I in the Head domain of desmoplakin, and the rare variant c.2687_2688insGA (p.A897KfsX4) in DSC2 gene (Figure 19) (De Bortoli et al., 2010). The other variations found in the two probands consist of two missense mutations: p.G638R in desmoglein-2, found in patient #2 (and also in index case #73), and p.F552C, affecting Arm-4 domain of plakophilin-2, detected in proband #8. Both these variations haven't been found in 250 healthy subjects (Syrris et al., 2006; De Bortoli et al., 2010) and were considered mutations.

The genetic study was extended to available relatives of the two probands. In both families, only the two index cases carried all the three variants. Interestingly, among relatives of index case #8 (II,1, Figure 23), the proband's niece (III,1, Figure 23), even if she doesn't carry none of the variations, is clinically affected. It can be speculated that the pathological phenotype in this subject could be due to another (or others) mutation in a known gene, or in a gene still unidentified.

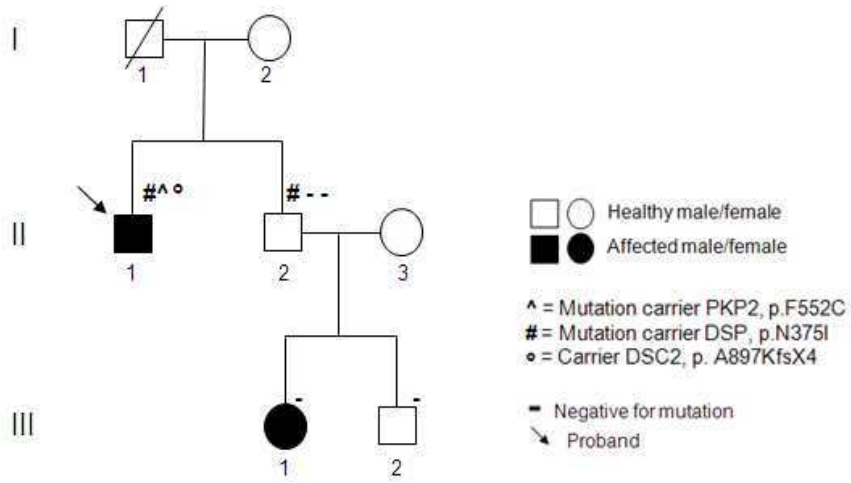

Fig. 23: Pedigree of family of patient #8. Index patient is indicated by an arrow. Black and white symbols represent clinically affected and unaffected individuals, respectively. The trait denotes the absence of mutation.

In other index cases, three mutations in two different genes have been found in the same patient.

Index case #34 carried a mutation in DSG2 gene, c.2773C>T, leading the missense variation p.P925S affecting RUD domain, and two mutations in DSP gene: the deletion c.3203_3204delAG, resulting in p.E1068VfsX19, and the point mutation c.5218G>A, resulting in p.E1740K, both affecting Rod domain of desmoplakin. Both missense mutations consist of non-conservative amino acid changes, as p.E1740K replaces a negative Glutamic acid with a positive Lysine, and p.P925S substitutes an hydrophobic Proline carrying a rigid structure, due to the presence of a cyclic ring in its side chain, by an hydrophilic and smaller Serine. None of the identified changes were reported in the literature, nor were detected in the control population. Genetic screening of proband's family members revealed that DSG2 mutation and DSP frameshift mutation were inherited from the father (I,1, Figure 24), while the DSP missense mutation was inherited from the mother (I,2, Figure 24). One of proband's sisters (II,2), carrying the two DSP mutations, showed a severe phenotype.

Fig. 24: Pedigree of family of patient #34. Index patient is indicated by an arrow. Black and white symbols represent clinically affected and unaffected individuals, respectively. The trait denotes the absence of mutation.

Other three different variations have been detected in patient #56: the known p.R1255K conservative amino acid change occurring in the Rod domain of desmoplakin (Bauce et al.,

2005) and two mutations in PKP2 gene, inherited *in trans*. One is the nonsense variation p.Q211X (c.631C>T) causing the insertion of a premature stop codon in the Head domain of the protein, and the other one is the nucleotide change c.2333T>C, resulting in the substitution of the hydrophobic Isoleucine 778 with an hydrophilic Threonine (p.I778T), altering a highly conserved residue in Arm-7 domain of plakophilin-2. None of the two novel substitutions was observed in 250 healthy subjects (Xu et al., 2009).

In proband #63, who showed a severe form of ARVC/D, three novel variations have been detected, consisting of the two-nucleotides deletion c.2447_2448delCC in PKP2 gene, that results in the frameshift mutation p.T816RfsX10 (also detected in proband #74), and the two nucleotide changes c.627C>G, in PKP2 gene, and c.437G>A, in DSG2 gene (Xu et al., 2010). The two resulting missense mutations, p.S209R and p.R146H, affect the Head domain of plakophilin-2, and the EC1 domain of desmoglein-2, respectively. While p.S209R replaces an hydrophilic Serine by a positive-charged Arginine in plakophilin-2, p.R146H is a conservative change, as the basic Arginine 146 of desmoglein-2 is substituted by an Histidine, another basic amino acid, that however brings a wider sterical crowding due to an imidazole ring in its sidechain. This substitution could alter the homophilic intercellular associations of desmoglein-2. All the identified variations weren't detected in the control population.

4.2.2 Mutation screening in CTNNA3 gene

CTNNA3 gene, coding for alphaT-catenin, was considered a good candidate ARVC gene, because of its expression and function in cardiomyocytes.

Patients' DNA was investigated by dHPLC and direct sequencing. PCR primers flanking each exon of the human CTNNA3 gene were designed by PRIMER3 software. For amplicons size, primers sequences, amplification and analysis conditions see Appendix. dHPLC analysis conditions were set up by the NAVIGATOR^{TM} software (Transgenomics). Samples showing a change in dHPLC elution pattern were sequenced. Human CTNNA3 gene (cDNA and translation sequences available in NCBI website, NM_013266 and NP_037398, respectively) contains 18 coding exons. Alternative splicing of CTNNA3 gene produces two isoforms of alphaT-catenin that differ in length. Mutation screening was performed in CTNNA3 corresponding to the longest isoform. All the amplified fragments consisted of a single exon flanked by intronic regions. Exons 1, 2, 8, 10, 14 and 18 were analyzed only by direct sequencing, because the nucleotide sequences showed denaturation domains unsuitable for dHPLC analysis.

Several polymorphisms listed in the dbSNP database were found (not reported). Moreover, four exonic unknown variations have been identified and weren't found in 250 ethnically-matched healthy controls (Table 11).

EXON	# INDEX CASE	NT SUBSTITUTION	AA SUBSTITUTION	POSITION (PROTEIN DOMAIN)	SIFT prediction	Poly-Phen2 prediction
3	71	c.281T>A	p.V94D	Beta-catenin binding site/homodimerization domain overlapping sequence	Affect protein funcion	Probably damaging PSIC: 0.964
6	38	c.779A>G	p.Q260R	Homodimerization domain	Tolerated	Possibly damaging PSIC: 0.508
13	21	c.1748T>C	p.V583A	Actin binding domain	Tolerated	Benign
17	41	c.2293_2295delTTG	p.del765L	Actin binding domain	-	-

Tab. 11: Heterozygous CTNNA3 mutations identified in the present study.

.

Relative position of mutations detected in this study are reported in Figure 25.

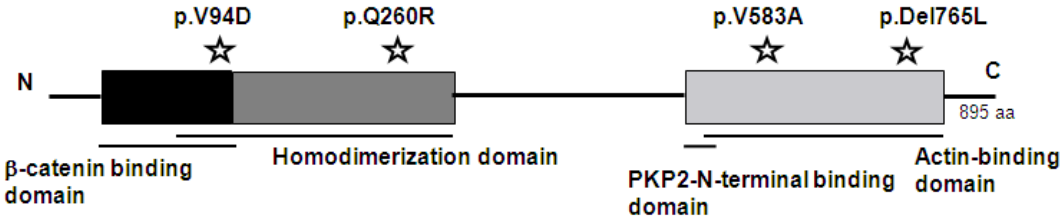

Fig. 25: Schematic representation of human alphaT-catenin and relative position of identified mutations. All of them are located in important interaction domains.

c.281T>A, p.V94D

By means of dHPLC analysis of exon 3 of CTNNA3, an abnormal elution profile was identified in index case #71 (Figure 26). DNA sequencing of the amplicon showed the c.281T>A nucleotide change carried in heterozygosity (Figure 26).

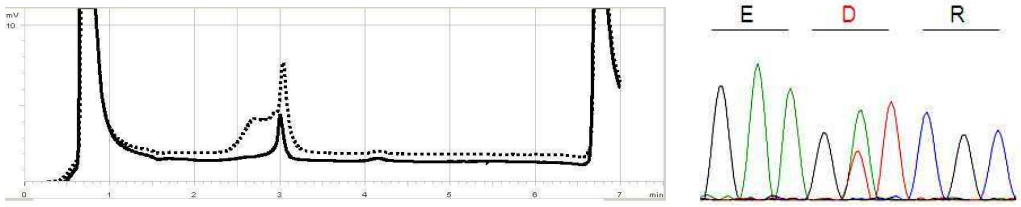

Fig. 26: (Left) dHPLC elution patterns of CTNNA3 amplicon 3 in the proband #71 (dotted) and in healthy control at 58.2°C analysis temperature. (Right) DNA sequencing of CTNNA3 fragment 3 revealing c.281T>A variation (p.V94D).

This change results in the missense mutation p.V94D, that interests a residue highly conserved among different species and alpha-catenin family members (Figure 27), located in the β-catenin binding site and homodimerization domain overlapping region of alphaT-catenin. The mutation replaced an hydrophobic residue (Valine) by a negative-charged one (Aspartic acid), that brings a different sterical crowding, given by the carbonilic group in the lateral chain.

Using SIFT and Poly-Phen2 software tools this mutation resulted to affect protein function and to be probably damaging (Table 11).

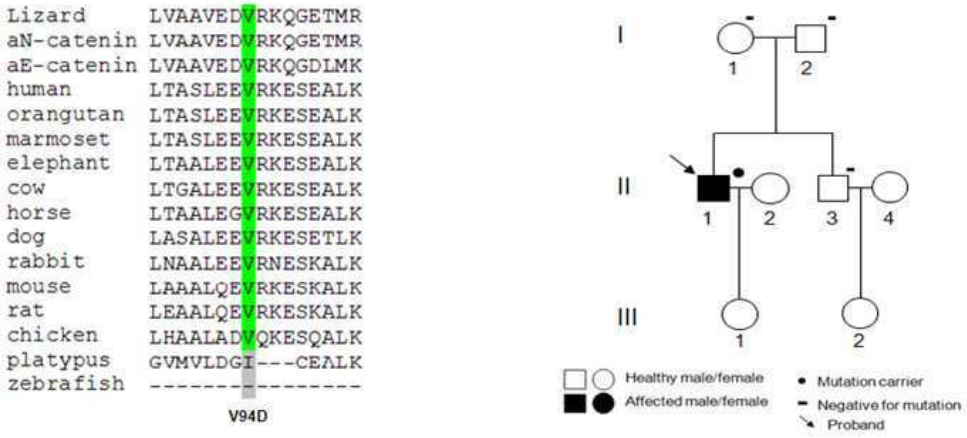

Fig. 27: (Left) ClustalW alignment of portion of beta-catenin-binding site overlapping homodimerization domain in alphaT-catenin among different species and alpha-catenin family members, showing the high conservation of V94. (Right) Pedigree of family of patient carrying p.V94D missense mutation. Index patient #71 is indicated by an arrow. Black and white symbols represent clinically affected and unaffected individuals, respectively. The black dot indicates the presence of the mutation, while the trait denotes its absence.

The proband (II,1, Figure 27) was diagnosed at the age of 14 years, at a prepartecipation screening for sport activity. The patient showed ECG abnormalities, consisting of sustained VT of LBBB morphology with superior axis, and negative T waves in V1-V4 in the absence of complete RBBB QRS ≥ 120 ms. Late potentials were evidenced with 25, 40, and 80 filter setting in the absence of a QRS duration of ≥ 110 msec. 2D-echocardiogram showed a severe dilatation of the RV with marked hypokinesia of the free wall, reduced right ventricular ejection fraction (EF), anterior, apical and subtricuspidal akinesia, and mild dilatation of the LV. Moreover, MRI showed mild dilatation of the RV, apical sacculation, and regional right ventricular akinesia with RVEF of 30%. After three transcatheter ablations, the proband received an implantable cardioverter defibrillator, at the age of 36 years.

The variation resulted to be a *de novo* mutation, as the parents (I,1; I,2, Figure 27) and the brother (II,3, Figure 27) are asymptomatic with clinically negative history and don't carry the p.V94D mutation.

c.779A>G p.Q260R

The unknown c.779A>G nucleotide variation was found in exon 6 of patient #38 through dHPLC analysis (Figure 28). It resulted in the missense mutation p.Q260R that involves a conserved amino acid in the homodimerization domain of alphaT-catenin (Figure 28). In this mutation, an hydrophilic aminoacid is replaced by a positive-charged one. Using Poly-Phen2 tool, the variation resulted to be possibly damaging (Table 11).

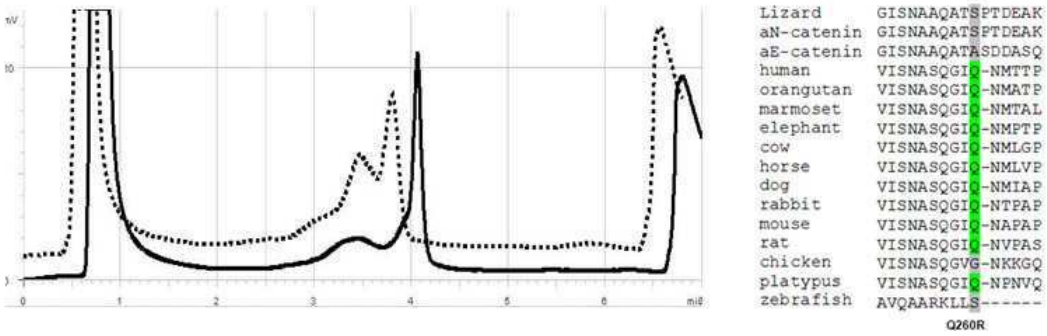

Fig. 28: (Left) dHPLC elution patterns of CTNNA3 amplicon 6 in proband #38 (dotted) and in healthy control at 55.2°C analysis temperature. (Right) ClustalW alignment of portion of homodimerization domain in alphaT-catenin among species and alpha-catenin family members, showing the conservation of Q260.

The proband (I,1, Figure 28) was diagnosed at the age of 41 years, due to an episode of non-sustained VT (NSVT) with superior axis. More recently, he manifested NSVT of LBBB morphology with inferior axis. He also showed positive SAECG at 25, 40 and 80 filter setting in the absence of a QRS duration of ≥ 110 msec. Echocardiogram demonstrated an akinetic right ventricular free wall together with moderate right ventricular dilatation (PLAX RVOT > 32 mm), and posterior wall hypokinesia. He's currently undergoing an antiarrhythmic therapy with sotalol. His two sons are also carriers of the p.Q260R missense mutation (II,1 and II,2, Figure 29). The older, examined at the age of 20 years due to ARVC/D family history, showed minor signs of the disease (apical and subtricuspidal hypokinesia with mild right ventricular dilatation on 2D-echo, and positive SAECG). The other son, aged 21 years, is completely asymptomatic and refused clinical investigation.

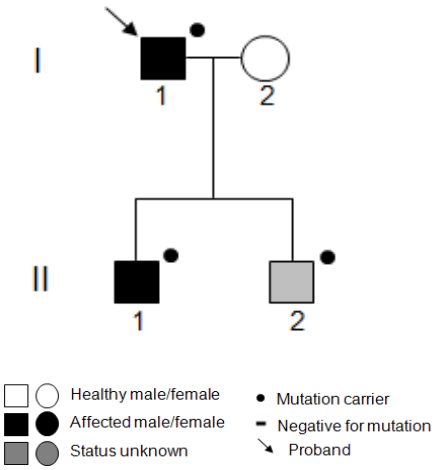

Fig.29: Pedigree of family of patient carrying p.Q260R missense mutation. Index patient #38 is indicated by an arrow. Black, white and grey symbols represent clinically affected and unaffected individuals and subjects of unknown disease status, respectively. The black dot indicates the presence of the mutation, while the trait denotes its absence.

c.1748T>C, p .V583A

The novel variation c.1748T>C (p.V583A) was detected by dHPLC (Figure 30) analysis followed by DNA sequencing in exon 13 of patient #21. It involves an aminoacid conserved among different species and alpha-catenin family members (Figure 30) and it is located in the actin binding domain. p.V583A is a conservative substitution, as both aminoacids are hydrophobic.

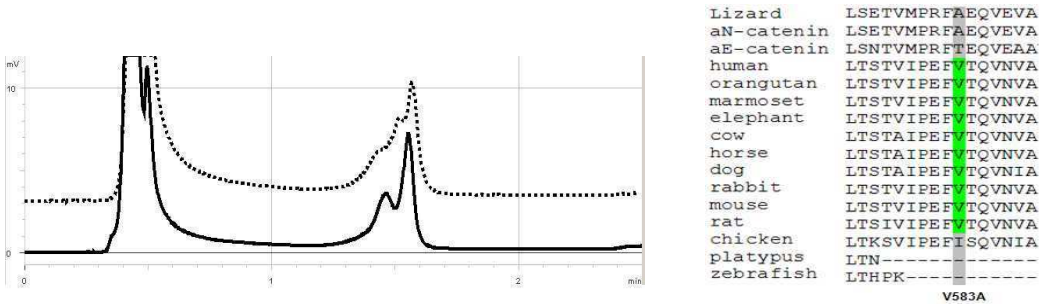

Fig. 30: (Left) dHPLC eluition patterns of CTNNA3 amplicon 13 in the proband #21 (dotted) and in healthy control at 52.9°C analysis temperature. (Right) ClustalW alignment of portion of actin binding domain in alphaT-catenin among species and alpha-catenin family members, showing the conservation of V583.

The proband (III,2, Figure 31) was examined at the age of 15 years, due to familial sudden death. His father (II,1, Figure 31) died suddenly at the age of 39 because of ARVC/D. The autoptic examination showed fibro-fatty tissue replacement in the whole right ventricular wall and aneurysms. Also two proband's uncles (II, 3 and II,4, Figure 31) died suddenly at the age of 31, but autopsy was not performed.

The proband showed at ECG more than 500 extrasystoles/24 hours, while the echocardiogram demonstrated mild dilatation of the RV and hypokinesia of posterior right ventricular free wall. Moreover, he underwent cardiopalm and he is currently treated with antiarrhythmic drugs.

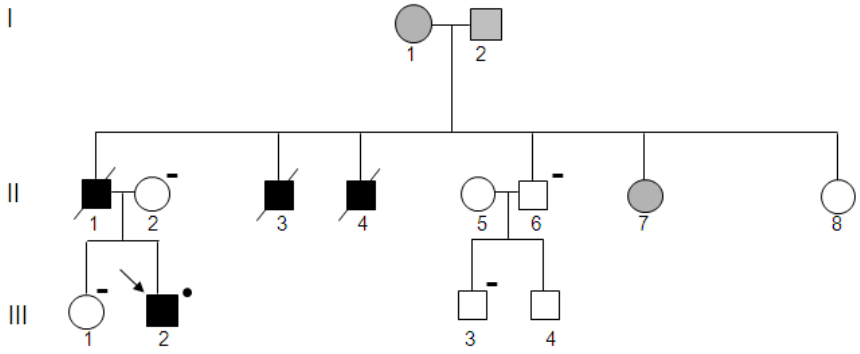

Fig. 31: Pedigree of family of patient carrying p.V583A missense mutation. Proband #21 is indicated by an arrow. Black, white and grey symbols represent clinically affected and unaffected individuals and subjects of unknown disease status, respectively. The black dot indicates the presence of the mutation, while the trait denotes its absence.

c.2293_2295delTTG, p.765DelL

By dHPLC analysis and following sequencing of amplicon 17 a novel three base pairs deletion was identified in patient #41 (Figure 32). This variation causes the loss of the highly conserved Leucine 765 in the actin binding site (Figure 32).

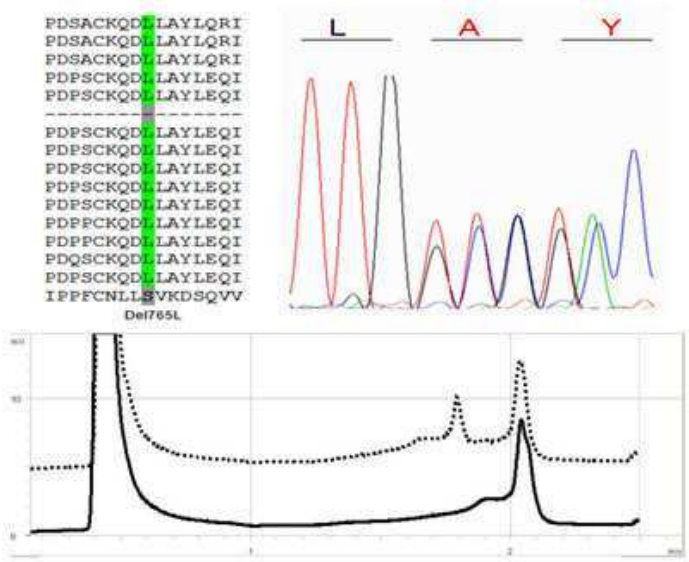

Fig. 32: Top:(Left) ClustalW alignment of portion of actin-binding domain in alphaT-catenin among species and alpha-catenin family members, showing the high conservation of L765. (Right) DNA sequencing of CTNNA3 fragment 3 revealing c.2293_2295delTTG deletion (p.del765L). Bottom: dHPLC eluition patterns of CTNNA3 amplicon 17 in the proband #41 (dotted) and in healthy control at 58.5°C analysis temperature.

The proband (III,23, Figure 33) was examined at the age of 15 years, due to an episode of syncope. The ECG and the ECG Holter showed non sustained ventricular arrhythmias with LBBB with superior axis. Moreover, late potentials were present at 40 and 80 filter setting in the absence of a QRS duration of ≥ 110 msec. Echocardiogram evidenced a mild right ventricular dilatation. The proband is currently undergoing an antiarrhythmic therapy with sotalol. Her father (II,12, Figure 33), carrying the same mutation, did not fulfil the current diagnostic criteria of ARVC/D. He showed a mild right ventricular dilatation (PLAX RVOT= 30 mm) at 2D-echo. Two asymptomatic investigated relatives (II,1 and II,5, Figure 33) don't carry this variation. On the contrary, other two family members (II,7 and III, 18, Figure 33), clinically unaffected carry the same variant. The absence of signs of the disease could be due to the incomplete penetrance typical of ARVC/D.

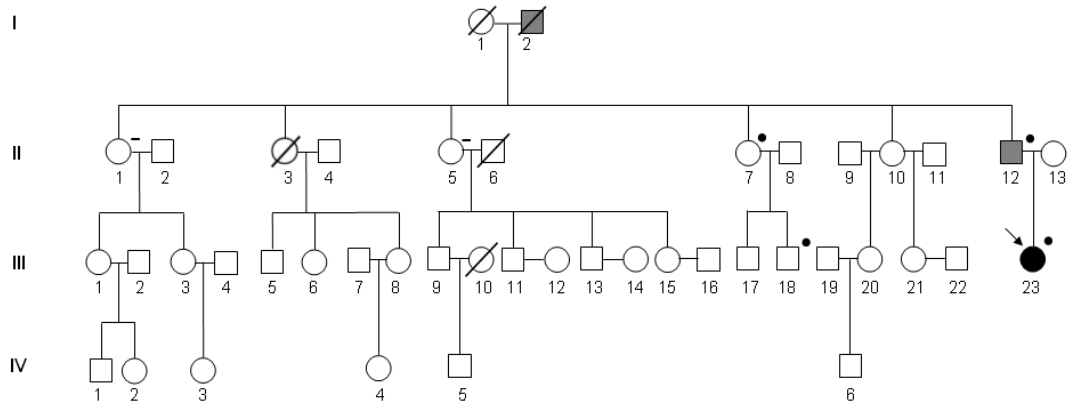

Fig. 33: Pedigree of family of patient carrying p.del765L deletion. Proband #41 is indicated by an arrow. Black and white symbols represent clinically affected and unaffected individuals, respectively. The black dot indicates the presence of the mutation, while the trait denotes its absence.

4.3 FUNCTIONAL STUDIES TO EVALUATE THE PATHOGENIC EFFECTS OF CTNNA3 MUTATIONS

4.3.1 Transfection experiments in HL-1 cells and in neonatal rat cardiomyocytes

To evaluate pathogenicity of missense mutations p.V94D, p.Q260R, p.V583A, and of deletion p.del765L found in CTNNA3 gene in ARVC/D patients, transfection experiments were performed in HL-1 cells and in neonatal rat cardiomyocytes. Site-specific mutagenesis PCR was performed to obtain constructs containing full length CTNNA3 cDNA in frame with EGFP encoding sequence, under the control of hCMV promoter. Constructs were transfected in the desmosome-forming HL-1 cell line, characterized by a differentiated cardiac phenotype and contractile activity *in vitro*, and in neonatal rat cardiomyocytes. In all transfected cells, wild-type fusion protein was detected in the cell membrane, at the intercellular junctions level (Figure 34 Panels A-A'' and Figure 35 Panels A-A''), and co-localized with endogenous beta-catenin, marked in red (Figure 34, Panels A'-A'' and Figure 35, Panels A'-A''). Beta-catenin is a protein present both in AJs and in *area composita* and it interacts with alphaT-catenin. The same pattern was observed in all cells transfected with constructs carrying the mutations p.Q260R, p.V583A, and p.del765L (Figure 34, Panels C-C'', D-D'', E-E'' and Figure 35, Panels C-C'', D-D'', E-E''). On the contrary, in all transfected cells, p.V94D alphaT-catenin was present in the plasma membrane at lower levels, while it was predominantly localized in the cytoplasm (Figure 34, Panels B-B'' and Figure 35, Panels B-B''). Immunofluorescence experiments were performed into transfected cells staining also endogenous plakoglobin (Figures 36 and 37), which interacts with alphaT-catenin. As seen for endogenous beta-catenin, the mutated proteins don't alter the correct cellular localization of plakoglobin, which is correctly present in the plasma membrane (Figure 36, Panels B-B", C-C'', D-D'', E-E'' and Figure 37, Panels B-B", C-C'', D-D'', E-E''). Similarly, cellular localization of cytoskeletric F-actin wasn't affected by any of the mutated proteins, both in HL-1 cells and in neonatal rat cardiomyocytes (Figure 38, Panels Panels B-B", C-C'', D-D'', E-E'' and Figure 39, Panels B-B", C-C'', D-D'', E-E'').

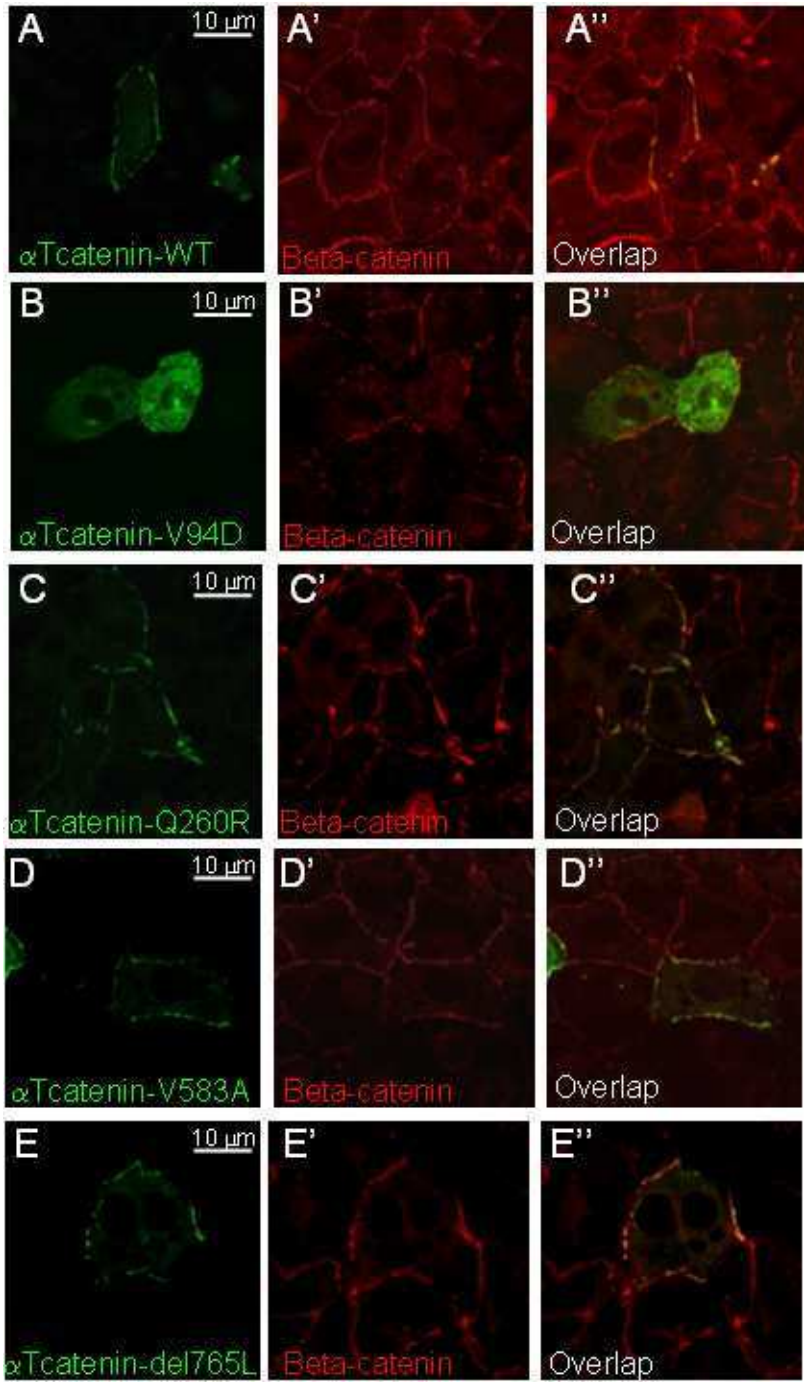

Fig. 34: Transfection studies in HL-1 cells. Note the p.V94D-alphaT-catenin-EGFP fusion protein localized in the cytoplasm (Panels B-B''). Immunostaining with monoclonal beta-catenin antibody showed both the presence of normal appearing desmosomes and reduced co-localization between endogenous beta-catenin and p.V94D-alphaT-catenin EGFP fusion protein (Panels B'-B'').

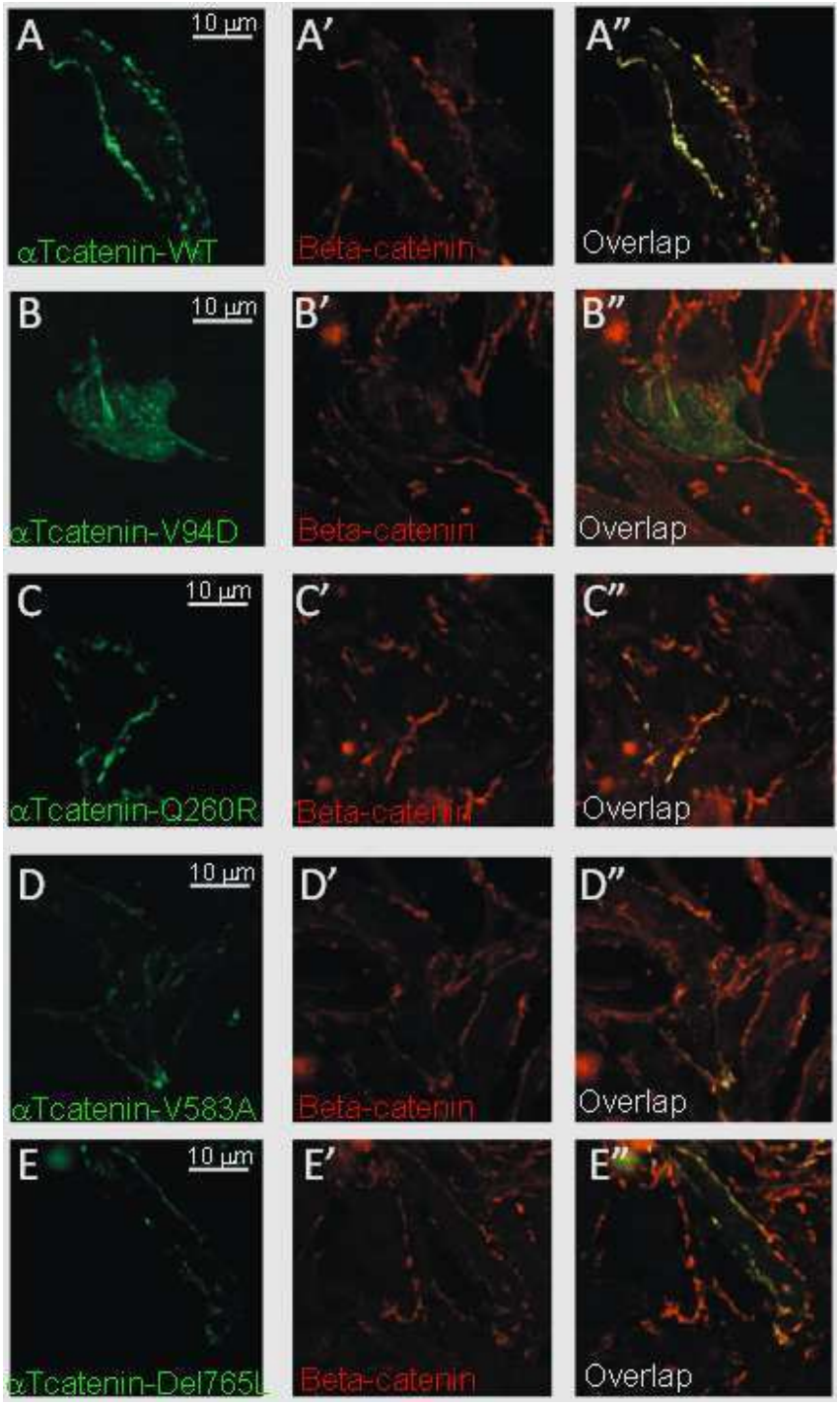

Fig. 35: Transfection studies in neonatal rat cardiomyocytes. Note the p.V94D-alphaT-catenin-EGFP fusion protein localized in the cytoplasm (Panels B-B''). Immunostaining with monoclonal beta-catenin antibody showed both the presence of normal appearing desmosomes and reduced co-localization between endogenous beta-catenin and p.V94D-alphaT-catenin-EGFP fusion protein (Panels B'-B'').

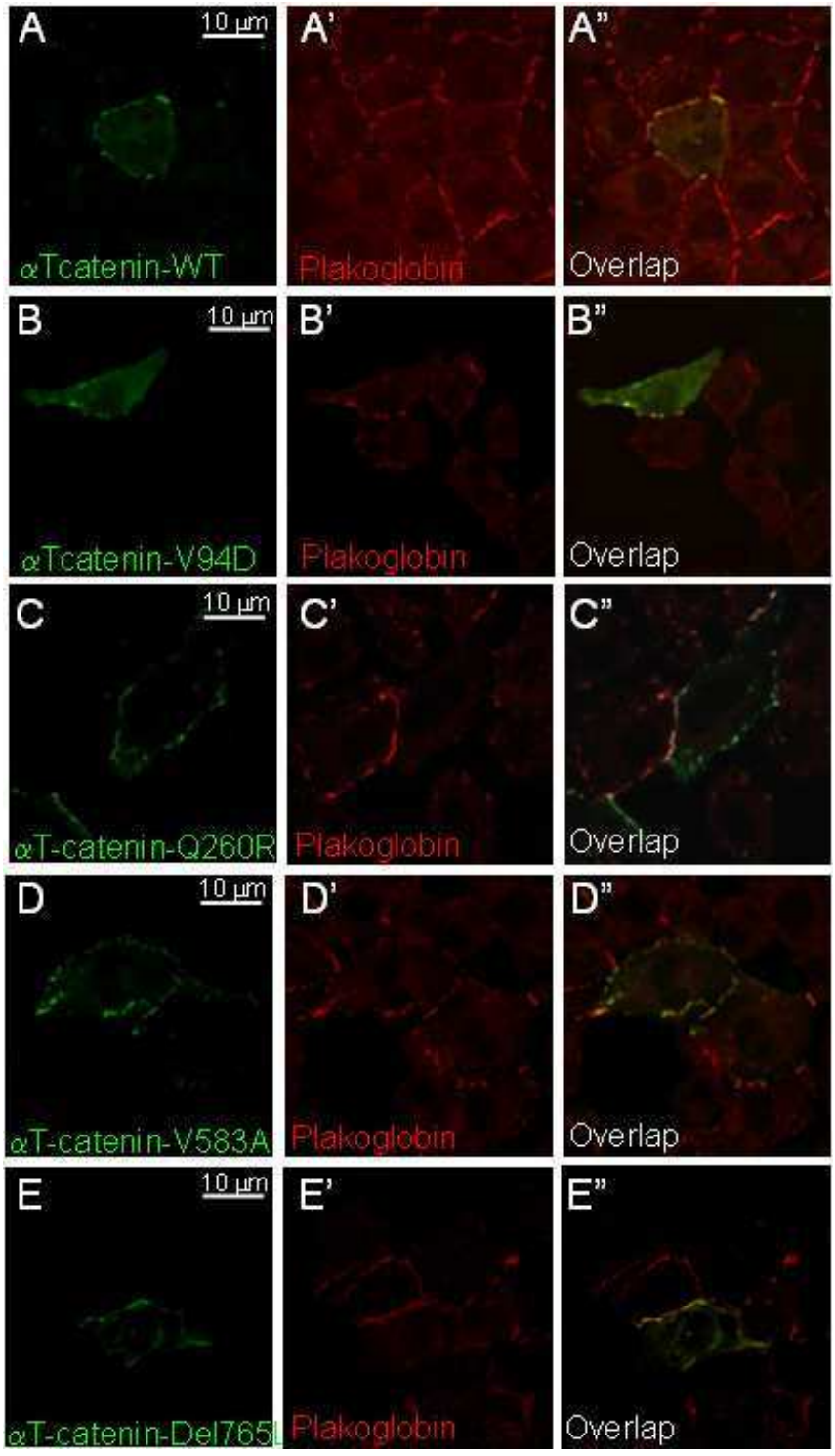

Fig. 36: Transfection studies in HL-1 cells. Note the p.V94D-alphaT-catenin-EGFP fusion protein localized in the cytoplasm (Panels B-B''). Immunostaining with monoclonal plakoglobin antibody showed both the presence of normal appearing desmosomes and reduced co-localization between endogenous plakoglobin and p.V94D-alphaT-catenin-EGFP fusion protein (Panels B'-B'').

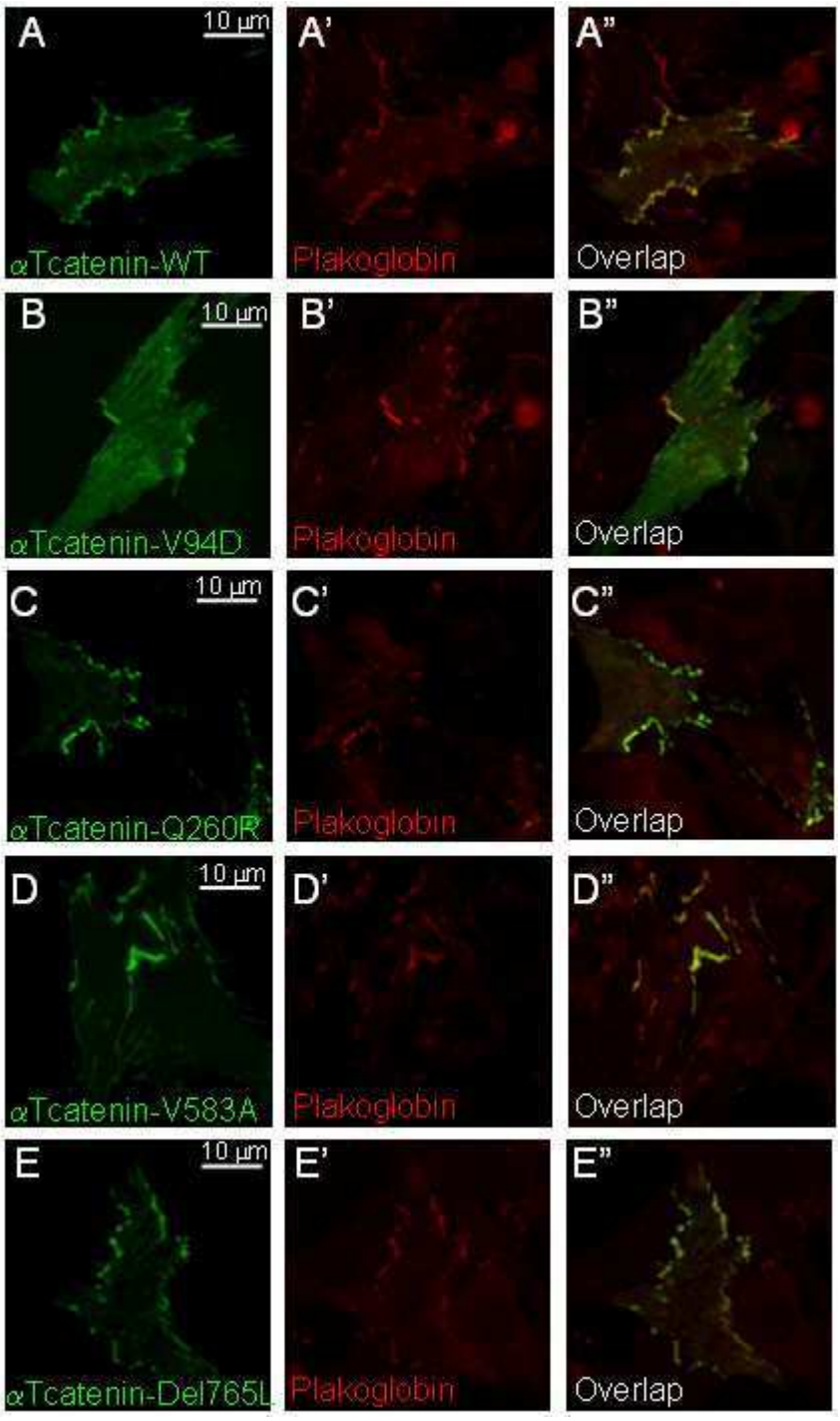

Fig. 37: Transfection studies in neonatal rat cardiomyocytes. Note the p.V94D-alphaT-catenin-EGFP fusion protein localized in the cytoplasm (Panels B-B''). Immunostaining with monoclonal plakoglobin antibody showed both the presence of normal appearing desmosomes and reduced co-localization between endogenous plakoglobin and p.V94D-alphaT-catenin-EGFP fusion protein (Panels B'-B'').

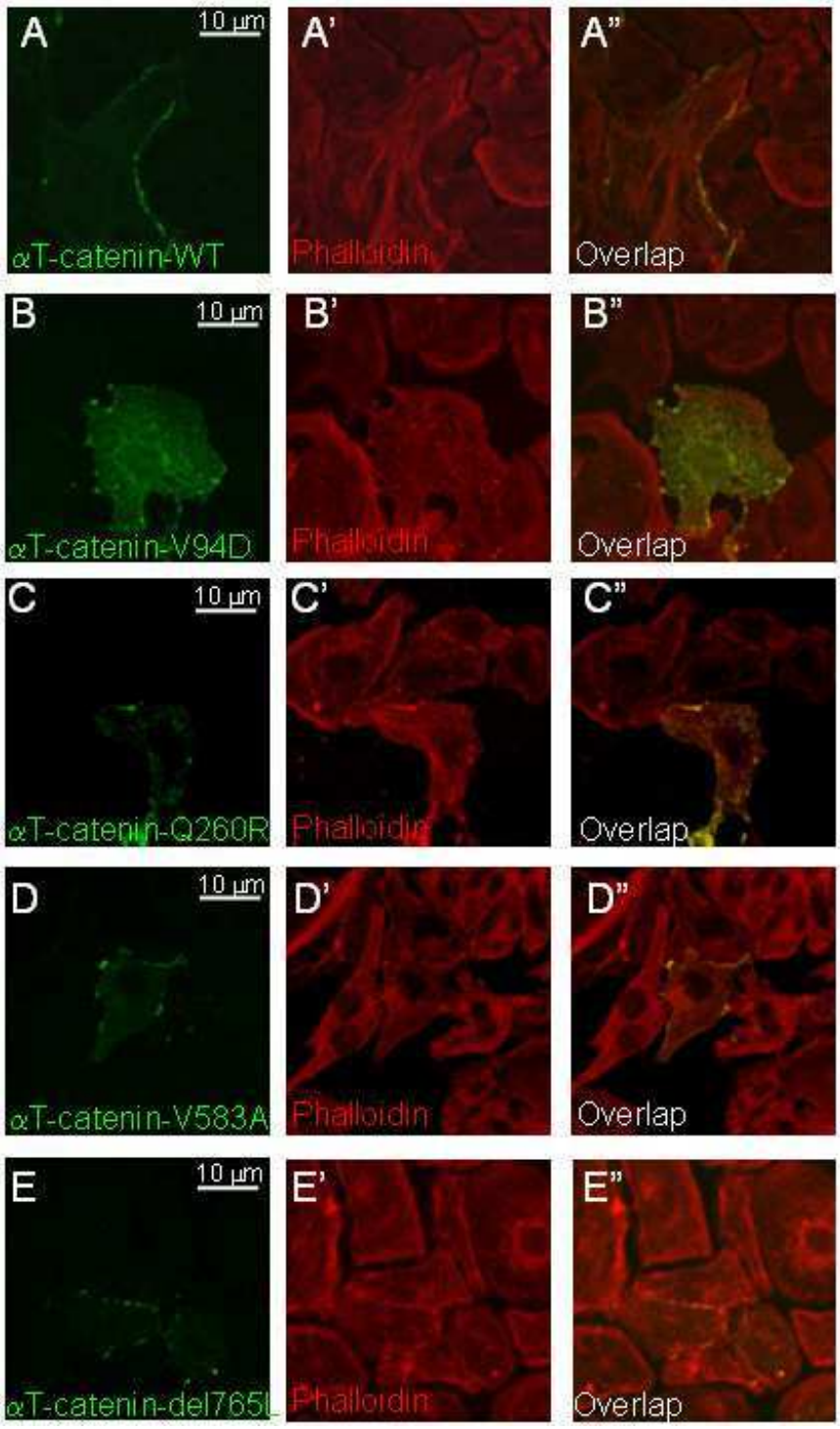

Fig. 38: Transfection studies in HL-1 cells. Note the p.V94D-alphaT-catenin-EGFP fusion protein localized in the cytoplasm (Panels B-B''). Immunostaining with phalloidin showed that the presence of mutant proteins don't affect the structure of F-actin microfilaments in the cytoskeleton (Panels B'-B'', C-C", D-D", E-E").

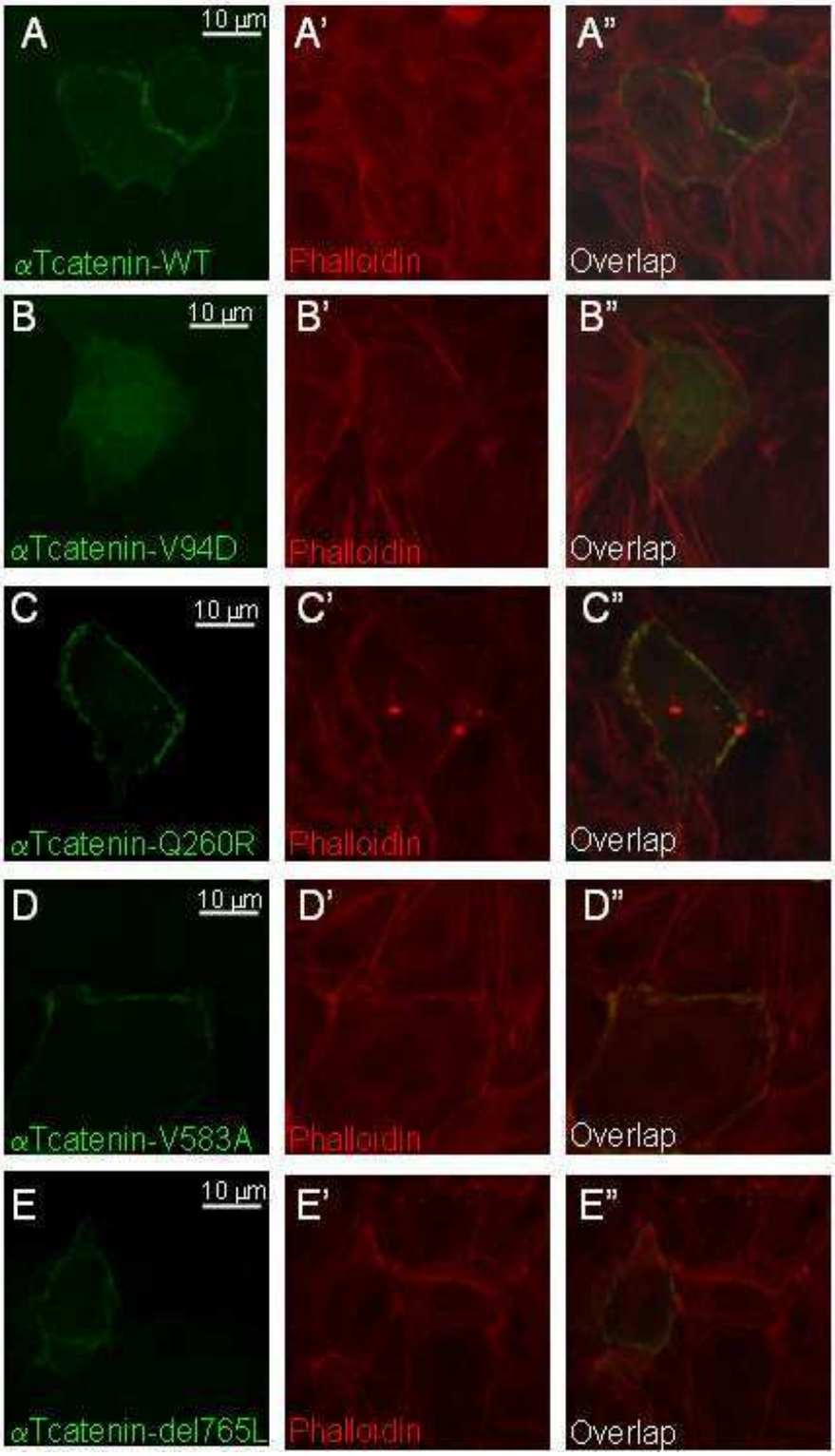

Fig. 39: Transfection studies in neonatal rat cardiomyocytes. Note the p.V94D-alphaT-catenin-EGFP fusion protein localized in the cytoplasm (Panels B-B''). Immunostaining with phalloidin showed that the presence of mutant proteins don't affect the structure of F-actin microfilaments in the cytoskeleton (Panels B'-B'', C-C", D-D", E-E").

4.3.2 Y2H assay

Since identified variations occur in conserved interaction domains of alphaT-catenin, Y2H assays were performed to check the interaction of wild type and different mutated alphaT-catenins with several molecular partners. These experiments were performed in collaboration with Prof. F. Van Roy's group of Ghent University, Belgium.

Specific bait and prey constructs containing the mutated full length CTNNA3 cDNA fused with DNA-BD and AD transcription factors, respectively, were obtained by site-specific mutagenesis PCR. Thus, interactions were checked in two directions.

Several interactions were studied, such as those of alphaT-catenin with beta-catenin, plakoglobin, plakophilin-2, and also dimerization both between a wild-type protein and a mutated one and between two mutated alphaT-catenins.

Mutated proteins carrying p.Q260R and p.V583A missense mutations showed a behaviour comparable to wild type, as they still interacted correctly with their molecular partners (Figure 40 Lanes 1, 3, 4). On the contrary, alphaT-catenin carrying p.V94D didn't interact with beta-catenin and plakoglobin (Figure 40, Lane 2). Interestingly, for the first time it has been demonstrated the interaction of alphaT-catenin with plakoglobin (Figure 40).

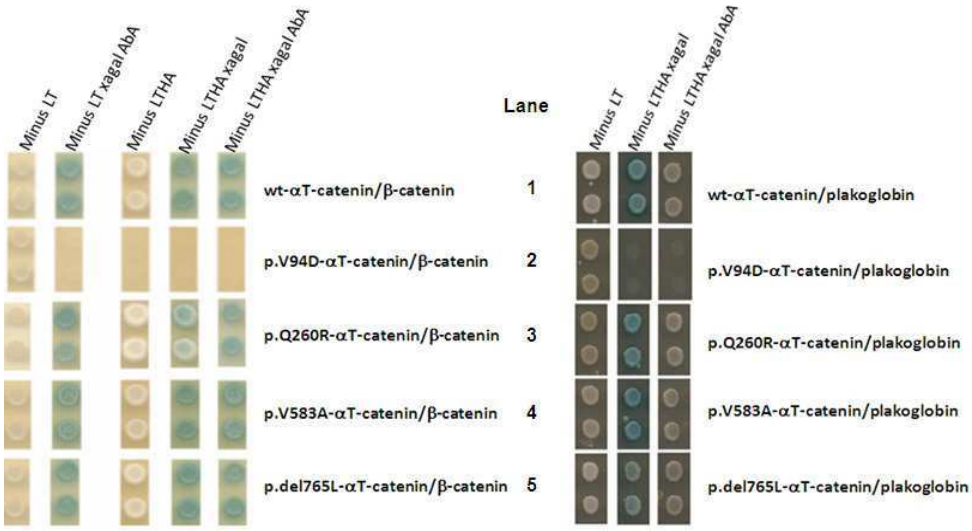

Fig. 40:
Y2H assay results showing the loss of interaction of p.V94D-alphaT-catenin both with beta-catenin and plakoglobin (Lane 2).

The homodimerization potential was checked using AbA, an antibiotic that prevents the yeast growth at low concentrations. The relative ability of the strains to grow in the presence of AbA reflects the strength of the interaction between bait and prey proteins.

Titration of AbA showed that p.del765L has a much stronger homodimerization potential compared to wild type and to other mutant alphaT-catenins (Figure 41, Lane 5, left). As the patients are heterozygote for the mutation, interaction between a mutated and a wild-type protein was also checked. Again, the interaction between p.del765L carrier protein and wild type alphaT-catenin is stronger (Figure 41, Lane 5, right).

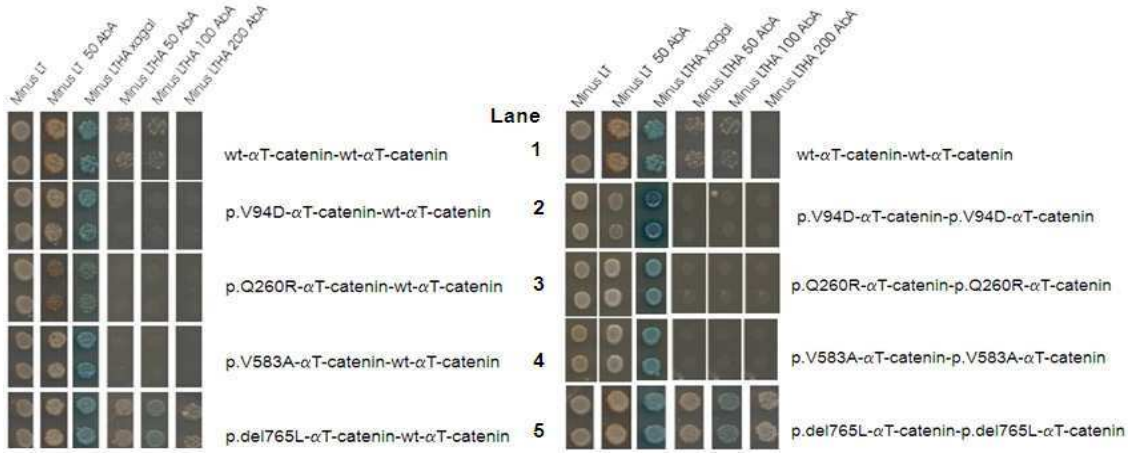

Fig. 41: Y2H assay results showing the stronger dimerization of p.del765L-alphaT-catenin interacting both with a wild type protein (Lane 5, left) and with p.del765L-alphaT-catenin (Lane 5, right).

4.3.3 Transfection experiments in HEK293T cells

Transfections experiments were also performed in human embryonic kidney HEK293T cells, using the construct carrying p.del765L-alphaT-catenin sequence, in the absence of the wild type protein. As reported in Figure 42, in contrast to the wild-type protein, mutant alphaT-catenin forms aggregates into the cytoplasm, that correspond to aggresomes, generically considered cellular deposits of misfolded proteins (Beaudoin et al., 2008).

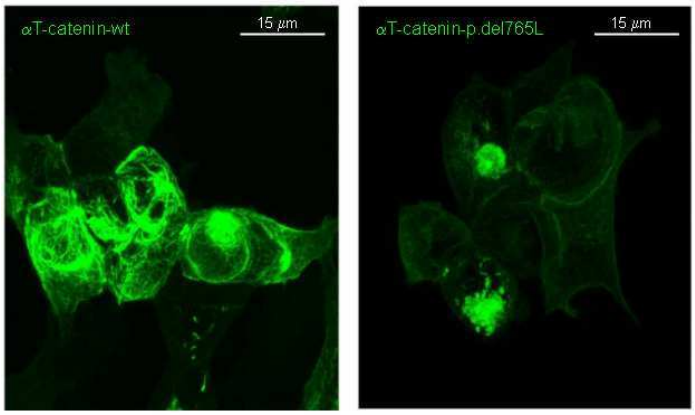

Fig.42: Confocal images of Hek293T cells transfected with either wild type or p.del765L. The right panel shows p.del765L aggregates that are not present in cells expression the WT.

Since Johnston et al. described aggresomes surrounded by vimentin microtubules (Johnston et al., 1998), immunofluorescence experiments were performed in HEK293T cells transfected with the p.del765L-alphaT-catenin construct to stain endogenous vimentin. Vimentin immunofluorescence pattern in transfected cells showed this particular organization (Figure 43), thus suggesting that p.del765L-alphaT-catenin aggregate into aggresomes.

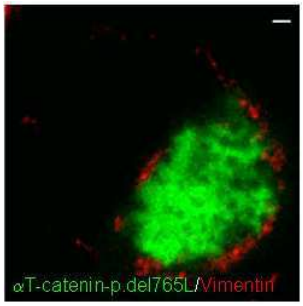

Fig.43 Aggresome formation (in green) is accompanied by reorganization of the vimentin cytoskeleton. HEK293T cells were transfected with p.del765L. Note in red the cage-like appearance of vimentin fluorescence in p.del765L-expressing cells.

5. DISCUSSION

Arrhythmogenic right ventricular cardiomyopathy (ARVC/D) (MIM # 107970) is an inherited cardiac disease characterized by progressive fibro-fatty myocardial replacement, primarily in the right ventricle. The main clinical features are structural and functional abnormalities of the ventricles, electrocardiographic depolarization/repolarization changes, re-entrant arrhythmias, and sudden death, that can be the first manifestation of the disease (Marcus et al., 1982; Thiene G., et al., 1988; Nava et al., 1988). ARVC/D is mostly inherited as an autosomal dominant trait with reduced penetrance and variable expressivity, although autosomal recessive forms have been reported (Nava et al., 2000; McKoy et al., 2000). The majority of the pathogenic mutations have been identified in genes encoding the desmosomal proteins plakoglobin (JUP), desmoplakin (DSP), plakophilin-2 (PKP2), desmoglein-2 (DSG2), and desmocollin-2 (DSC2) (McKoy et al., 2000; Asimaki et al., 2007; Rampazzo et al., 2002 ; Gerull et al., 2004 ; Pilichou et al., 2006 ; Syrris et al., 2006). Few additional mutations have been found in the cardiac ryanodine receptor 2 (RYR2), in transforming growth factor beta 3 (TGFβ3), in TMEM43 (LUMA), in desmin (DES), and most recently, in titin (TTN) genes (Tiso et al., 2001; Beffagna et al., 2005; Merner et al., 2008; Klauke et al., 2010; Taylor et al., 2011).

The involvement in ARVC/D of different genes encoding desmosomal components has led to the “desmosomal model“ hypothesis. Desmosomes are one of the two major cell-cell junction complexes of ICD in cardiomyocytes. They provide cardiomyocytes adhesion and mechanical integrity of heart tissue through a net of interactions from desmosomal cadherins to desmin intermediate filaments (Huber, 2003). It has be speculated that mutations affecting desmosomal genes could compromise both function and integrity of intercellular junctions, determining cardiac intercalated discs remodeling. In these conditions, mechanical stress that typically affects heart tissue, could induce cardiomyocytes detachment and subsequent death, followed by fibro-fatty replacement and conductance abnormalities (Kostetskii et al., 2005).

The wide genetic heterogeneity of the disease can be, at least in part, the reason of its impressive phenotypic variability. This aspect, together with the incomplete penetrance and the absence of symptoms in the “concealed” phase of the disease, accounts for the complexity of its diagnosis. Key clinical applications of mutation screening include confirmatory testing of index cases to facilitate interpretation of borderline investigations and cascade screening of families. The benefits of mutation screening in family members are 2-fold: early identification of symptom-free family members carrying the mutation and at risk of developing ARVC and reassurance to mutation-negative relatives.

5.1 Mutation screening of desmosomal genes

In the present study, mutation screening of five desmosomal genes (PKP2, DSP, DSG2, DSC2, and JUP) was performed in 80 Italian unrelated ARVC/D probands, fulfilling 2010 diagnostic criteria. Mutations were detected in 44% (35 out of 80) of index cases: 15% of

them (12 probands) resulted to carry a mutation in PKP2 gene, 7.5% (6 probands) one mutation in DSP gene, 6% (5 probands) a mutation in DSG2 gene, 2.5% (2 probands) one mutation in JUP gene, and 12.5% (10 probands) carried two or more mutations in the same gene or in different genes. No mutations have been detected in DSC2 gene.

Globally, 41 mutations in desmosomal genes have been identified among 80 index cases. According to data reported in the literature (McKoy et al., 2000; Asimaki et al., 2007; Rampazzo et al., 2002 ; Gerull et al., 2004 ; Pilichou et al., 2006 ; Syrris et al., 2006) and to those previously obtained in our lab, the most extensively mutated genes are PKP2, DSP, and DSG2, with frequencies of 35,7% (15 mutations), 28,5% (12 mutations), and 26% (11 mutations), respectively; on the contrary, mutations in JUP gene have been detected only 7% (3 mutations) of cases and none in DSC2 gene.

Some probands resulted to carry the same mutation, especially in PKP2 gene. This aspect could be due to various causes, such as the presence of a founder effect, selection bias or the fact that some genomic regions represent a mutational hotspot. These reasons could also explain the diversity of mutation frequency of PKP2 gene, ranging from 7% to 45%, reported in literature by groups from different regions worldwide (Gerull et al., 2004; Van Tintelen et al., 2006; Pilichou et al., 2006; Dalal et al., 2006; Syrris et al., 2007; Awad et al., 2006; Heuser et al., 2006; Yang et al., 2006; Lahtinen et al., 2008; Christensen et al., 2010; Bhuiyan et al., 2009; Den Haan et al., 2009; Bauce et al., 2010; Fressart et al., 2010).

As reported in other cohorts, ten probands resulted to carry two or three mutations in the same gene or in different desmosomal genes (den Haan et al., 2009; Bauce et al., 2010; Xu et al., 2010; Fressart et al., 2010). This aspect underlines the importance to carry out in probands whole panel of genes rather than single-gene testing. Bauce and co-workers noticed that carriers of multiple mutations showed a more severe phenotype in terms of LV and RV dilation, if compared to single carriers (Bauce et al., 2010) and Fressart and colleagues speculated that multiple mutation carriers undergo more frequently to sudden death and systolic dysfunctions (Fressart et al., 2010).

Another crucial aspect of mutation screening is the assessment of pathogenicity of ARVC/D mutations, to discriminate pathogenic mutations from rare polymorphisms. This is particular relevant since in the last revision of the diagnostic criteria, the identification of a pathogenic mutation has been considered as a major diagnostic criteria (Marcus et al., 2011). However, this recommendation to include a pathogenic mutation in the major criteria could led to overdiagnosing ARVC/D, as in some instances non-pathogenic rare variants could be uncorrectly classified as pathogenic mutations. The classification of a genetic variant as a disease causing or benign is a known challenge in human genetics. In general we could consider as pathogenic mutations truncating mutations, splice-site mutations confirmed by *in vitro* functional studies and missense mutations with demonstrated functional effects. However, a significant proportion of genetic variants remains unclassified and this fact represents a gap in risk assessment for index patients and in genotype-phenotype correlation studies; moreover, unclassified variants are noninformative for family screening. Recently another step towards a classification of identified variations in ARVC/D patients has

been made (Kapplinger et al., 2011). That is about a mix of factors such as kind of variant (in/del, splice junction, nonsense, missense), mutation localization, conservation of involved amino acid and its boundaries across species, and race of the carrier.

Anyway, in the assessment of pathogenicity of an identified variation it must be taken into account that the presence of a mutation among few control subjects can't exclude its pathogenicity. In fact, mutation carriers can be fully asymptomatic due to the incomplete penetrance typical of ARVC/D, as evidenced by Lahtinen and Kapplinger and their co-workers (Lahtinen et al., 2011; Kapplinger et al., 2011). Pathogenic potential of a variation might be difficult to establish and it often creates disagreements in different groups. Discrepancies on classification of the same variation could be due to the use of different classification criteria, rather than to the presence of a founder effect, that together with the strictness in applying the task force criteria could leave several undiagnosed cases among healthy controls. An example of this disagreement is given by c.2687_2688insGA, found in DSC2 gene and resulting in p.A897KfsX4 frameshift mutation. It was reported by Syrris and co-workers as a pathogenic mutation, whereas in the present study it has been considered a polymorphism, as it was detected in the control population with an allelic frequency of 1,5%. den Haan et al. reported this variant as a polymorphism as well (den Haan et al., 2009). Moreover, this variation was carried by several probands (some of them also carry other variants in desmosomal genes) and it affects the last portion of ICS domain of isoform DSC2a, which is absent in the shorter DSC2b, the most expressed in the heart, that is then completely functional and could compensate the relative deficiency of DSC2a. This variant could be then considered a polymorphism that may affect the phenotypic expression of concomitant ARVC/D mutations identified in three probands investigated in this study. Only in one of them no other variations have been observed up to now. It can be speculated that he may carry a pathogenic mutation in an unknown ARVC/D gene.

An accurate genotyping and the identification of disease-causing mutations facilitate timely diagnosis and consequently allow the prevention of complications and the reduction of morbidity and mortality. Moreover, once a causative mutation is detected in an ARVC/D patient, family members screening for the presence of the same mutation enables the identification asymptomatic subjects at risk of developing the disease. Thus, mutation carriers may modify their lifestyle to decrease the likelihood of SCD. Anyway, the absence of a mutation alone cannot override clinical diagnosis. An example is represented by the niece of proband #8, who, although doesn't carry any of the three mutations recurring in the family, shows an affected phenotype.

According to data reported in literature, mutation screening of five desmosomal genes performed in the present study failed to detect causative mutations in 56% of investigated probands, suggesting that additional genes could be involved in ARVC/D (Fressart et al., 2010; Bauce et al., 2010; Christensen et al., 2010; Den Haan et al., 2009).

5.2 Mutation screening of CTNNA3 candidate gene

The main methods used to identify novel disease-genes are the linkage analysis and the candidate-gene approach. Linkage analysis implies that the more two chromosomal *loci* are closer, the less they'll be separated during the mitosis. Hence, if polymorphic known markers segregate with the disease phenotype among affected members in a family, it means that the involved gene maps in the same chromosomal *locus* of the markers and it can be then identified among all the genes located in that limited genomic region. In the candidate gene approach, a gene is chosen to be a potential disease gene due to its tissue expression, to the cellular localization of its proteic product, to the function of the encoded protein. In the present study, a candidate gene approach was adopted in order to identify a novel ARVC/D gene.

Together with desmosomes, AJs represent a tool to assure heart tissue integrity and mechanical coupling. Indeed, AJs are intercellular structures providing a strong mechanical connection in adjacent cardiomyocytes linking their extracellular and cytoplasmic components to cytoskeletal actin (Tepass et al., 2000). This structure consists of cadherins and catenins: cytoplasmic tails of cadherin homodimers are linked to cytoskeletal actin through direct or indirect binding of plakoglobin, beta- and alpha-catenins, and accessories proteins, such as vinculin and alpha-actinin (Imamura et al., 1999; Birchmeier et al., 1994). AJs hence keep cells tightly together in the contraction and expansion of the cardiac muscle. Moreover, representing the anchor-point where myofibrils are attached, they enable the transmission of contractile force from one cell to another (Ferreira-Cornwell et al., 2002).

One of the main members of cardiac AJs is alphaT-catenin, which is the most recently characterized protein of the alpha-catenin family. It is encoded by CTNNA3 gene, located in 10q21 locus and considered the fifth largest gene in the human genome, as it spans 1.78 Mbs, organized in 18 exons (Janssens et al., 2003). Alternative splicing originates two different proteins, of 895 and 628 amino acids respectively, whereof the shorter is specifically expressed in testis. The longer isoform has a predicted molecular weight of about 100 kDa and it is highly expressed in several tissues, like brain, kidney, liver, or skeletal muscle, and, mostly, in peritubular myoid cells of testis tissue and in cardiomyocytes (Janssens et al., 2001). The main functional domains of alphaT-catenin include a beta-catenin binding site, partially overlapping the homodimerization domain, and an actin binding site, extending along portion of the plakophilin-2 binding domain (Goossens et al., 2007; Pokutta and Weis 2000). Compared to the better characterized alphaE-catenin and alphaN-catenin, the other two members of alpha-catenin family, alphaT-catenin maintains a very high amino acid conservation, especially in the C-terminal and in the beta-catenin and actin binding domains (Janssens et al., 2001). This suggests that all members of this family may have diverged from a common ancestor. AlphaT-catenin is a relatively new protein, not deeply investigated. On the contrary, much more is known about the ubiquitous alphaE-catenin. Considering that these two proteins share a high percentage of sequence homology, it can be speculated that data emerged from studies on alphaE-catenin may seemingly recapitulate the behaviour of alphaT-catenin. As far as alphaT-catenin function is

specifically concerned, different results underline the central role of this protein in providing strong cell-cell adhesion. Janssens and colleagues in 2001 demonstrated that overexpressing CTNNA3 in a CTNNA1 (coding for alphaE-catenin) negative colon carcinoma cell line, adherens and tight junctions reassembled through the recruitment of alphaT-catenin interacting partners, such as beta-catenin, plakoglobin, and E-cadherin (Janssens et al., 2001). More recently, using Y2H and co-immunoprecipitation, Goossens and co-workers showed that alphaT-catenin specifically interacts with the N-terminal domain of plakophilin-2 in ICD of cardiomyocytes and that the same interaction doesn't involve alphaE-catenin. This specific interaction occurs in the so-called "*area composita*", a mixed junction type specific of ICD of cardiomyocytes, in which both proteins of desmosomes and of AJs are present (Goossens et al., 2007; Borrmann et al., 2006; Franke et al., 2006). These results shed light on a possible specific and necessary role for alphaT-catenin in ICD of heart. The authors suggested that this protein could act as a means of strengthening cell-cell adhesion in contractile cells, probably recruiting desmosomal proteins to hybrid intercellular junctions, thus forming a mixed-type, reinforced junction at the ICD that is attached to both desmin intermediate filaments and actin cytoskeleton (Goossens et al., 2007). Due to alphaT-catenin localization in ICD of cardiomyocytes, to its function, and to its specific interaction with plakophilin-2 occurring exclusively in the *area composita*, CTNNA3 has been considered in our lab a good candidate gene for ARVC/D.

Three missense mutations and a three base-pairs deletion have been detected in 4 (5,3%) out of 76 ARVC/D probands negative for mutations in desmosomal genes. Comparing to mutation frequency of desmosomal genes, CTNNA3 resulted to be more commonly mutated than JUP and DSC2 genes, and showed a variation recurrence comparable to DSP and DSG2, which are two out of the three most extensively altered genes among ARVC/D patients. Among the three missense substitutions, only p.V583A is a conservative change, while p.V94D and p.Q260R involve amino acids with different chemical properties. Moreover, all of the four mutations interest amino acids conserved among different species.

Missense mutation p.V94D is located in the common region of beta-catenin-binding site and homodimerization domain. These two domains have an overlapping portion: in fact, homodimerization domain encompasses amino acids 82-279, while beta-catenin-binding domain is located within residues 54-148 (Kobielak and Fuchs, 2004; Pokutta and Weis, 2000). This overlap determines the mutual exclusion of homodimerization and beta-catenin binding (Dawes, 2009). Assays performed by Drees et al. demonstrated that alphaE-catenin acts allosterically: heterodimer alpha-beta-catenin has a bigger affinity for cadherin and a lower one for actin, while homodimer acts in the opposite way (Drees et al., 2005). Moreover, the most recent experiments performed to establish the correlation between cadherin-catenin complex and actin showed that alpha-catenins can't bind simultaneously beta-catenin and actin and attempts to detect a quaternary complex composed by cadherins/beta-catenin/alpha-catenin and actin failed (Harris and Tepass, 2010; Yamada et al., 2005). Taking these data together, it has been proposed that dissociation of alpha-catenins from the catenin-cadherin complexes clustered in the nascent cell-cell contacts

make available high local concentrations of free alpha-catenins. Subsequent originated alpha-catenin homodimers preferentially interact with actin, stimulating its polymerization and its association with AJs through accessories proteins in mature contacts (Harris and Tepass 2010).

Transfection experiments both in HL-1 and in neonatal rat cardiomyocytes performed in the present study showed that p.V94D-alphaT-catenin localizes in the cytoplasm, while the wild type and all the other mutated proteins join correctly the plasma membrane. In all cases, immunofluorescence stainings of endogenous beta-catenin and plakoglobin showed that cellular localization of these two proteins isn't appearently compromised, as both signals are correctly detected in the plasma membrane. F-actin cytoskeletal filaments showed a correct immunofluorescence pattern in all transfected cells, as well. Moreover, by Y2H assays it has been demonstrated that only p.V94D-alphaT-catenin loses its skill to bind beta-catenin and plakoglobin. This result could justify the presence of p.V94D-alphaT-catenin in the cytoplasm of transfected cells. In the heterozygous patient carrying p.V94D, both mutated and wild type alphaT-catenin are present and wild type protein may interact correctly with beta-catenin and plakoglobin.

Y2H assays demonstrated also that p.V94D variation doesn't increase the homodimerization strength. Y2H assay performed in the present study revealed also a novel interaction between alphaT-catenin and plakoglobin. In fact, while the interaction between alphaT-catenin and beta-catenin has been previously reported (Janssens et al., 2001), the binding of plakoglobin represents a novel data and up to now the amino acid residues of both proteins involved in this interaction haven't been identified yet.

Also p.del765L mutation resulted to affect alphaT-catenin behavior if compared to wild-type protein. In fact, even if the mutated protein localizes correctly into the plasma membrane in cardiomyocytes, in HEK293T cells, which don't express endogenous alphaT-catenin, it forms aggregates surrounded by a vimentin cage, called aggresomes. This structure consists of juxtanuclear aggregated protein deposits surrounded by vimentin microtubules, whose formation may be induced by the accumulation of misfolded proteins, not degraded in proteasome (Johnston et al., 1998). Beaudoin and co-workers underlined that aggresome formation may be determined by several factors existing in a cell line, such as kinetics of coalescence of individual aggregates, or the organization of the microtubule network (Beaudoin et al., 2008). This underlines the complexity and the variability of misfolded proteins in cells and that aggresomes couldn't be obligatory end-products of protein misfolding. This could explain why in transfected cardiomyocytes no protein aggregation has been observed. Moreover, Y2H assay showed that p.del765L-alphaT-catenin dimerizes more strongly both with wild-type and p.del765L-alphaT-catenins. Taken together, these results suggest that deletion of Leucine 765 in alphaT-catenin could compromise the folding of the whole protein, possibly leading to an haploinsufficiency condition.

Two other missense mutations, p.Q260R and p.V583A, have been detected in this study. Transfection experiments in cardiomyocytes showed for both of them a normal localization into the plasma membrane. Moreover, Y2H assays didn't show loss or abnormal interactions

with different investigated proteins. It would be useful to check by Y2H or co-immunoprecipitation analyses interactions of these two mutated alphaT-catenin with other partners, such as vinculin, or alpha-actinin. Anyway, up to now, it cannot be excluded that they could be very rare polymorphisms having a modifier potential that can be expressed in the presence of other mutations.

CTNNA3 gene had been previously considered a good candidate gene for different cardiomyopathies. In 2003, Janssens and colleagues, postulating the involvement of CTNNA3 in dilated cardiomyopathy (DCM), screened all 18 exons in a DCM family showing linkage to the 10q21-q23 locus, but no mutation was detected (Janssens et al., 2003). More recently, this gene elicited interest also in ARVC/D studies (Christensen et al., 2011). A mutation screening in CTNNA3 gene was performed in 65 ARVC/D Danish patients; p.A689V variant was found in an affected subject carrying also a novel polymorphism in DSP gene. The same substitution in CTNNA3 gene was identified also in 2 healthy subjects out of 1400 (allelic frequency of 0.14%) and affected a highly conserved residue. The authors considered this substitution as an unclassified variant. However, it cannot be excluded that p.A689V detected in CTNNA3 gene could be a pathogenic mutation, present in two asymptomatic subjects among the healthy controls. Danish population is pretty close and the detected variation could be present in two healthy subjects because of a founder effect. Hence, it would be interesting to perform in vitro functional studies to evaluate its pathogenic potential.

Finally, to better understand the molecular mechanism involved in ARVC/D pathogenesis due to p.V94D and p.del765L mutations in CTNNA3 gene, it could be useful to generate transgenic and knock-in mice, that allow to dig into this disease in a biological system *in vivo*.

Desmosomes and AJs are intercellular junctions, composed by different proteins and involved in maintaining adhesion and integrity among cardiomyocytes. In both cases, cell-cell mechanical anchoring occurs at two crucial points: the extracellular space, where desmosomal and classical cadherin dimerization occurs, and in the intracellular space, where the cytoplasmic end of cadherins is attached indirectly to desmin intermediate filaments, in the case of desmosomes, or to actin filaments, in the case of AJs. Similarly to what has been suggested for desmosomal mutations in ARVC/D patients, it can be proposed that variations in AJ components could lead to the aberrant incorporation or the absence of the altered protein into the junction. This may result in an incorrect functioning of the intercellular connection in stress conditions, subsequent cardiomyocyte death and fibro-fatty replacement. Moreover, since components of desmosomes and of AJs are also present in the *area composita*, aberrations in these proteins can also compromise the reinforcing role played by this mixed junction.

It has been also reported that changes in the functions of desmosomal proteins lead to abnormal distribution of gap junctions that can induce the arrhythmogenic vulnerability in ARVC/D patients (Pieperhoff et al., 2008; Oxford et al., 2007; Kaplan et al., 2004). For example, decay of PKP2 expression causes loss of both connexin-43 from the ICD and gap-junction-mediated coupling between cells (Oxford et al., 2007). Similarly, it has been

demonstrated that mutations in AJ components have large effects on gap junctions expression and function (Li et al., 2008; Li et al., 2005; Matsushita et al., 1999). For example, cardiac specific deletion of N-cadherin in mouse causes the rupture of AJs, desmosomes, and area composita, and a marked reduction of gap junction protein connexin-43, leading to VT and SCD (Li et al., 2005). ICD should be then imagined not as the summation of separate components with different functions, but rather as an "organelle" where macromolecular complexes (desmosomes, AJs, *area composita*, gap junctions) interact synergically. It can be then speculated that impaired mechanical coupling in intercellular junctions such as desmosomes, AJs, and also in *area composita*, may lead to electrical dysfunctions with increased arrhythmogeneity, explaining the clinical phenotype of ARVC/D. In particular, alterations in alphaT-catenin function may interfere directly or indirectly with intercellular coupling between alphaT-catenin, plakophilin-2, cytoskeleton and gap junctions, which may subsequently result in destabilization of the ICD structure, cardiac dysfunction, as well as cardiac arrhythmias. Since alphaE-catenin lacks plakophilin-2 binding domain, it is supposed that it cannot supply to structural and functional alterations of alphaT-catenin (Goossens et al., 2007). Interestingly, the discovery of the interaction of plakophilin-2 with alphaT-catenin could provide a new key to interpret the possible pathological mechanism of mutations in plakophilin-2 and maybe of variations affecting also the other desmosomal proteins. Unfortunately, at present it isn't specifically known which other molecular interactions occur among alphaT-catenin and other proteins in AJs and in *area composita*, nor which elements are involved in the passage from mechanical to electrical coupling. Further studies are needed to clarify these aspects. It would be interesting to perform functional studies on plakophilin-2 mutations to detect possible abnormalities in alphaT-catenin, which is an ascertained molecular partner, but also to check if mutations in other desmosomal components could affect localization or behaviour of proteins of AJs, belonging also to *area composita*. ARVC/D so far has been considered a "desmosomal disease", as the majority of mutations have been detected in genes encoding desmosomal components. However, results obtained in this study demonstrate the involvement in this disorder of a gene of *area composita*, expanding the concept of ARVC/D to the definition of a "disease of *area composita*". This represents an innovative and important information to be kept into consideration in the near future in the study of ARVC/D. For example, these data can orient towards new insights to explain the pathogenic mechanism of the disease, spreading the interpretation beyond the desmosomes and considering the whole junctional complexes in ICD. Also, the impact of identification of mutations in a gene encoding an intercellular junction component different from desmosomal proteins can be wide, addressing the research of other candidate genes in new directions. Genes encoding proteins of AJs and *area composita*, such as p120, beta-catenin, vinculin, etc, can be considered for future studies to dig wider both in ARVC/D diagnosis and in its complex and still unclear pathological mechanism.

6. CONCLUSIONS

Arrhythmogenic right ventricular cardiomyopathy (ARVC/D) is a genetic disease inherited as an autosomal trait with incomplete penetrance and variable expressivity, associated with ventricular tachycardia, syncope, and sudden death. The main pathologic feature is the loss of myocardium and fatty or fibro-fatty replacement, predominantly in the right ventricle. Genetically, it is a heterogenous disease: so far, 10 disease genes have been identified, but the vast majority of pathogenic mutations detected in affected subjects have been observed in desmosomal genes, leading to the definition of ARVC/D as “a desmosomal disease”. In the present study, mutation screening in five desmosomal genes involved in ARVC/D led to the identification of mutations in 44% of the 80 investigated subjects. Accordingly to data reported in literature, variants in PKP2 are relatively common and the three genes the most frequently mutated are PKP2, DSP, and DSG2. Moreover, as previously described, complex genetic status with multiple mutations was observed in ten (12,5%) probands. This result underlines the importance of both continuing mutation screening after the identification of a first variant and of a correct classification of detected changes. It is as much important the assessment of pathogenicity of a detected variation from both a clinical and a genetic point of view, considering the wide phenotipic variability of ARVC/D. Concordant to previous data, in 56% of subjects investigated in this study, any pathogenic mutation was detected, suggesting that additional genes should be involved in ARVC/D. Mutation screening in CTNNA3 candidate gene subsequently performed in 76 affected probands led to identification of four novel mutations. For the first time, pathogenic mutations have been detected in a gene encoding a protein belonging to a cardiac intercellular junction, different from desmosomes. This data sheds light on a new, wider concept of ARVC/D, that should not be considered only a cardiac “desmosomal disease” anymore, but rather a “disease of *area composita*”. Accordingly, in the very next future the research on new ARVC/D candidate genes should be pointed to those encoding components of this mixed-type intercellular junction.

7. REFERENCES

-Abraham SC., DeNofrio D, Loth E, Minda JM, Tomaszewski JE, Pietra GG, Reynolds C.. Desmin myopathy involving cardiac, skeletal, and vascxular smooth muscle: report of a case with immunoelectron microscopy. Hum Pathol. 1998;29:876-82.

-Ackerman MJ, Priori SG, Willems S, Berul C, Brugada R, Calkins H, Camm AJ, Ellinor PT, Gollob M, Hamilton R, Hershberger RE, Judge DP, Le Marec H, McKenna WJ, Schulze-Bahr E, Semsarian C, Towbin JA, Watkins H, Wilde A, Wolpert C, Zipes DP. HRS/EHRA expert consensus statement on the state of genetic testing for the channelopathies and cardiomyopathies this document was developed as a partnership between the Heart Rhythm Society (HRS) and the European Heart Rhythm Association (EHRA). Heart Rhythm. 2011;8:1308-39.

-Angelini A, Basso C, Nava A, Thiene G. Endomyocardial biopsy in arrhythmogenic right ventricular cardiomyopathy. Am Heart 1996;132:203-6.

-Armstrong DK, McKenna KE, Purkis PE, Green KJ, Eady RA, Leigh IM, Hughes AE. Haploinsufficiency of desmoplakin causes a striate subtype of palmoplantar keratoderma. Hum Mol Genet. 1999;8:143-8.

-Arnold N, Gross E, Schwarz-Boeger U, Pfisterer J, Jonat W, Kiechle M. A highly sensitive, fast, and economical technique for mutation analysis in hereditary breast and ovarian cancers. Hum Mutat 1999,14:333-9.

-Asimaki A and Saffitz JE. The role of endomyocardial biopsy in ARVC: looking beyond histology in search of new diagnostic markers. J Cardiovasc Electrophysiol. 2011;22:111-7.

-Asimaki A, Tandri H, Huang H, Halushka MK, Gautam S, Basso C, Thiene G, Tsatsopoulou A, Protonotarios N, McKenna WJ, Calkins H, Saffitz JE. A new diagnostic test for arrhythmogenic right ventricular cardiomyopathy. N Engl J Med. 2009;360:1075-84.

-Asimaki A, Syrris P, Wichter T, Matthias P, Saffitz JE, McKenna WJ. A novel dominant mutation in plakoglobin causes arrhythmogenic right ventricular cardiomyopathy. Am J Hum Genet. 2007;81:964-73.

-Avella A, d'Amati G, Pappalardo A et al. Diagnostic value of endomyocardial biopsy guided by electroanatomic voltage mapping in arrhythmogenic right ventricular cardiomyopathy/dysplasia. J Cardiovasc Elecrophysiol 2008; 19:1127-34.

-Awad MM, Calkins H, Judge DP; Medscape. Mechanisms of disease: molecular genetics of arrhythmogenic right ventricular dysplasia/cardiomyopathy. Nat Clin Pract Cardiovasc Med. 2008;5:258-67.

-Awad MM, Dalal D, Tichnell C, James C, Tucker A, Abraham T, Spevak PJ, Calkins H, Judge DP. Recessive arrhythmogenic right ventricular dysplasia due to novel cryptic splice mutation in PKP2. Hum Mutat. 2006;27:1157.

-Bagattin A, Veronese C, Bauce B, Wuyts W, Settimo L, Nava A, Rampazzo A, Danieli GA. Denaturing HPLC-based approach for detecting RYR2 mutations involved in malignant arrhythmias. Clin Chem 2004, 50:1148-55.

-Basso C, Corrado D, Marcus FI, Nava A, Thiene G. Arrhythmogenic right ventricular cardiomyopathy. Lancet. 2009;373:1289-300.

-Basso C, Ronco F, Marcus FI, Abuduereheman A, Rizzo S, frigo AC, Bauce B, Maddalena F, Nava A, Corrado D, Grigoletto F, Tiene G. Quantitative assessment of endomyocardial biopsy in arrhythmogenic right ventricular cardiomyopathy/dysplasia: an in vitro validation of diagnostic criteria. Eur Heart J 2008;29:2760-71.

-Basso C. and Thiene G. Autopsy and endomyocardial biopsy findings. In: Arrhythmogenic Right Ventricular Cardiomyopathy/Dysplasia. Marcus FI, Nava A, Thiene G, editors. Milan, Italy Springer Verlag; 2007: pp. 29-44.

-Basso C, Czarnowska E, Della Barbera M, Bauce B, Beffagna G, Wlodarska EK, Pilichou K, Ramondo A, Lorenzon A, Wozniek O, Corrado D, Daliento L, Danieli GA, Valente M, Nava A, Thiene G, Rampazzo A. Ultrastructural evidence of intercalated disc remodelling in arrhythmogenic right ventricular cardiomyopathy: an electron microscopy investigation on endomyocardial biopsies. Eur Heart J 2006, 27:1847-54.

-Basso C and Thiene G. Adipositas cordis, fatty infiltration of the right ventricle, and arrhythmogenic right ventricular cardiomyopathy. Just a matter of fat? Cardiovasc Pathol 2005, 14:37-41

-Basso C, Fox PR, Meurs KM, Towbin JA, Spier AW, Calabrese F, Maron BJ, Thiene G. Arrhythmogenic right ventricular cardiomyopathy causing sudden cardiac death in boxer dogs: a new animal model of human disease. Circulation. 2004;109:1180-5.

-Basso C, Thiene G, Corrado D, Angelini A, Nava A, Valente M. Arrhythmogenic right ventricular cardiomyopathy. Dysplasia, dystrophy, or myocarditis? Circulation. 1996; 94: 983-91.

-Bauce B, Rampazzo A, Basso C, Mazzotti E, Rigato I, Steriotis A, Beffagna G, Lorenzon A, De Bortoli M, Pilichou K, Marra MP, Corbetti F, Daliento L, Iliceto S, Corrado D, Thiene G, Nava A. Clinical phenotype and diagnosis of arrhythmogenic right ventricular cardiomyopathy in pediatric patients carrying desmosomal gene mutations. Heart Rhythm. 2011;8:1686-95.

-Bauce B, Nava A, Beffagna G, Basso C, Lorenzon A, Smaniotto G, De Bortoli M, Rigato I, Mazzotti E, Steriotis A, Marra MP, Towbin JA, Thiene G, Danieli GA, Rampazzo A. Multiple mutations in desmosomal proteins encoding genes in arrhythmogenic right ventricular cardiomyopathy/dysplasia. Heart Rhythm. 2010;7:22-9.

-Bauce B, Frigo G, Marcus FI, Basso C, Rampazzo A, Maddalena F, Corrado D, Winnicki M, Daliento L, Rigato I, Steriotis A, Mazzotti E, Thiene G, Nava A. Comparison of clinical features of arrhythmogenic right ventricular cardiomyopathy in men versus women. Am J Cardiol. 2008;102:1252-7.

-Bauce B, Basso C, Rampazzo A, Beffagna G, Daliento L, Frigo G, Malacrida S, Settimo L, Danieli G, Thiene G, Nava A. Clinical profile of four families with arrhythmogenic right ventricular cardiomyopathy caused by dominant desmoplakin mutations. Eur Heart J 2005; 26:1666-75.

-Beaudoin S, Goggin K, Bissonnette C, Grenier C, Roucou X. Aggresomes do not represent a general cellular response to protein misfolding in mammalian cells. BMC Cell Biol.2008;9:59.

-Beffagna G, De Bortoli M, Nava A, Salamon M, Lorenzon A, Zaccolo M, Mancuso L, Sigalotti L, Bauce B, Occhi G, Basso C, Lanfranchi G, Towbin JA, Thiene G, Danieli GA, Rampazzo A. Missense mutations in desmocollin-2 N-terminus, associated with arrhythmogenic right ventricular cardiomyopathy, affect intracellular localization of desmocollin-2 in vitro. BMC Med Genet. 2007;8:65.

-Beffagna G, Occhi G, Nava A, Vitiello L, Ditadi A, Basso C, Bauce B, Carraro G, Thiene G, Towbin JA, Danieli GA, Rampazzo A. Regulatory mutations in transforming growth factor-beta3 gene cause arrhythmogenic right ventricular cardiomyopathy type 1. Cardiovasc Res. 2005; 65: 366-73.

-Ben-Ze'ev A and Geiger B. Differential molecular interactions of beta-catenin and plakoglobin in adhesion, signaling and cancer. Curr Opin Cell Biol. 1998;10:629-39.

-Bengtsson L, Otto H. LUMA interacts with emerin and influences its distribution at the inner nuclear membrane. J Cell Sci 2008: 121: 536–48.

-Bhuiyan ZA, Jongbloed JD, van der Smagt J, Lombardi PM, Wiesfeld AC, Nelen M, Schouten M, Jongbloed R, Cox MG, van Wolferen M, Rodriguez LM, van Gelder IC, Bikker H, Suurmeijer AJ, van den Berg MP, Mannens MM, Hauer RN, Wilde AA, van Tintelen JP. Desmoglein-2 and desmocollin-2 mutations in dutch arrhythmogenic right ventricular dysplasia/cardiomypathy patients: results from a multicenter study. Circ Cardiovasc Genet. 2009;2:418-27.

-Bierkamp C, Schwarz H, Huber O, Kemler R. Desmosomal localization of beta-catenin in the skin of plakoglobin null-mutant mice. Development. 1999;126:371-81.

-Bierkamp C, Mclaughlin KJ, Schwarz H, Huber O, Kemler R. Embryonic heart and skin defects in mice lacking plakoglobin. Dev Biol. 1996;180:780-5.

-Birchmeier W and Behrens J. Cadherin expression in carcinomas: role in the formation of cell junctions and the prevention of invasiveness. Biochim Biophys Acta. 1994;1198:11-26.

-Blomström-Lundqvist C, Sabel KG, Olsson SB. A long term follow up of 15 patients with arrhythmogenic right ventricular dysplasia. Br Heart J. 1987; 58: 477-88.

-Bornslaeger EA, Corcoran CM, Stappenbeck TS, Green KJ. Breaking the connection: displacement of the desmosomal plaque protein desmoplakin from cell-cell interfaces disrupts anchorage of intermediate filament bundles and alters intercellular junction assembly. J Cell Biol. 1996;134:985-1001.

- Borrmann CM, Grund C, Kuhn C, Hofmann I, Pieperhoff S, Franke WW. The area composita of adhering junctions connecting heart muscle cells of vertebrates. II. Colocalizations of desmosomal and fascia adhaerens molecules in the intercalated disk. Eur J Cell Biol. 2006;85:469-85.

-Chen AE, Ginty DD, Fan CM. Protein kinase A signalling via CREB controls myogenesis induced by Wnt proteins. Nature. 2005;433:317-22.

-Chimenti P, Pieroni M, Maseri A, Frustaci A. Histologic findings in patients with clinical and instrumental diagnosis of sporadic arrhythmogenic right ventricular dysplasia. J Am Coll Cardiol 2004; 43: 2305-13.

-Choi HJ, Park-Snyder S, Pascoe LT, Green KJ, Weis WI. Structures of two intermediate filament-binding fragments of desmoplakin reveal a unique repeat motif structure. Nat Struct Biol. 2002; 9:612-20.

-Christensen AH, Andersen CB, Tybjaerg-Hansen A, Haunso S, Svendsen JH. Mutation analysis and evaluation of the cardiac localization of TMEM43 in arrhythmogenic right ventricular cardiomyopathy. Clin Genet. 2011;80:256-64.

-Christensen AH, Benn M, Tybjaerg-Hansen A, Haunso S, Svendsen JH. Missense variants in plakophilin-2 in arrhythmogenic right ventricular cardiomyopathy patients--disease-causing or innocent bystanders? Cardiology. 2010;115:148-54.

-Ciaramella P, Basso C, Di Loria A, Piantedosi D. Arrhythmogenic right ventricular cardiomyopathy associated with severe left ventricular involvement in a cat. J Vet Cardiol. 2009;11:41-5.

-Claycomb WC, Lanson NA Jr, Stallworth BS, Egeland DB, Delcarpio JB, Bahinski A, Izzo NJ Jr. HL-1 cells: a cardiac muscle cell line that contracts and retains phenotypic characteristics of the adult cardiomyocyte. Proc Natl Acad Sci U S A.1998;95:2979-84.

-Corrado D, Basso C, Pavei A, Michieli P, Schiavon M, Thiene G. Trends in sudden cardiovascular death in young competitive athletes after implementation of a prepartecipation screening program. JAMA 2006, 296:1593-601.

-Corrado D and Thiene G. Arrhythmogenic right ventricular cardiomyopathy/dysplasia: clinical impact of molecular genetic studies. Circulation 2006;113:1634-7.

-Corrado D, Basso C, Leoni L, Tokajuk B, Bauce B, Frigo G, Tarantini G, Napodano M, Turrini P, Ramondo A, Daliento L, Nava A, Buja G, Iliceto S, Thiene G. Three-dimensional electroanatomic voltage mapping increases accuracy of diagnosing arrhythmogenic right ventricular cardiomyopathy/dysplasia. Circulation. 2005;111:3042-50.

-Corrado D, Leoni L, Link MS, Della Bella P, Gaita F, Curnis A, Salerno JU, Igidbashian D, Raviele A, Disertori M, Zanotto G, Verlato R, Vergara G, Delise P, Turrini P, Basso C, Naccarella F, Maddalena F, Estes NA 3rd, Buja G, Thiene G. Implantable cardioverter-defibrillator therapy for prevention of sudden death in patients with arrhythmogenic right ventricular cardiomyopathy/dysplasia. Circulation. 2003;108:3084-91.

-Corrado D., Basso C., Schiavon M., Thiene G. Screening for hypertrophic cardiomyopathy in young athletes. N Engl J Med. 1998;339:364-9.

-Corrado D, Basso C, Thiene G, McKenna WJ, Davies MJ, Fontaliran F, Nava A, Silvestri F, Blomstrom-Lundqvist C, Wlodarska EK, Fontaine G, Camerini F. Spectrum of clinicopathologic manifestations of arrhythmogenic right ventricular cardiomyopathy/dysplasia: a multicenter study. J Am Coll Cardiol. 1997;30:1512-20.

-Corrado D., Thiene G., Nava A., Rossi L., Pennelli N. Sudden death in young competitive athletes: clinicopathologic correlations in 22 cases. Am J Med. 1990; 89: 588-96.

-Cox MG, van der Zwaag PA, van der Werf C, van der Smagt JJ, Noorman M, Bhuiyan ZA, Wiesfeld AC, Volders PG, van Langen IM, Atsma DE, Dooijes D, van den Wijngaard A, Houweling AC, Jongbloed JD, Jordaens L, Cramer MJ, Doevendans PA, de Bakker JM, Wilde AA, van Tintelen JP, Hauer RN. Arrhythmogenic right ventricular dysplasia/cardiomyopathy: pathogenic desmosome mutations in index-patients predict outcome of family screening: Dutch arrhythmogenic right ventricular dysplasia/cardiomyopathy genotype-phenotype follow-up study. Circulation. 2011;123:2690-700.

-d'Amati G, di Gioia CR, Giordano C, Gallo P. Myocyte transdifferentiation: a possible pathogenetic mechanism for arrhythmogenic right ventricular cardiomyopathy. Arch Pathol Lab Med. 2000;124:287-90.

-Dalakas MC, Park KY, Semino-Mora C, Lee HS, Sivakumar K, Goldfarb LG. Desmin myopathy, a skeletal myopathy with cardiomyopathy caused by mutations in the desmin gene. N Engl J Med. 2000;342:770-80.

- Dalal D, Molin LH, Piccini J, Tichnell C, James C, Bomma C, Prakasa K, Towbin JA, Marcus FI, Spevak PJ, Bluemke DA, Abraham T, Russell SD, Calkins H and and Judge DP. Clinical features of arrhythmogenic right ventricular dysplasia/cardiomyopathy associated with mutations in plakophilin-2. Circulation 2006, 113:1641-9.

-Daliento L, Turrini P, Nava A, Rizzoli G, Angelini A, Buja G, Scogmaniglio R, Thiene G. Arrhythmogenic right ventricular cardiomyopathy in young versus adult patients: similarities and differences. J Am Coll Cardiol 1995,25:655-64.

-Daliento L, Rizzoli G, Thiene G, Nava A, Rinuncini M, Chioin R, Dalla Volta S. Diagnostic accuracy of right ventriculography in arrhythmogenic right ventricular cardiomyopathy. Am J Cardiol. 1990; 66: 741-5.

-Dalla Volta S., Battaglia G, Zerbini E. “Auricularization” of right ventricular pressure curve. Am. Heart J 1961; 61:25-33; Dalla Volta S., et al.,Le syndrome Clinique et hemodynamique de l’auricularisation du ventricule droit. Arch Mal Coeur Vaiss 1965;58:1129-43.

-Dawes AT. A mathematical model of alpha-catenin dimerization at adherens junctions in polarized epithelial cells. J Theor Biol. 2009;257:480-8.

-De Bortoli M, Beffagna G, Bauce B, Lorenzon A, Smaniotto G, Rigato I, Calore M, Li Mura IE, Basso C, Thiene G, Lanfranchi G, Danieli GA, Nava A, Rampazzo A. The p.A897KfsX4 frameshift variation in desmocollin-2 is not a causative mutation in arrhythmogenic right ventricular cardiomyopathy. Eur J Hum Genet. 2010;18:776-82.

-Delmar M, McKenna WJ. The cardiac desmosome and arrhythmogenic cardiomyopathies: from gene to disease. Circ Res. 2010;107:700-14.

-Delmar M. The intercalated disk as a single functional unit. Heart Rhythm. 2004;1:12-3.

-den Haan AD, Tan BY, Zikusoka MN, Lladó LI, Jain R, Daly A, Tichnell C, James C, Amat-Alarcon N, Abraham T, Russell SD, Bluemke DA, Calkins H, Dalal D, Judge DP. Comprehensive desmosome mutation analysis in north americans with arrhythmogenic right ventricular dysplasia/cardiomyopathy. Circ Cardiovasc Genet. 2009;2:428-35.

-Don RH, Cox PT, Wainwright BJ, Baker K, Mattick JS. 'Touchdown' PCR to circumvent spurious priming during gene amplification. Nucleic Acids Res 1991,19:4008.

-Drees F, Pokutta S, Yamada S, Nelson WJ, Weis WI. Alpha-catenin is a molecular switch that binds E-cadherin-beta-catenin and regulates actin-filament assembly. Cell. 2005;123:903-15.

-Elliott P., Andersson B., Arbustini E., Bilinska Z., Cecchi F., Charron P., Dubourg O., Kühl U., Maisch B., McKenna W.J., Monserrat L., Pankuweit S., Rapezzi C., Seferovic P., Tavazzi L., Keren A. Classification of the cardiomyopathies: a position statement from the European Society Of Cardiology Working Group on Myocardial and Pericardial Diseases. Eur Heart J. 2008;29:270-6.

-Ellis LA, Taylor CF, Taylor GR. A comparison of fluorescent SSCP and denaturing HPLC for high throughput mutation scanning. Hum Mutat 2000,15:556-64.

-Eshkind L, Tian Q, Schmidt A, Franke WW, Windoffer R, Leube RE. Loss of desmoglein 2 suggests essential functions for early embryonic development and proliferation of embryonal stem cells. Eur J Cell Biol. 2002;81:592-8.

-Fernández del Palacio, M. J., Bernal, L. J., Bayón, A., Barnabé A., Montes de Oca, R. and Seva,J. Arrhythmogenic right ventricular dysplasia/cardiomyopathy in a Siberian husky. J. Small Anim. Pract. 2001; 42:137–42.

-Ferreira-Cornwell MC, Luo Y, Narula N, Lenox JM, Lieberman M, Radice GL. Remodeling the intercalated disc leads to cardiomyopathy in mice misexpressing cadherins in the heart. J Cell Sci. 2002;115:1623-34.

- Fixman M and Freire JJ. Theory of DNA melting curves. Biopolymers. 1977,16:2693-2704.

-Fontaine G, Fontaliran F, Frank R. Arrhythmogenic right ventricular cardiomyopathies: clinical forms and main differential diagnoses. Circulation. 1998, 97:1532-5. Review.

-Fontaine G, Fontaliran F, Guiraudon G, Frank R, Laurenceau JL, Malergue C, Grosgogeat Y. The arrhythmogenic right ventricle. In : Iwa T, Fontaine G (eds) Cardiac arrhythmias. Recent progress in investigation and management. Amsterdam: Elsevier Science BV 1988,189-202.

-Fontaine G, Frank R, Guiraudon G, Pavie A, Tereau Y, Chomette G, Grosgogeat Y. Signification des troubles de conduction intraventriculaire observés dans la dysplasia ventriculaire droite arhythmogène. Arc Mal Coeur 1984;77:872-9.

-Fountoulakis M, Soumaka E, Rapti K, Mavrodis M, Tsangaris G, Maris A, Weisleder N, Capetanaki Y. Alterations in the heart mitochondrial proteome in a desmin null heart failure model. J Mol Cell Cardiol. 2005;38:461-74.

-Fox PR, Maron BJ, Basso C, Liu S, Thiene G. Spontaneously occurring arrhythmogenic right ventricular cardiomyopathy in the domestic cat. A new animal model similar to the human disease. Circulation 2000;102:1863-70.

-Franke WW, Borrmann CM, Grund C, Pieperhoff S. The area composita of adhering junctions connecting heart muscle cells of vertebrates. I. Molecular definition in intercalated disks of cardiomyocytes by immunoelectron microscopy of desmosomal proteins. Eur J Cell Biol. 2006;85:69-82.

-Fressart V, Duthoit G, Donal E, Probst V, Deharo JC, Chevalier P, Klug D, Dubourg O, Delacretaz E, Cosnay P, Scanu P, Extramiana F, Keller D, Hidden-Lucet F, Simon F, Bessirard V, Roux-Buisson N, Hebert JL, Azarine A, Casset-Senon D, Rouzet F, Lecarpentier Y, Fontaine G, Coirault C, Frank R, Hainque B, Charron P. Desmosomal gene analysis in arrhythmogenic right ventricular dysplasia/cardiomyopathy: spectrum of mutations and clinical impact in practice. Europace. 2010;12:861-8.

-Furlanello F, Bertoldi A, Dallago M, Furlanello C, Fernando F, Inama G, Pappone C, Chierchia S. Cardiac arrest and sudden death in competitive athletes with arrhythmogenic right ventricular displasia. Pacing Clin Electrophysiol 1998, 21:331-5.

-Gallicano GI, Bauer C, Fuchs E. Rescuing desmoplakin function in extra-embryonic ectoderm reveals the importance of this protein in embryonic heart, neuroepithelium, skin, and vasculature. Development 2001,128:929-41.

-Gallicano GI, Kouklis P., Bauer C, Yin M, Vasioukhin V, Degenstein L, Fuchs E. Desmoplakin is required early in development for assembly of desmosomes and cytoskeletal linkage. J Cell Biol 1998,143:2009-22.

-Garcia-Gras E, Lombardi R, Giocondo MJ, Willerson JT, Schneider MD, Khoury DS, Marian AJ. Suppression of canonical Wnt/beta-catenin signaling by nuclear plakoglobin recapitulates phenotype of arrhythmogenic right ventricular cardiomyopathy. J Clin Invest. 2006;116:2012-21.

-Garrod DR, Chidgey M. Desmosome structure, composition and function. Biochim Biophys Acta. 2008;1778:572-87.

- Garrod DR, Merritt AJ, Nie Z. Desmosomal cadherins. Curr Opin Cell Biol 2002,14:537–45.

-George CH, Sorathia R, Bertrand BM, Lai FA. In situ modulation of the human cardiac ryanodine receptor (hRyR2) by FKBP12.6. Biochem J. 2003;370(Pt 2):579-89.

-Gerull B, Heuser A, Wichter T, Paul M, Basson CT, McDermott DA, Lerman BB, Markowitz SM, Ellinor PT, MacRae CA, Peters S, Grossmann KS, Drenckhahn J, Michely B, Sasse-Klaassen S, Birchmeier W, Dietz R, Breithardt G, Schulze-Bahr E, Thierfelder L. Mutations in the desmosomal protein plakophilin-2 are common in arrhythmogenic right ventricular cardiomyopathy. Nat Genet. 2004;36:1162-4.

-Getsios S, Amargo EV, Dusek RL, Ishii K, Sheu L, Godsel LM, Green KJ. Coordinated expression of desmoglein 1 and desmocollin 1 regulates intercellular adhesion. Differentiation 2004, 72:419–33.

- Getsios S, Huen AC, Green KJ. Working out the strength and flexibility of desmosomes. Nat.Rev. Mol. Cell Biol. 5, 271-81.

-Goldfarb LG and Dalakas MC. Tragedy in a heartbeat: malfunctioning desminb causes skeletal and cardiac muscle disease. J Clin Invest 2009; 119:1806-13.

-Goossens S, Janssens B, Bonné S, De Rycke R, Braet F, van Hengel J, van Roy F. A unique and specific interaction between alphaT-catenin and plakophilin-2 in the area composita, the mixed-type junctional structure of cardiac intercalated discs. J Cell Sci. 2007;120:2126-36.

-Gotthardt M, Hammer RE, Hübner N, Monti J, Witt CC, McNabb M, Richardson JA, Granzier H, Labeit S, Herz J. Conditional expression of mutant M-line titins results in cardiomyopathy with altered sarcomere structure. J Biol Chem. 2003;278:6059-65.

-Granzier HL, Radke MH, Peng J, Westermann D, Nelson OL, Rost K, King NM, Yu Q, Tschöpe C, McNabb M, Larson DF, Labeit S, Gotthardt M. Truncation of titin's elastic PEVK region leads to cardiomyopathy with diastolic dysfunction. Circ Res. 2009;105:557-64.

-Granzier HL and Labeit S. The giant protein titin: a major player in myocardial mechanics, signaling, and disease. Circ Res.2004;94:284–95.

-Granzier HL and Irving TC.Passive tension in cardiac muscle: contribution of collagen, titin, microtubules, and intermediate filaments. Biophys J 1995;68:1027-44.

-Green KJ and Simpson CL. Desmosomes: new perspectives on a classic. J Invest Dermatol 2007,127:2499-515.Review.

-Gramlich M, Michely B, Krohne C, Heuser A, Erdmann B, Klaassen S, Hudson B, Magarin M, Kirchner F, Todiras M, Granzier H, Labeit S, Thierfelder L, Gerull B. Stress-induced dilated cardiomyopathy in a knock-in mouse model mimicking human titin-based disease. J Mol Cell Cardiol. 2009;47:352-8.

-Gross E, Arnold N, Goette J, Schwarz-Boeger U, Kiechle M. A comparison of BRCA1 mutation analysis by direct sequencing, SSCP and DHPLC. Hum Genet 1999,105:72-8.

-Grossmann KS, Grund C, Huelsken J, Behrend M, Erdmann B, Franke WW, Birchmeier W. Requirement of plakophilin 2 for heart morphogenesis and cardiac junction formation. J Cell Biol 2004, 67:149-60.

-Gumbiner BM. Regulation of cadherin adhesive activity. J Cell Biol. 2000;148:399-404. Review.

-Hamid MS, Norman M, Quraishi A, Firoozi S, Thaman R, Gimeno JR, Sachdev B, Rowland E, Elliott PM, McKenna WJ. Prospective evaluation of relatives for familial arrhythmogenic right ventricular cardiomyopathy/dysplasia reveals a need to broaden diagnostic criteria. J Am Coll Cardiol. 2002;40:1445-50.

-Harpster, N. Boxer cardiomyopathy. Kirk's Current Veterinary Therapy VIII, (Kirk, R., ed.), WB Saunders, Philadelphia 1983:329–37.

-Harris TJ, Tepass U. Adherens junctions: from molecules to morphogenesis. Nat Rev Mol Cell Biol. 2010;11:502-14.

-Harvey AM, Battersby IA, Faena M, Fews PG, Darke G, Ferasin L. Arrhythmogenic right ventricular cardiomyopathy in two cats. J Small Anim Pract 2005;46:151-6.

-Heuser A, Plovie ER, Ellinor PT, Grossmann KS, Shin JT, Wichter T, Basson CT, Lerman BB, Sasse-Klaassen S, Thierfelder L, MacRae CA, Gerull B. Mutant desmocollin-2 causes arrhythmogenic right ventricular cardiomyopathy. Am J Hum Genet. 2006;79:1081-8.

-Huang H, Asimaki A, Lo D, McKenna W, Saffitz J. Disparate effects of different mutations in plakoglobin on cell mechanical behavior. Cell Motil Cytoskel 2008;65:964–78.

-Huber AH, Nelson WJ, Weis WI. Three-dimensional structure of the armadillo repeat region of beta-catenin. Cell. 1997;90:871-82.

- Huber O. Structure and function of desmosomal proteins and their role in development and disease. Cell Mol Life Sci. 2003;60:1872-90.

-Hulot JS, Jouven X, Empana JP, Frank R, Fontaine G. Natural history and risk stratification of arrhythmogenic right ventricular dysplasia/cardiomyopathy. Circulation. 2004;110:1879-84.

-Imamura Y, Itoh M, Maeno Y, Tsukita S, Nagafuchi A. Functional domains of alpha-catenin required for the strong state of cadherin-based cell adhesion. J Cell Biol. 1999;144:1311-22.

-Janssens B, Mohapatra B, Vatta M, Goossens S, Vanpoucke G, Kools P, Montoye T, van Hengel J, Bowles NE, van Roy F, Towbin JA. Assessment of the CTNNA3 gene encoding human alpha T-catenin regarding its involvement in dilated cardiomyopathy.Hum Genet. 2003;112:227-36.

-Janssens B, Goossens S, Staes K, Gilbert B, van Hengel J, Colpaert C, Bruyneel E, Mareel M, van Roy F. AlphaT-catenin: a novel tissue-specific beta-catenin-binding protein mediating strong cell-cell adhesion. J Cell Sci. 2001;114:3177-88.

- Johnston JA, Ward CL, Kopito RR. Aggresomes: a cellular response to misfolded proteins. J Cell Biol. 1998;143:1883-98.

- Jones AC, Austin J, Hansen N, Hoogendoorn B, Oefner PJ, Cheadle JP, O'Donovan MC. Optimal temperature selection for mutation detection by denaturing HPLC and comparison to single-stranded conformation polymorphism and heteroduplex analysis. Clin Chem 1999,45:1133-40.

-Kannankeril PJ, Mitchell BM, Goonasekera SA, Chelu MG, Zhang W, Sood S, Kearney DL, Danila CI, De Biasi M, Wehrens XH, Pautler RG, Roden DM, Taffet GE, Dirksen RT, Anderson ME, Hamilton SL. Mice with the R176Q cardiac ryanodine receptor mutation catecholamine induced ventricular tachycardia and cardiomyopathy. Proc Natl Acad Sci U S A 2006, 103:12179-84.

-Kaplan SR, Gard JJ, Carvajal-Huerta L, Ruiz-Cabezas JC, Thiene G, Saffitz JE. Structural and molecular pathology of the heart in Carvajal syndrome. Cardiovasc Pathol 2004, 13:26-32.

- Kaplan SR, Gard JJ, Protonotarios N, Tsatsopoulou A, Spiliopoulou C, Anastasakis A, Squarcioni CP, McKenna WJ, Thiene G, Basso C, Brousse N, Fontaine G, Saffitz JE. Remodeling of myocyte gap junctions in arrhythmogenic right ventricular cardiomyopathy due to a deletion in plakoglobin (Naxos disease). Heart Rhythm. 2004;1:3-11.

-Kapplinger JD, Landstrom AP, Salisbury BA, Callis TE, Pollevick GD, Tester DJ, Cox MG, Bhuiyan Z, Bikker H, Wiesfeld AC, Hauer RN, van Tintelen JP, Jongbloed JD, Calkins H, Judge DP, Wilde AA, Ackerman MJ. Distinguishing arrhythmogenic right ventricular cardiomyopathy/dysplasia-associated mutations from background genetic noise. J Am Coll Cardiol. 2011;57:2317-27.

-Kirchhof P, Fabritz L, Zwiener M, Witt H, Schäfers M, Zellerhoff S, Paul M, Athai T, Hiller KH, Baba HA, Breithardt G, Ruiz P, Wichter T, Levkau B. Age- and training-dependent development of arrhythmogenic right ventricular cardiomyopathy in heterozygous plakoglobin-deficient mice. Circulation. 2006;114:1799-806.

-Klauke B, Kossmann S, Gaertner A, Brand K, Stork I, Brodehl A, Dieding M, Walhorn V, Anselmetti D, Gerdes D, Bohms B, Schulz U, Zu Knyphausen E, Vorgerd M, Gummert J, Milting H. De novo desmin-mutation N116S is associated with arrhythmogenic right ventricular cardiomyopathy. Hum Mol Genet. 2010;19:4595-607.

-Klymkowsky MW, Williams BO, Barish GD, Varmus HE, Vourgourakis YE. Membrane-anchored plakoglobins have multiple mechanisms of action in Wnt signaling. Mol Biol Cell. 1999;10:3151-69.

-Kobielak A, Fuchs E. Alpha-catenin: at the junction of intercellular adhesion and actin dynamics. Nat Rev Mol Cell Biol. 2004;5:614-25. Review.

-Kostareva A, Sjöberg G, Bruton J, Zhang SJ, Balogh J, Gudkova A, Hedberg B, Edström L, Westerblad H, Sejersen T. Mice expressing L345P mutant desmin exhibit morphological and functional changes of skeletal and cardiac mitochondria. J Muscle Res Cell Motil. 2008;29:25-36.

-Krusche CA, Holthöfer B, Hofe V, van de Sandt AM, Eshkind L, Bockamp E, Merx MW, Kant S, Windoffer R, Leube RE. Desmoglein 2 mutant mice develop cardiac fibrosis and dilation. Basic Res Cardiol. 2011;106:617-33.

-Labeit S, Kolmerer B, Linke WA. The giant protein titin. Emerging roles in physiology and pathophysiology. Circ. Res. 1997;80:290-4.

-Lacroix D, Lions C, Klug D, Prat A. Arrhythmogenic right ventricular dysplasia: catheter ablation, MRI, and heart transplantation. J Cardiovasc Electrophysiol. 2005;16:235-6.

-Lancisi GM De Motu Cordis et Aneurysmatibus. Naples 1736.

-Lapouge, K., Fontao, L., Champliaud, M.F., Jaunin, F., Frias, M.A.,Favre, B., Paulin, D., Green, K.J. and Borradori, L. New insightsinto the molecular basis of desmoplakin- and desmin-related cardiomyopathies. J. Cell. Sci. 2006;119:4974–85.

-Lahtinen AM, Lehtonen E, Marjamaa A, Kaartinen M, Heliö T, Porthan K, Oikarinen L, Toivonen L, Swan H, Jula A, Peltonen L, Palotie A, Salomaa V, Kontula K. Population-prevalent desmosomal mutations predisposing to arrhythmogenic right ventricular cardiomyopathy. Heart Rhythm. 2011; 8:1214-21.

-Lahtinen AM, Lehtonen A, Kaartinen M, Toivonen L, Swan H, Widén E, Lehtonen E, Lehto VP, Kontula K. Plakophilin-2 missense mutations in arrhythmogenic right ventricular cardiomyopathy. Int J Cardiol. 2008;126:92-100.

-Le Guludec D, Slama MS, Frank R, Faraggi M, Grimon G, Bourguignon MH, Motte G. Evaluation of radionuclide angiography in diagnosis of arrhythmogenic right ventricular cardiomyopathy. J Am Coll Cardiol. 1995;26:1476-83.

-Leask A and Abraham DJ. TGF-beta signaling and the fibrotic response. FASEB J. 2004;18:816-27.

-Li D, Liu Y, Maruyama M, Zhu W, Chen H, Zhang W, Reuter S, Lin SF, Haneline LS, Field LJ, Chen PS, Shou W. Restrictive loss of plakoglobin in cardiomyocytes leads to arrhythmogenic cardiomyopathy. Hum Mol Genet. 2011;20:4582-96.

-Li J, Swope D, Raess N, Cheng L, Muller EJ, Radice GL. Cardiac tissue-restricted deletion of plakoglobin results in progressive cardiomyopathy and activation of {beta}-catenin signaling. Mol Cell Biol. 2011;31:1134-44.

- Li J, Levin MD, Xiong Y, Petrenko N, Patel VV, Radice GL. N-cadherin haploinsufficiency affects cardiac gap junctions and arrhythmic susceptibility. J Mol Cell Cardiol. 2008;44:597-606

- Li J, Patel VV, Kostetskii I, Xiong Y, Chu AF, Jacobson JT, Yu C, Morley GE, Molkentin JD, Radice GL. Cardiac-specific loss of N-cadherin leads to alteration in connexins with conduction slowing and arrhythmogenesis. Circ Res. 2005;97:474-81.

-Liu J and Farmer SR. Regulating the balance between peroxisome proliferator-activated receptor gamma and beta-catenin signaling during adipogenesis. A glycogen synthase kinase 3beta phosphorylation-defective mutant of beta-catenin inhibits expression of a subset of adipogenic genes. J Biol Chem. 2004;279:45020-7.

-Lodish H, Berk A, Matsudaria P, Kaiser CA, Krieger M, Scott MP, Zipursky L, Darnell J. Molecular Cell Biology 5th ed, WH Freeman,2003.

-Lombardi R, Dong J, Rodriguez G, Bell A, Leung TK, Schwartz RJ, Willerson JT, Brugada R, Marian AJ. Genetic fate mapping identifies second heart field progenitor cells as a source of adipocytes in arrhythmogenic right ventricular cardiomyopathy. Circ Res. 2009;104:1076-84.

-Ly S, Marcus FI, Xu T, Towbin JA. A woman with incidental findings of ventricular aneurysms and a desmosomal cardiomyopathy. Heart Rhythm. 2008;5:1455-7.

-Mallat Z, Tedgui A, Fontaliran F, Frank R, Durigon M, Fontaine G. Evidence of apoptosis in arrhythmogenic right ventricular dysplasia. N Engl J Med. 1996;335:1190-6.

-Marcus FI, McKenna WJ, Sherrill D, Basso C, Bauce B, Bluemke DA, Calkins H, Corrado D, Cox MG, Daubert JP, Fontaine G, Gear K, Hauer R, Nava A, Picard MH, Protonotarios N, Saffitz JE, Sanborn DM, Steinberg JS, Tandri H, Thiene G, Towbin JA, Tsatsopoulou A, Wichter T, Zareba W. Diagnosis of arrhythmogenic right ventricular cardiomyopathy/dysplasia: proposed modification of the Task Force Criteria. Eur Heart J. 2010;31:806-14.

-Marcus FI and Fontaine G. Arrhythmogenic right ventricular dysplasia/cardiomyopathy: a review. Pacing Clin Electrophysiol. 1995;18:1298-314.

-Marcus FI, Fontaine GH, Guiraudon G, Frank R, Laurenceau JL, Malergue C, Grosgogeat Y. Right ventricular dysplasia: a report of 24 adult cases. Circulation. 1982; 65:384-98.

-Maron BJ, Towbin JA, Thiene G, Antzelevitch C, Corrado D, Arnett D, Moss AJ, Seidman CE, Young JB; American Heart Association; Council on Clinical Cardiology, Heart Failure and Transplantation Committee; Quality of Care and Outcomes Research and Functional Genomics and Translation Biology Interdisiplinary Working Groups, Council on Epidemiology and Prevention. Contemporary definitions and classification of the cardiomyopathies: an American Heart Association Scientific Statement from the Council on Clinical Cardiology, Heart Failure and Transplantation Committee; Quality of Care and Outcomes Research and Functional Genomics and Translational Biology Interdisciplinary Working Groups; and Council on Epidemiology and Prevention. Circulation 2006;113:1807-16.

-Martin ED, Moriarty MA, Byrnes L, Grealy M. Plakoglobin has both structural and signalling roles in zebrafish development. Dev Biol. 2009;327:83-96.

-Matsushita T, Oyamada M, Fujimoto K, Yasuda Y, Masuda S, Wada Y, Oka T, Takamatsu T. Remodeling of cell-cell and cell-extracellular matrix interactions at the border zone of rat myocardial infarcts. Circ Res. 1999;85:1046-55.

-McKenna WJ, Thiene G, Nava A, Fontaliran F, Blomstrom-Lundqvist C, Fontaine G, Camerini F. Diagnosis of arrhythmogenic right ventricular dysplasia/cardiomyopathy. Task Force of the Working Group Myocardial and Pericardial Disease of the European Society of Cardiology and of the Scientific Council on Cardiomyopathies of the International Society and Federation of Cardiology. Br Heart J 1994, 71:215-8.

-McKoy G, Protonotarios N, Crosby A, Tsatsopoulou A, Anastasakis A, Coonar A, Norman M, Baboonian C, Jeffery S, McKenna WJ. Identification of a deletion in plakoglobin in arrhythmogenic right ventricular cardiomyopathy with palmoplantar keratoderma and woolly hair (Naxos disease). Lancet. 2000;17;355:2119-24.

-Merner ND, Hodgkinson KA, Haywood AF, Connors S, French VM, Drenckhahn JD, Kupprion C, Ramadanova K, Thierfelder L, McKenna W, Gallagher B, Morris-Larkin L, Bassett AS, Parfrey PS, Young TL. Arrhythmogenic right ventricular cardiomyopathy type 5 is a fully penetrant, lethal arrhythmic disorder caused by a missense mutation in the TMEM43 gene. Am J Hum Genet. 2008;82:809-21.

-Mertens C, Hofmann I, Wang Z, Teichmann M, Sepehri Chong S, Schnölzer M, Franke WW. Nuclear particles containing RNA polymerase III complexes associated with the junctional plaque protein plakophilin 2. Proc Natl Acad Sci U S A. 2001;98:7795-800.

-Missiaen L, Robberecht W, van den Bosch L, Callewaert G, Parys JB, Wuytack F, Raeymaekers L, Nilius B, Eggermont J, De Smedt H. Abnormal intracellular ca(2+)homeostasis and disease. Cell Calcium 2000, 28:1-21. Review.

-Möhr, A. J. and Kirberger, R. M. Arrhythmogenic right ventricular cardiomyopathy in a dog. J. S. Afr. Vet. Assoc. 2000;71:125–30.

-Munkholm J, Christensen AH, Svendsen JH, Andersen CB. Usefulness of immunostaining for plakoglobin as a diagnostic marker of arrhythmogenic right ventricular cardiomyopathy. Am J Cardiol. 2011.

-Muthappan P and Calkins H. Arrhythmogenic right ventricular dysplasia. Prog Cardiovasc Dis. 2008;51:31-43.

-Nava A., Bauce B., Basso C., Muriago M., Rampazzo A., Villanova C., Daliento L., Buja G., Corrado D., Danieli G.A., Thiene G. Clinical profile and long-term follow-up of 37 families with arrhythmogenic right ventricular cardiomyopathy. J Am Coll Cardiol. 2000; 36:2226-33.

-Nava A., Thiene G., Canciani B., Scognamiglio R., Daliento L., Buja G., Martini B., Stritoni P., Fasoli G. Familial occurrence of right ventricular dysplasia: a study involving nine families. J Am Coll Cardiol. 1988;12:1222-8.

-Norgett EE, Hatsell SJ, Carvajal-Huerta L, Cabezas JC, Common J, Purkis PE, Whittock N, Leigh IM, Stevens HP, Kelsell DP. Recessive mutation in desmoplakin disrupts desmoplakin-intermediate filament interactions and causes dilated cardiomyopathy, woolly hair and keratoderma. Hum Mol Genet. 2000;9:2761-6.

-Norman MW, McKenna WJ. Arrhythmogenic right ventricular cardiomyopathy: perspectives on disease. Z Kardiol. 1999; 88: 550-4.

-Olivé M, Goldfarb L, Moreno D, Laforet E, Dagvadorj A, Sambuughin N, Martínez-Matos JA, Martínez F, Alió J, Farrero E, Vicart P, Ferrer I. Desmin-related myopathy: clinical, electrophysiological, radiological, neuropathological and genetic studies. J Neurol Sci. 2004;219:125-37.

-Osler W. The principles and practice of medicine. 6th edition. New York: D. Appleton & Co; 1905. p. 20.

-Ota T, Fujii M, Sugizaki T, Ishii M, Miyazawa K, Aburatani H, Miyazono K.Targets of transcriptional regulation by two distinct type I receptors for transforming growth factor-beta in human umbilical vein endothelial cells.J Cell Physiol.2002;193:299-318.

-Ott P, MarcusFI, Sobonya RE. Cardiac sarcoidosis masquerading as right ventricular dysplasia. Pacing Clin Electrophysiology 2003; 26: 1498-503.

-Overall CM, Wrana JL, Sodek J. Independent regulation of collagenase, 72-kDa progelatinase, and metalloendoproteinase inhibitor expression in human fibroblasts by transforming growth factor-beta. J Biol Chem. 1989;264:1860-9.

-Oxford EM, Musa H, Maass K, Coombs W, Taffet SM, Delmar M. Connexin43 remodeling caused by inhibition of plakophilin-2 expression in cardiac cells. Circ Res. 2007;101:703-11.

-Pieperhoff S, Franke WW. The area composita of adhering junctions connecting heart muscle cells of vertebrates. VI. Different precursor structures in non-mammalian species. Eur J Cell Biol. 2008;87:413-30.

-Pilichou K, Remme CA, Basso C, Campian ME, Rizzo S, Barnett P, Scicluna BP, Bauce B, van den Hoff MJ, de Bakker JM, Tan HL, Valente M, Nava A, Wilde AA, Moorman AF, Thiene G, Bezzina CR. Myocyte necrosis underlies progressive myocardial dystrophy in mouse dsg2-related arrhythmogenic right ventricular cardiomyopathy. J Exp Med. 2009;206:1787-802.

-Pilichou K, Nava A, Basso C, Beffagna G, Bauce B, Lorenzon A, Frigo G, Vettori A, Valente M, Towbin J, Thiene G, Danieli GA, Rampazzo A. Mutations in desmoglein-2 gene are associated with arrhythmogenic right ventricular cardiomyopathy.Circulation.2006;113:1171-9.

-Pokutta S, Weis WI. Structure of the dimerization and beta-catenin-binding region of alpha-catenin. Mol Cell. 2000;5:533-43.

-Polesskaya A, Seale P, Rudnicki MA. Wnt signaling induces the myogenic specification of resident CD45+ adult stem cells during muscle regeneration. Cell. 2003;113:841-52.

-Posch MG, Posch MJ, Perrot A, Dietz R, Ozcelik C. Variations in DSG2: V56M, V158G and V920G are not pathogenic for arrhythmogenic right ventricular dysplasia/cardiomyopathy. Nat Clin Pract Cardiovasc Med. 2008;5:E1.

-Priori SG, Napolitano C, Tiso N, Memmi M, Vignati G, Bloise R, Sorrentino V, Danieli GA. Mutations in the cardiac ryanodine receptor gene (hRyR2) underlie catecholaminergic polymorphic ventricular tachycardia. Circulation. 2001;103:196-200.

-Quarta G, Muir A, Pantazis A, Syrris P, Gehmlich K, Garcia-Pavia P, Ward D, Sen-Chowdhry S, Elliott PM, McKenna WJ. Familial evaluation in arrhythmogenic right ventricular cardiomyopathy: impact of genetics and revised task force criteria. Circulation. 2011;123:2701-9.

-Radke MH, Peng J, Wu Y, McNabb M, Nelson OL, Granzier H, Gotthardt M. Targeted deletion of titin N2B region leads to diastolic dysfunction and cardiac atrophy. Proc Natl Acad Sci U S A. 2007;104:3444-9.

-Rampazzo A, Nava A, Malacrida S, Beffagna G, Bauce B, Rossi V, Zimbello R, Simionati B, Basso C, Thiene G, Towbin JA, Danieli GA. Mutation in human desmoplakin domain binding to plakoglobin causes a dominant form of arrhythmogenic right ventricular cardiomyopathy. Am J Hum Genet. 2002;71:1200-6.

-Rampazzo A, Nava A, Erne P, Eberhard M, Vian E, Slomp P, Tiso N, Thiene G, Danieli GA. A new locus for arrhythmogenic right ventricular cardiomyopathy (ARVD2) maps to chromosome 1q42-q43. Hum Mol Genet 1995, 4:2151-4.

-Rampazzo A, Nava A, Danieli GA, Buja G, Daliento L, Fasoli G, Scognamiglio R, Corrado D, Thiene G. The gene for arrhythmogenic right ventricular cardiomyopathy maps to chromosome 14q23-q24. Hum Mol Genet 1994,3:959-62.

-Ross SE, Hemati N, Longo KA, Bennett CN, Lucas PC, Erickson RL, MacDougald OA. Inhibition of adipogenesis by Wnt signaling. Science. 2000;289:950-3.

-Ruiz P, Brinkmann V, Ledermann B, Behrend M, Grund C, Thalhammer C, Vogel F, Birchmeier C, Günthert U, Franke WW, Birchmeier W. Targeted mutation of plakoglobin in mice reveals essential functions of desmosomes in the embryonic heart. J Cell Biol. 1996;135:215-25.

-Saffitz JE, Asimaki A, Huang H. Arrhythmogenic right ventricular cardiomyopathy: new insights into disease mechanisms and diagnosis. J Investig Med. 2009;57:861-4. Review.

-Santilli, R. A., Bontempi, L. V., Perego, M., Fornai, L. and Basso, C.Outflow tract segmental arrhythmogenic right ventricular cardiomyopathy in an English Bulldog. J. Vet. Cardiol. 2009;11:47–51.

-Sen-Chowdhry S, Syrris P, Prasad SK, Hughes SE, Merrifield R, Ward D, Pennell DJ, McKenna WJ. Left-dominant arrhythmogenic cardiomyopathy: an under-recognized clinical entity. J Am Coll Cardiol. 2008;52:2175-87.

-Sen-Chowdhry S, Syrris P, McKenna WJ. Role of genetic analysis in the management of patients with arrhythmogenic right ventricular dysplasia/cardiomyopathy. J Am Coll Cardiol. 2007;50:1813-21.

-Sen-Chowdhry S, Syrris P, McKenna WJ. Genetics of right ventricular cardiomyopathy. J Cardiovasc Electrophysiol 2005, 16:927-35.

-Shan Q, Cao K, Huang Y, Liao M, Chen M, Li W, Zou J, Zhu B, Ma W. Clinical and familial study of arrhythmogenic right ventricular cardiomyopathy. Chin Med J. 2001;114:369-73.

-Simpson, KW, Bonagura, JD and Eaton, KA. Right ventricular cardiomyopathy in a dog. J. Vet. Intern. Med. 1994;8:306–9.

-Stappenbeck TS, Bornslaeger EA, Corcoran CM, Luu HH, Virata ML, Green KJ. Functional analysis of desmoplakin domains: specification of the interaction with keratin versus vimentin intermediate filament networks. J Cell Biol. 1993;123:691-705.

-Stokes DL and Wagenknecht T. Calcium transport across the sarcoplasmic reticulum: structure and function of Ca2+-ATPase and the ryanodine receptor. Eur J Biochem 2000, 267:5274-9. Review.

- Syrris P, Ward D, Asimaki A, Evans A, Sen-Chowdhry S, Hughes SE, McKenna WJ. Desmoglein-2 mutations in arrhythmogenic right ventricular cardiomyopathy: a genotypephenotype characterization of familial disease. Eur Heart J 2007, 28:581-8.

-Syrris P, Ward D, Evans A, Asimaki A, Gandjbakhch E, Sen-Chowdhry S, McKenna WJ. Arrhythmogenic right ventricular dysplasia/cardiomyopathy associated with mutations in the desmosomal gene desmocollin-2. Am J Hum Genet. 2006;79:978-84.

-Tabib A, Miras A, Taniere P, Loire R. Undetected cardiac lesions cause unexpected sudden cardiac death during occasional sport activity. A report of 80 cases. Eur Heart J. 1999;20:900-3.

-Tandri H, Saranathan M, Rodriguez ER, Martinez C, Bomma C, Nasir K, Rosen B, Lima JA, Calkins H, Bluemke DA: Noninvasive detection of myocardial fibrosis in arrhythmogenic right ventricular cardiomyopathy using delayed-enhancement magnetic resonance imaging. J Am Coll Cardiol 2005, 45:98-103.

-Taylor M, Graw S, Sinagra G, Barnes C, Slavov D, Brun F, Pinamonti B, Salcedo EE, Sauer W, Pyxaras S, Anderson B, Simon B, Bogomolovas J, Labeit S, Granzier H, Mestroni L. Genetic variation in titin in arrhythmogenic right ventricular cardiomyopathy-overlap syndromes. Circulation. 2011;124:876-85.

- Tepass U, Truong K, Godt D, Ikura M, Peifer M. Cadherins in embryonic and neural morphogenesis. Nat Rev Mol Cell Biol. 2000;1:91-100. Review.

-Thiene G, Corrado D, Basso C. Arrhythmogenic right ventricular cardiomyopathy/dysplasia. Orphanet J Rare Dis. 2007;14;2:45.

-Thiene G and Basso C. Arrhythmogenic right ventricular cadiomyopathy. An Update. Cardiovasc Pathol. 2001; 10:109-11.

-Thiene G, Basso C, Danieli GA, Rampazzo A, Corrado D, Nava A. Arrhythmogenic right ventricular cardiomyopathy: a still underrecognised clinical entity. Trends Cardiovascular Med 1997,7:84-90.

-Thiene G, Corrado D, Nava A, Rossi L, Poletti A, Boffa GM, Daliento L, Pennelli N. Right ventricular cardiomyopathy: is there evidence of an inflammatory aetiology? Eur Heart J. 1991;12 Suppl D:22-5.

-Thiene G, Nava A, Corrado D, Rossi L, Pennelli N. Right ventricular cardiomyopathy and sudden death in young people. N Engl J Med. 1988;318:129-33.

-Tiso N, Stephan DA, Nava A, Bagattin A, Devaney JM, Stanchi F, Larderet G, Brahmbhatt B, Brown K, Bauce B, Muriago M, Basso C, Thiene G, Danieli GA, Rampazzo A. Identification of mutations in the cardiac ryanodine receptor gene in families affected with arrhythmogenic right ventricular cardiomyopathy type 2 (ARVD2). Hum Mol Genet. 2001;10:189-94.

-Troyanovsky SM, Troyanovsky RB, Eshkind LG, Krutovskikh VA, Leube RE, Franke WW. Identification of the plakoglobin-binding domain in desmoglein and its role in plaque assembly and intermediate filament anchorage. J Cell Biol. 1994;127:151-60.

-Turrini P, Corrado D, Basso C, Nava A, Bauce B, Thiene G: Dispersion of ventricular depolarization-repolarization: a non-invasive marker for risk stratification in arrhythmogenic right ventricular cardiomyopathy. Circulation 2001;103:3075-80.

-Uhl HS. A previously undescribed congenital malformation of the heart: almost total absence of the myocardium of the right ventricle. Bull John Hopkins Hosp 1952,91:197-209.

-Valente M, Calabrese F, Angelini A, Caforio A, Basso C, Thiene G. Pathobiology. In: Arrhythmogenic right ventricular cardiomyopathy/dysplasia Nava A, Rossi L and Thiene G, Editors, Elsevier, Amsterdam, 1997:147–58.

-van Tintelen JP, Van Gelder IC, Asimaki A, Suurmeijer AJ, Wiesfeld AC, Jongbloed JD, van den Wijngaard A, Kuks JB, van Spaendonck-Zwarts KY, Notermans N, Boven L, van den Heuvel F, Veenstra-Knol HE, Saffitz JE, Hofstra RM, van den Berg MP. Severe cardiac phenotype with right ventricular predominance in a large cohort of patients with a single missense mutation in the DES gene. Heart Rhythm. 2009;6:1574-83.

-Van Tintelen JP, Entius MM, Bhuiyan ZA, Jongbloed R, Wiesfeld AC, Wilde AA, van der Smagt J, Boven LG, Mannens MM, van Langen IM, Hofstra RM, Otterspoor LC, Doevendans PA, Rodriguez LM, van Gelder IC, Hauer RN: Plakophilin-2 mutations are the major determinant of familial arrhythmogenic right ventricular dysplasia/cardiomyopathy. Circulation 2006,113:1650-8.

-Varga J, Jimenez SA. Stimulation of normal human fibroblast collagen production and processing by transforming growth factor-beta. Biochem Biophys Res Commun. 1986;138:974-80.

-Vatta M, Yang Z, Towbin JA. Arrhythmogenic in right ventricular cardiomyopathy/dysplasia. Transgenic animal models. In Arrhythmogenic Right Ventricular Cardiomyopathy/Dysplasia. Edited by Marucs FI, Nava A, Thiene G. Milano: Springer, 2007:61-8.

-Wang X, Osinska H, Dorn GW 2nd, Nieman M, Lorenz JN, Gerdes AM, Witt S, Kimball T, Gulick J, Robbins J. Mouse model of desmin-related cardiomyopathy. Circulation. 2001;103:2402-7.

-Wichter T, Paul M, Wollman C, Acil T, Gerdes P, Ashraf O, Tjan TD, Soeparwata R, Block M, Borggrefe M, Scheld HH, Breithardt G, Bocker D. Implantable cardioverter/defibrillator therapy in arrhythmogenic right ventricular cardiomyopathy: singlecenter experience of longterm follow-up and complications in 60 patients. Circulation 2004,109:1503-8.

-Whittock NV, Ashton GH, Dopping-Hepenstal PJ, Gratian MJ, Keane FM, Eady RA, McGrath JA. Striate palmoplantar keratoderma resulting from desmoplakin haploinsufficiency. J Invest Dermatol. 1999;113:940-6.

-Wu Y, Cazorla O, Labeit D, Labeit S, Granzier H. Changes in titin and collagen underlie diastolic stiffness diversity of cardiac muscle. J Mol. Cell. Cardiol 2000;32:2151-62.

- Xiao W and Oefner PJ. Denaturng high-performance liquid chromatography: A rewiew. Hum Mut 2001,17:439-74.

-Xu T, Yang Z, Vatta M, Rampazzo A, Beffagna G, Pilichou K, Scherer SE, Saffitz J, Kravitz J, Zareba W, Danieli GA, Lorenzon A, Nava A, Bauce B, Thiene G, Basso C, Calkins H, Gear K, Marcus F, Towbin JA; Multidisciplinary Study of Right Ventricular Dysplasia Investigators. Compound and digenic heterozygosity contributes to arrhythmogenic right ventricular cardiomyopathy. J Am Coll Cardiol. 2010;55:587-97.

- Yamada S, Pokutta S, Drees F, Weis WI, Nelson WJ. Deconstructing the cadherin-catenin-actin complex. Cell. 2005;123:889-901.

-Yang Z, Bowles NE, Scherer SE, Taylor MD, Kearney DL, Ge S, Nadvoretskiy VV, DeFreitas G, Carabello B, Brandon LI, Godsel LM, Green KJ, Saffitz JE, Li H, Danieli GA, Calkins H, Marcus F, Towbin JA. Desmosomal dysfunction due to mutations in desmoplakin causes arrhythmogenic right ventricular dysplasia/cardiomyopathy. Circ Res 2006,99:646-55.

-Zhurinsky J, Shtutman M, Ben-Ze'ev A. Differential mechanisms of LEF/TCF family-dependent transcriptional activation by beta-catenin and plakoglobin. Mol Cell Biol. 2000;20:4238-52.

-Zou J, Cao K, Yang B, Chen M, Shan Q, Chen C, Li W, Haines DE. Dynamic substrate mapping and ablation of ventricular tachycardias in right ventricular dysplasia. J Interv Card Electrophysiol. 2004;11:37-45.

LINKS

http://www.ncbi.nlm.nih.gov/books/NBK21334/
http://www.transgenomic.com/pd/Systems.asp?tab=2

8. APPENDIX

DNA Taq polymerases used and relative protocol:

-Taq Gold (Roche) Protocol

DNA	(50 ng/μL)	1	μL
Primer F	(10 pmol/μL)	1	μL
Primer R	(10 pmol/μL)	1	μL
Buffer	5x	2.5	μL
$MgCl_2$		2.5	μL
dNTPs	(1 mM)	5	μL
GoTaq®	(5 U/μL)	0,16	μL
H_2O		To 25	μL

-Go Taq (Promega) Protocol:

DNA	(50 ng/μL)	1	μL
Primer F	(10 pmol/μL)	1	μL
Primer R	(10 pmol/μL)	1	μL
Buffer	5x	5	μL
dNTPs	(1 mM)	5	μL
GoTaq®	(5 U/μL)	0,125	μL
H_2O		To 25	μL

Conditions of screened genes

PKP2, Taq Gold

Amplicon	bp	Forward 5'-3'	Reverse 5'-3'	PCR T_{ann}°C	T°C dHPLC
1	414	ACTCGAGCGGGGCGGGGCTCG	ACTCCCAGCACGCGGGGTGAG	68	Direct sequencing
2	329	ACTTGTTCTTGGCCTTCATT	TTGGGAAAAGTAAACACTCAAA	TD70>60	53.0 / 55.6 / 58.0
3	971	GGGGCAAACTTCTCGTCATC	GCAGCTGCCTGAAAAGTCATT	TD70>60	Direct sequencing
4	310	TGCTTCCCAGTATTCGCTGA	GGTTTCAGTGTGCAAAGTCACC	TD70>60	61.0
5a	273	GCCTCAGTTGTGCTACACATAG	CAGCCACCTCCAATTTGTTG	TD70>60	56.0 / 60.0
5b	304	CGTGGCATCCTCAAGCTTCT	TGAGCCCATCAATCATTTGC	TD70>60	58.1 / 59.1
6	308	TTCAGGGGAGGTGATGTTTG	GGATTACAGGCGCAGACC	TD70>60	Direct sequencing
7	333	GGAGTTGATGGCCTTGACTG	TCCTGACTTCCTTGGGGCTA	TD70>60	58.5
8	307	TGCCAGTTTCCAAACACCTG	AAACCTAAAACCAAGCGGCTA	TD70>60	55.2 / 56.5 / 58.7
9	291	TGATATCACACCTGCAAGGA	CACAAACACACACTCTCTCTCAT	TD70>60	56.9 / 58.7
10	330	CTGGTCTCCTGGTTTGAGTG	TTTCATCTCTGAATTGAATGTAG	TD70>60	57.8 / 60.8
11	330	AAACATCTTCATCAACCTCTGGT	CGGGAGGTGATACAGACAACA	TD70>60	55.3 / 57.1 / 61.2
12a	231	GAAAAAGAATGTTCTTCACCCA	TCGCGTGCATTCTGGTAACT	TD70>60	Direct sequencing
12b	278	TTCCTGACACAGTCCCGAGT	CATCCTGTTTGCTGCCATGT	TD70>60	Direct sequencing
13	307	ACCGAGTGGCCTGACTTCAT	CGATTTCTTCCCAGGGTCAA	TD70>60	58.5 / 59.9 / 61.0
14a	284	TTGACCCTGGGAAGAAATCG	CAGGGGACCACGGAAATAGA	TD70>60	58.2
14b	300	GGACTGCCAAAGCCTACCAC	TTCCCAGGAAGCCATGTACCA	TD70>60	57.4

DSP, Taq Gold

Amplicon	bp	Forward 5'-3'	Reverse 5'-3'	PCR T_{ann}°C	T°C DHPLC
1	422	GGTAGCGAGCAGCGACCTC	AAAACCTTTCCACCTTCGGG	65	65.9 / 66.5
2	365	GATTCCGGGTAAAGGGTCTC	TCTGTTCTGAAAAAGCGTGTCT	62	60.5 / 62.6
3	433	TGGTTCATGAATCTCCGTCTGT	GGGAACATTTGTGCTGCCTT	62	57.2 / 59.2
4	471	TTAAGTCCTGGGGTAAAGAAAA	GGAGGAAAATCCTGCAAACAG	55	58.6 / 61.3
5	443	GCATTAGCCATTTGGGAACC	TTCCCCATTTAAGAAGTGGGATT	62	56.4 / 59.7 / 61.8
6	262	GGGATCTGAGGCCAGTATCTGA	ATCGATGAACAGGTGCCTCC	62	58.0
7	309	ACCTGCAGAGAACACCAGTCA	AGACCAATCATTCCCCGAGA	62	61.1 / 62.1
8	382	AACAGCGTGATTCTTTGGCA	CCAACCCCTGGTGTAGGGTA	55	Direct sequencing
9	312	AGCTTTCATGCAGGCTCACC	GCACTCAAAATCAATGAAGAGG	62	53.7 / 56.8 / 58.7
10	414	ATAGTTTCCCGCTGCCACAT	AAATGCTTGCTTGGCTCTGG	65	57.6 / 60.4
11	442	TGCCGACGAATTTGTGATTT	TTGTTCCATAGCTGCTGATTTC	60	55.7 / 56.4
12	394	TCAGCTTCATTTGAGGGGAAA	GGCAAGGCATCGTGTGTCTA	62	59.3 / 61.8
13	359	GGTTTTTGTGCAGTGGTGTGA	AGGAGGGCTGAGCTGACTTG	62	60.3
14	372	CCCATCTAGTGGGTGGCATT	CCAGTTTTATGCAAACTCCCTT	62	58.9 / 59.6
15	505	TTCTTCGTGCACTAAATTTTCA	AATCCTGCCAGAAGCCTGTT	62	56.6 / 58.0
16	480	CCATGGAAGTTGACTGATGTG	ATGCGAGGCTAGCGGAATTA	62	55.9
17	370	TCTGCTTTGACGTTGTTCCC	AACCTGTGTGGCCACTGAAA	62	57.6 / 58.2
18	437	TTTTATAAACTTTGCCGCCCA	GGCAGTCCATGAAAAGAGCAT	62	Direct sequencing
19	382	TCAAGTGAATTTCTGGGTGA	AAGCCTTCACAAAATGGGTT	58	57.0
20	323	TGCTCATCTCCTAAGCTGTAAC	CGCTTTACAACAAATCAGCA	62	53.6 / 55.3
21	312	TAGACGTGCAGCCCAATGAT	AAGACAGGCAGGAGACAGGG	65	57.0 / 58.8
22	489	TAGGGGAAACAGCCTGGAGA	CAGCGTATTGGAGCATGGAA	TD72>62	Direct sequencing
23a	455	GAATGCACATTGGTCTGGGA	CACATTGCCTTGCTTTCTGC	62	56.9 / 58.5
23b	477	TACCAGGCAGAGTGTTCCCA	CTCCTTGATGGTGGTCTTCG	62	58.0
23c	471	AGGCACCCGGAAGAGAGAAT	GCCTCCTCCTGAAACTCAGC	62	56.0 / 57.0 / 60.7
23d	461	ACTGAAGCAGGTCATGCAGC	CCAGCTGCTGTTTCCTCTGA	62	56.7 / 59.0
23eBg	326	TCACCCGAGAAAACAGGAGC	TCTCGCGTTTTCATCTTCCA	62	57.4 / 59.6
23eEnd	271	TTGATGATGCTGCCAAAACC	AACCGCGTGATATCCTGGTC	62	57.0 / 59.4
23f	503	GCAAACAGTAGTGCGACGGA	TGCTCATTCCTCAAGTGAGCTT	62	60.6 / 61.6
23fg	371	CACCTGAGGGAAAAGCAGAG	AGTTCCAGGGTCCGGTTG	62	58.7/59.9
23g	407	CGGAACCTGAGGCTGGAGTA	AAAGAACAGCAGGGCACACA	TD72>62	54.8 / 56.2 / 59.8
24a	488	CAAGCTCACAGTGTATCCAGGG	TGCTTGGAGTCTTTCGATCTCA	62	Direct sequencing
24b	471	GGAAGACTCAATATTCCCGCA	AAGCAGATGCTCCAGCGATA	62	57.8 / 59.3 / 59.8
24c	476	GAAGGTGACAGCAATGCAGC	CTGAAGCAATCTGGGCTTCC	62	57.8 / 58.7
24d	490	TTGATGATCCATTTTCAGGCA	CAGCTTGAACCCTGGAGGAA	62	58.0 / 59.1 / 59.7
24e	472	CCTTCCAAGGAATCAGACAACC	CGAATACCGTGGCCCTTTT	65	58.3 / 59.3
24f	502	CAGAACGAGCTGTCACTGGG	TGCTCACACAGTTCTTTGAAGG	62	Direct sequencing
24g	493	CCTCAGGAAGCGTAGAGTGG	GTCAAAGATGGCTGCAATGG	TD72>62	57.2 / 58.5 / 59.3
24h	500	TTAGCAGCTCCCGACATGAA	TTCGGTGCTTATCCTCCCAT	62	58.8 / 61.2 / 62.0
24i	467	CATAGGCTTCGAGGGTGTGA	GTGGCGTCAAAGCTTCCTCT	65	Direct sequencing
24l	479	GGATGCCATAAATCGCTCCA	GACGCACTGCATCCAAGTGTA	65	55.3 / 56.8

DSG2, Taq Gold

Amplicon	bp	Forward 5'-3'	Reverse 5'-3'	PCR T_{ann}°C	T°C DHPLC
1	314	CCAGGGAGGAGCCGAGTG	GATTTTCCGAAGCCCCAGGT	TD70>60	67.0 / 69,1
2	391	AGATTTCTCCTCGGGCACTT	TGCACTGAATACCCCTGGAT	TD70>60	54.8 / 55.1 / 57.5
3	463	GCCTCATAGGAAATACGAAGCA	CCGGAATGGGAAAGAGAATC	TD70>60	Direct sequencing
4	393	GGCTTTTGGCTAAGATCAAATC	GCATCCAAAGCGTAACCTGT	TD70>60	53.1 / 55.0
5	491	TCTTGATCGAGAAGAAACACCA	AAGCAATGGCATGTAAAGTCC	TD70>60	Direct sequencing
6	490	CCCATTCACGCTTATGTCCT	TGGACAGCACATCCCTAAAA	TD70>60	53.8 / 55.0 / 55.8
7+8	700	TCTGCAAAAGCTCTGACTGC	TTTTAAGTGTTCAGGGCTCAAA	TD70>60	Direct sequencing
9a	343	TGCTGCTATATTTCCTGTGCAT	TCCAATTATTTGGCCTTTGC	TD70>60	54.7 / 55.7 / 56.5
9b	355	CCTACACCCATTCCCATCAA	GGTGAAAATTCCCCCTCATC	TD70>60	54.8 / 56.9
10	373	AGAGGTTTCCAATTCATGCAG	CTTGACCTCGTGATCCACCT	TD70>60	52.3 / 53.7 / 54.3
11	421	TCTGTTGTCAGCAATAGGAACA	GGTTCAGGACCTCATTTCATAA	TD68>58	55.4 / 56.8 / 59.0
12	455	GCAATGAAAGAACATTTGTGGA	TTGTTTCCCTATTCACCCTCA	TD70>60	Direct sequencing
13	289	GACAAGTCCAGGAAGGGACA	CACTTCCCTAGGCCCCTTTA	TD70>60	55.0 / 57.5 / 59.5
14a	292	CTGGCCTCAGTGGAAATAGC	GCAGGCTTCTGTGTTCTTCC	TD70>60	58.9 / 60.1
14b	299	TCATTTCTGCCAGTGGATCA	TCTTCGTTCAGTGCAACAGC	TD70>60	60.6
14c	225	GATGGAAGGTGGGAAGAACA	CCCCCACCACCAATACATAA	TD70>60	61.0 / 62.8
14d	286	TGACCACTGAAACCACGAAG	GGGTCCCATTTCTCTTTCCT	TD70>60	Direct sequencing
15a	273	TTTCCCTGATGGTTCCTTGT	GCGGTCATCTAGCTCTCCTT	TD70>60	53.8 / 54.5 / 57.5
15b	331	CGGCCTCTTACACTGAGGAA	ACTGGGAAGCTACTGCCAGA	TD70>60	57
15c	377	TCGCTGAATGCTTCTATTGG	CTAGAAGCCATTGGGTCAGG	TD70>60	56.5 / 57.9
15d	263	TCTGGCAGTAGCTTCCCAGT	GCTGGAGCATACACCCTCTC	TD70>60	60.1
15e	261	CACCTCTTCCTGACCCAATG	GAAGATGCTGAGTGCCTTCC	TD70>60	59.8
15f	412	CCTTGGTAGATCAGCCTTATGC	TGCTTGGTAACTCTGGTGGA	TD70>60	58.0 / 59.0 / 60.0
15g	305	ACGGTGTCTGGAGCTGGA	GGAAGCAGAGACAGTGTGGTC	TD70>60	57.2 / 58.5

DSC2, Taq Gold

Amplicon	bp	Forward 5'-3'	Reverse 5'-3'	PCR T_{ann}°C	T°C DHPLC
1	708	TCAGACCTCGCTCTGTAATTGA	TATCCCCGTTCCCCTAGTTT	58	Direct sequencing
2	199	ACACATTAAAGTTTTCTTTTTAT	GGCGTATATGTACCACAGCA	62	Direct sequencing
3	400	CCCCACGTGCATACATTACT	TGGTTTTCATTCGTCTTTAAGC	58	54.8 / 55.4
4	269	CCCCTACCCAGCTAATCCTC	GGAAACTATAGACTCCCACAGCA	58	55.6 / 58.5
5	332	TGAAAGCTCTGCTGAAATAAAGA	GGAGTAGCCAGAGCATTGGT	58	56.5 / 57.2
6	266	GCCAAAATGAATTTGAAGCATAC	TTGAAACACAGTTAATTTGCCATA	60	54.7
7	384	CATAGAACATGTGAATGTTTTGGA	CAAAACCAGCATACTCCAAGG	58	55.0 / 58.0 / 59.5
8	252	GTTGGTGCTTTCCCCCAATA	AGGCCAGAGATGTGCATATTA	58	54.3 / 55.6
9	324	CATCGTGTTCAATTTTTGTGA	CCTTTCTTTCCATTAAATTCTAGC	60	52.2 / 53.5 / 55.3
10	374	ACTCGTTAGCATTGCCAAAT	TAACGTAACAAAATAAGCTA	58	56.5 / 57.9
11	375	CAAGAAGTAGCAGTGGCATAAGG	AACAGAGTGCATGTATCCAGCTT	60	51.7 / 56.0
12	345	GTGTTCAGTGCATACTTTTGTGG	GCAGACATCCTGATGTTGAAAA	58	57.0 / 58.0 / 59.0
13	356	TGTTCAGAAGAAATCAGTGACA	GTGTCTTGAAAGTTACTTTAAAGG	58	57.2 / 58.0
14	263	GATTTATGTGTGTATTAACCATTG	CGCATTATAAGCGAATTCATCC	58	57.7
15a	194	CATAATTTTGTGTTCCTCTCTGT	AGGATTCCGAGGTCTGGTGT	58	56.2 / 60.6 / 61.8
15b	332	GGCTTCACAACCCAAACTGT	TGAAAATTATAGTCAGAATCCAGT	58	61.0 / 61.4 / 62.2
15'	226	GCCACATGCGTGACTTTTAG	ACTTTCTGCCAAGGGGAAAA	58	53.7 / 55.2
16	397	CAATGAAAGGTAAATCAAAGCAA	AAAAACCCCCACAAATAGCA	58	56.3 / 56.8

JUP, Go Taq

Amplicon	bp	Forward 5'-3'	Reverse 5'-3'	PCR T_{ann}°C	T°C DHPLC
1	474	GGACAGTCAGGCGAGATAGC	GCCTTGCTCAGATCTCTGGT	60	Direct sequencing
2	399	GCCAGGTGACTTCCTGCT	GTGGGCCCCTAGTTAGCAT	62	61.3 / 62.5+1 / 63+1.5
3	390	CTGCTCCCCAGTGTCTGC	CTCCCCTGAGGACATCTGC	62	63.4 / 64.3+0.5 / 64.8+1
4	427	GACTCTCCCGTGTGTGATGA	TTATGGAAGCTCAGGGAAGG	62	63.6+0.5 / 64.1+1 / 65+1
5	395	ATATTTCCAGAGGGGCGTCA	CCAAGGCTGTGCAGGATAGA	62	63.7
6_7	580	CGAACTATTCGTGCTTTAGCTG	GGACTGGGGGCTCTAAATCT	62	60.2+0.5 / 62.6+1 / 63.6+1.5
8	517	CCCCTTTAGGTCATCCCACT	CTTTGCTACAGCGGCTTTG	62	62.3+0.5 / 62.7+1
9	300	GAGGGAAGGGATACTTGAAGC	CCACAGAGGACACCCTGAC	65	61.8+0.5 / 63.9+1
10	276	CTGTCATGGGGAGGAGTTGT	GTCCAGGCCTCCCAAATC	65	63.2
11_12	550	ATTGCTACAGGGTGGAGGTG	AGGAGACCCCCAAAAGTGTT	65	Direct sequencing
13	250	GCCCCCTCTTTTAGAAGCAT	GCAGTTGCCACTGGTCCT	62	61.2
14'UTR	487	GTAGAGGAGGCAGCTGAAGG	AAGCCACTCCGTGTCACC	65	62.4
14A	477	TGTCTTTGGTGGGGATGGGG	CAGACCCAGAGAAGGAACCA	TD 65-75	Direct sequencing
14B	482	TGGCCACTAAAGCTTCAGACT	GGGGTCTGAAACAGGAAGG	65	61.4
14C	290	CCTGTCCCACCCACACAGCT	CTAGGGAAGCCCCTCAACTTT	65	Direct sequencing

CTNNA3, Go Taq

An	bp	Forward 5'-3'	Reverse 5'-3'	PCR T ann°C	T°C dHPLC
1	395	TTGCTTGTAACCTCCCCTTT	GCGTGAAAGCCTACGTTTCT	62	Direct sequencing
2	407	TAATTTGTTACAGGACCTAAGC	TCTTCATTATTCATTTTTCCCAC	60	Direct sequencing
3	491	GCCCCTAGCCCTTGAGTT	ACTGAGCCTTGGAGCTGTCT	TD72>62	56.5 / 58.2
4	583	TTGAGCACAACTTTCTTGCAG	CTCTGGCTTCCTTATTTTGAGG	60	56.4 / 57.8+1 / 58.4+1
5	406	GGACTGAACAGGCTTCTCAT	GCAGGAAGCCTAAAGTGTTC	TD72>62	56.5 / 59.9
6	700	TGCTCTACGGGGACCTTTAC	GGCAGAGATGTACAGGAGTCAG	62	55.2 / 58.7+1
7	326	TGAAATGCCATGGAGCTCTAA	ACGGAAAGTATCTCAGCCTAT	62	56.2 / 58.7+0,5 / 60.7+1
8	156	CCATTGCTTATGTCGTTTTTTC	TTAGCCCCTATGTTTCTGACT	62	Direct sequencing
9	267	TTTCTTTTTGCCTGGATATTTTG	GACAAGCCAATGTGGAGTGA	TD72>62	54.3 / 56.3+2
1	454	TTTTGTTTTTCCAGTCTCACAA	AGGAAGCAGAAGTTGCAGTC	62	Direct sequencing
1	578	TTCCTATTGTCGATGATGAAT	ACCATGCCTGTCCCAGTATT	TD70>60	55+3 / 57+3
1	350	CCATTTCCAATGTGCACTCTA	AATTGTGCAGCTGTTATTGGC	TD72>62	56,7+1 / 61+3
1	586	GCCTTTAATTGTCTTTGATTCG	GCAGCAGTAAAATGCACTCA	62	53,5 / 55,3+1
1	395	CATGACTGATGCTCCTGTGAA	CAGGAGTCCCACCCATTAGA	62	Direct sequencing
1	326	TGCTTTTGACATAGTGGAATGA	TGGCACTTGACACTCAGAGA	60	55.7 / 57.5+1
1	295	CCGTTCTTTGGGATGCGAAT	GGCAAAGAGCAATTAGCATGA	TD70>60	57.6+1
1	313	AAGGTACCTGCCATGTGAATA	AGATTTGGTCATGTAAACAAGG	62	55.8+1 / 58.5+2
1	550	CCACGCTTGGCAATAATTAAC	TGCTGACCATACAGAATGAC	62	Direct sequencing

Restriction enzymes used to digest pEGFPC2-haTctn, pEGADT7-haTctn and pEGBKT7-haTctn constructs

	Enzymes
pEGFPC2-haTctn	BamHI (Promega); BglII (Promega)
pEGADT7-haTctn	HindIII (Promega); BglII (Promega)
pEGBKT7-haTctn	HindIII (Promega)